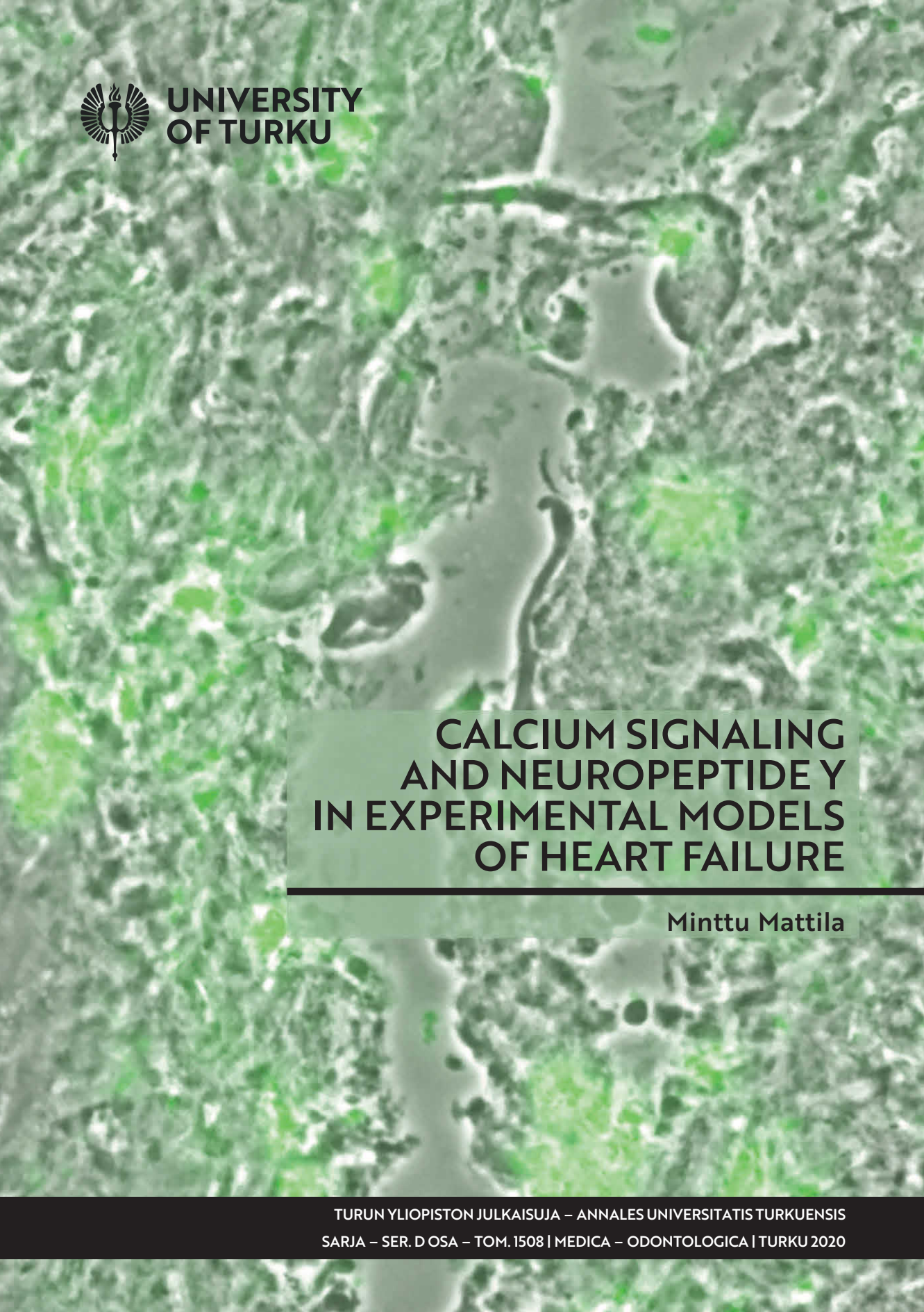

UNIVERSITY OF TURKU

CALCIUM SIGNALING AND NEUROPEPTIDE Y IN EXPERIMENTAL MODELS OF HEART FAILURE

Minttu Mattila

TURUN YLIOPISTON JULKAISUJA – ANNALES UNIVERSITATIS TURKUENSIS
SARJA – SER. D OSA – TOM. 1508 | MEDICA – ODONTOLOGICA | TURKU 2020

UNIVERSITY OF TURKU

CALCIUM SIGNALING AND NEUROPEPTIDE Y IN EXPERIMENTAL MODELS OF HEART FAILURE

Minttu Mattila

TURUN YLIOPISTON JULKAISUJA – ANNALES UNIVERSITATIS TURKUENSIS
SARJA – SER. D OSA – TOM. 1508 | MEDICA – ODONTOLOGICA | TURKU 2020

University of Turku

Faculty of Medicine
Institute of Biomedicine
Pharmacology, Drug Development and Therapeutics
Drug Research Doctoral Programme

Supervised by

Docent Mikko Savontaus, MD, PhD
Turku University Hospital
Department of Medicine
University of Turku
Turku, Finland

Associate Professor Eriika Savontaus
MD, PhD
Institute of Biomedicine
University of Turku
Turku, Finland

Reviewed by

Docent, Johanna Magga, PhD
Research Unit of Biomedicine
Faculty of Medicine
University of Oulu
Oulu, Finland

Professor, Anna-Liisa Levonen, MD,PhD
A.I. Virtanen Institute for Molecular Sciences
University of Eastern Finland
Kuopio, Finland

Opponent

Professor, Jaana Rysä, PhD
University of Eastern Finland
School of Pharmacy
Kuopio, Finland

The originality of this publication has been checked in accordance with the University of Turku quality assurance system using the Turnitin OriginalityCheck service.

Cover Image: Minttu Mattila

ISBN 978-951-29-8179-3 (PRINT)
ISBN 978-951-29-8180-9 (PDF)
ISSN 0355-9483 (Print)
ISSN 2343-3213 (Online)
Painosalama Oy, Turku, Finland 2020

To my family and all the other precious people in my life

UNIVERSITY OF TURKU
Faculty of Medicine
Institute of Biomedicine
Pharmacology, Drug Development and Therapeutics
MINTTU MATTILA: Calcium Signaling and Neuropeptide Y
in Experimental Models of Heart Failure
Doctoral Dissertation, 152 pp.
Drug Research Doctoral Programme (DRDP)
September 2020

ABSTRACT

Despite advances in medical therapy and interventional procedures, heart failure carries a dismal prognosis. Calcium has a central role in controlling the contractility of the heart, and the sarcoplasmic reticulum Ca^{2+} ATPase (SERCA2a) is a key player in calcium cycling in the cardiomyocyte. The expression and activity of SERCA2a have been shown to be decreased in cardiac dysfunction, resulting in inefficient relaxation of the cardiomyocytes. Another player in cardiac modulation is neuropeptide Y (NPY), a sympathetic nervous system neurotransmitter. NPY takes part in many processes in the heart, e.g. excitation–contraction coupling and calcium signaling.

These two factors were assessed in a model of doxorubicin-induced heart failure as well as in models of obesity and type 2 diabetes. Doxorubicin (DOX) is an effective anticancer drug but its use is limited by dose-dependent cardiomyopathy for which there is no clinically validated treatment. The therapeutic potential of lentiviral-mediated SERCA2a gene therapy was studied in this DOX-induced model of heart failure. Next, transgenic mice overexpressing NPY (OE-$NPY^{D\beta H}$) were studied in the same model. Lastly, the OE-$NPY^{D\beta H}$ mice were examined in a model of diet-induced obesity and type 2 diabetes, both associating strongly with pathological changes in the heart.

DOX treatment evoked significant cardiotoxicity, resulting in a disturbance in the expression levels of the genes involved in calcium cycling, and a slight decline in myocardial function. Furthermore, lentiviral SERCA2a gene transfer was able to improve the function of the heart. In OE-$NPY^{D\beta H}$ mice, DOX impaired lean mass accumulation; moreover, the observed tendency to a greater decline in myocardial function may imply that NPY overexpression increases the susceptibility to DOX-induced cardiotoxicity. Additionally, overexpression of NPY led to a cardiovascular phenotype resembling diet-induced obesity in some respects.

In summary, these results provide further knowledge about the role of SERCA2a and NPY in the pathological processes of heart failure, and may help to clarify the therapeutic potential of enhancing calcium cycling.

KEYWORDS: heart failure, calcium signaling, SERCA2a, neuropeptide Y, doxorubicin, gene therapy, obesity, type 2 diabetes

TURUN YLIOPISTO
Lääketieteellinen tiedekunta
Biolääketieteen laitos
Farmakologia, lääkekehitys ja lääkehoito
MINTTU MATTILA: Kalsiumsignalointi ja neuropeptidi Y
kokeellisissa sydämen vajaatoimintamalleissa
Väitöskirja, 152 s.
Lääketutkimuksen tohtoriohjelma
Syyskuu 2020

TIIVISTELMÄ

Lääkkeellisten ja kirurgisten hoitojen kehityksestä huolimatta sydämen vajaatoiminnan ennuste on huono. Sydämen supistuvuuden säätelyssä kalsiumilla on tärkeä rooli. Kalsiumin kierron keskeinen tekijä sydänlihassolussa on sarkoplasmisen kalvoston Ca^{2+} ATPaasi (SERCA2a). Sydämen vajaatoiminnassa SERCA2a:n määrän on todettu vähenevän ja aktiivisuuden laskevan, mikä johtaa sydänlihassolun puutteelliseen relaksaatioon. Sydämen toiminnan säätelyyn osallistuu myös sympaattisen hermoston välittäjäaine, neuropeptidi Y (NPY), jonka vaikutukset välittyvät sydämen soluihin hermoston lisäksi osin myös suorien reseptorivaikutusten kautta. NPY vaikuttaa muun muassa sydänlihassolun kalsiumvirtoihin ja supistuvuuteen.

Näitä kahta sydämen säätelyn osatekijää tutkittiin doksorubisiinin indusoimassa sydämen vajaatoimintamallissa ja lihavuuden sekä tyypin 2 diabeteksen malleissa. Doksorubisiini on tehokas syövän hoidossa käytetty lääke, mutta käyttöä rajaa sen aiheuttama sydänlihassairaus, johon ei tunneta kliinisesti validoitua hoitoa. Doksorubisiinimallin yhteydessä arvioitiin myös lentivirusvälitteisen SERCA2a-geeniterapian potentiaalia. NPY:tä siirtogeenisesti yli-ilmentäviä hiiriä (OE-$NPY^{D\beta H}$) tutkittiin doksorubisiinimallissa ja lisäksi kokeellisissa lihavuuden sekä tyypin 2 diabeteksen malleissa, joissa on todettu esiintyvän sydämen patologisia muutoksia.

Doksorubisiini johti sydämen kalsiumin kiertoon vaikuttavien geenien ilmenemisen häiriöön ja sydämen toiminnan lievään alenemiseen. SERCA2a-geeniterapia paransi sydämen toimintaa. OE-$NPY^{D\beta H}$-hiirillä doksorubisiini esti rasvattoman massan kasvua ja havaittu tendenssi voimakkaampaan sydämen toiminnan heikentymiseen saattaa viitata siihen, että NPY:n yli-ilmentäminen altistaa doksorubisiinin indusoimalle sydäntoksisuudelle. Lisäksi NPY:n yli-ilmentämisen todettiin johtavan runsasrasvaisen ruokavalion aiheuttaman lihavuuden ilmiasua muistuttavaan kardiovaskulariseen ilmiasuun.

Väitöskirjan tulokset tarjoavat uutta tietoa SERCA2a:n ja NPY:n roolista sydämen vajaatoiminnan patologisissa prosesseissa ja auttavat kalsiumsignaloinnin tehostamisen terapeuttisen potentiaalin selvittämisessä.

AVAINSANAT: sydämen vajaatoiminta, kalsiumsignalointi, SERCA2a, neuropeptidi Y, doksorubisiini, geeniterapia, lihavuus, tyypin 2 diabetes

Table of Contents

Abbreviations

ACh	Acetylcholine
AAV	Adeno-associated virus
ATPase	Adenosine triphosphatase
AHA	American Heart Association
ANP	Atrial natriuretic peptide
Beta1R	Beta-1 adrenergic receptor
BMI	Body mass index
BW	Body weight
BNP	Brain natriuretic peptide
Ca^{2+}	Calcium ion
COL I	Collagen I
COL1a2	Collagen I alpha 2
COL III	Collagen III
DNA	Deoxyribonucleic acid
DIO	Diet-induced obesity
DβH	Dopamine-beta-hydroxylase
DOX	Doxorubicin
EF	Ejection fraction
ELLA	Eläinkoelautakunta; National Animal Experimental Board
EDV	End-diastolic volume
ESV	End-systolic volume
EASD	the European Association for the Study of Diabetes
EMA	the European Medicines Agency
ESC	the European Society of Cardiology
FGF	Fibroblast growth factor
FDA	the Food and Drug Administration
FS	Fractional shortening
GTT	Glucose tolerance test
GFP	Green fluorescent protein
HF	Heart failure
HFpEF	Heart failure with preserved ejection fraction

HFrEF	Heart failure with reduced ejection fraction
HR	Heart rate
HW	Heart weight
HFD	High fat diet
HEK293T	Human embryonic kidney 293T cells
ITT	Insulin tolerance test
IL-1β	Interleukin 1 beta
IL-6	Interleukin 6
IL-10	Interleukin 10
IRES	Internal ribosome entry site
ICLAS	the International Council of Laboratory Animal Science
i.p.	Intraperitoneal
i.v.	Intravenous
IVSs	Intraventricular septum in systole
LVEDD	Left ventricular end-diastolic diameter
LVESD	Left ventricular end-systolic diameter
LVIDd	Left ventricular internal diameter in diastole
LVIDs	Left ventricular internal diameter in systole
LVmass	Left ventricular mass
LVPWs	Left ventricular posterior wall in systole
LVpres	Left ventricular pressure
MMP2	Matrix metalloproteinase 2
MMP9	Matrix metalloproteinase 9
MMP13	Matrix metalloproteinase 13
MAP	Mean arterial pressure
mRNA	Messenger ribonucleic acid
OE-NPY$^{D\beta H}$	Mouse model overexpressing NPY under DβH promoter
MOI	Multiplicity of infection
α-MHC	Myosin heavy chain alpha
β-MHC	Myosin heavy chain beta
NPY	Neuropeptide Y
Npy1R	Neuropeptide Y Y1-receptor
Npy2R	Neuropeptide Y Y2-receptor
Npy5R	Neuropeptide Y Y5-receptor
NO	Nitric oxide
L-NNA	N-nitro-L-arginine; Nitric oxide synthase inhibitor
n.s.	Not significant
PGC-1α	Peroxisome proliferator-activated receptor gamma coactivator 1 alpha
PGC-1β	Peroxisome proliferator-activated receptor gamma coactivator 1 beta
PE	Phenylephrine

PBS	Phosphate-buffered saline
PLN	Phospholamban
PCR	Polymerase chain reaction
PET	Positron emission tomography
qNMR	Quantitative nuclear magnetic resonance
qPCR	Quantitative polymerase chain reaction
ROS	Reactive oxygen species
RNA	Ribonucleic acid
RyR2	Ryanodine receptor 2
SERCA2a	Sarcoplasmic reticulum Ca2+ ATPase
α-SMA	Smooth muscle actin alpha
SNP	Sodium nitroprusside
SEM	Standard error of the mean
STZ	Streptozotocin
SNS	Sympathetic nervous system
TL	Tibia length
TU/ml	Transducing units/ml
TGF-β1	Transforming growth factor beta 1
TNF-α	Tumor necrosis factor alpha
T2D	Type 2 diabetes
TH	Tyrosine hydroxylase
VEGF	Vascular endothelial growth factor
WD	Western type diet
WT	Wild-type
wo	Week old

List of Original Publications

This dissertation is based on the following original publications, which are referred to in the text by their Roman numerals:

I Mattila M, Koskenvuo J, Söderström M, Eerola K, Savontaus M. Intramyocardial Injection of Serca2a-Expressing Lentivirus Improves Myocardial Function in Doxorubicin-Induced Heart Failure. *The Journal of Gene Medicine*, 2016; 18: 124–33

II Mattila M, Söderström M, Ailanen L, Savontaus E, Savontaus M. The Effects of Neuropeptide Y Overexpression on the Mouse Model of Doxorubicin-Induced Cardiotoxicity. *Cardiovascular Toxicology*, 2020; 20: 328–33

III Ailanen L, Mattila M, Ruohonen ST, Ruohonen S, Rinne P, Vähätalo L, Penttinen AM, Söderström M, Savontaus M, Savontaus E. The Effects of Neuropeptide Y Overexpression and Diet-Induced Obesity on Cardiovascular Phenotype in Male Mice. *Manuscript*.

In addition, the thesis contains some unpublished data.

1 Introduction

Heart failure (HF) is, beyond question, a major health issue, in fact it is the leading global cause of morbidity and mortality (Oh*, et al.* 2019). The prevalence of HF is still increasing due to the ageing of the population, and it has been estimated that the total costs of HF will more than double by 2030 from the year 2012 (Heidenreich*, et al.* 2013). HF is a broad term for a large number of pathophysiological elements manifesting as a common syndrome; the failure to pump enough blood to meet the demand of the organs. Manifestations may appear at many levels; for example, structural abnormalities in myocardium or in the coronary arteries; functional abnormalities in valves or arrhythmias; triggered by circulating substances such as sympathetic nervous system transmitters, natriuretic peptides and cytokines as well as being driven by other factors such as toxic drugs, obesity and diabetes (Jessup & Brozena 2003). Hypertension, myocardial infarction and valvular heart disease are common causes of HF, each of them having their own pathophysiological mechanism. On the other hand, inflammation and toxic mechanisms impair the heart in rather different ways. Pathophysiological factors promote a process of left ventricular remodeling resulting in hypertrophy, interstitial fibrosis and/or dilatation, leading eventually to permanent deleterious effects on the heart (Jessup & Brozena 2003).

Despite advances in medical therapy and invasive procedures, the prognosis of advanced HF remains dismal. To discover more efficient treatment methods, there is a strong need to understand more profoundly the diverse pathophysiological mechanisms behind the processes leading to the different types of HF. In this thesis, the attention has been focused on two significant mechanisms in the regulation of the heart, calcium signaling and the sympathetic neurotransmitter, neuropeptide Y (NPY). In the cardiomyocyte, the action potential initiates the cascade of excitation–contraction coupling, and calcium cycling plays a key role in this process. It is essential for proper relaxation phase that the calcium released in the contraction phase is efficiently extruded from the cytosol. It is recognized that disturbances in calcium cycling are common in the damaged heart (Olson 2004). NPY takes part in a vast number of processes in the heart, such as excitation–contraction coupling and the modulation of calcium currents in cardiomyocytes. The main function of NPY is

neuronal modulation, but in addition, NPY exerts direct effects on the cardiac cells. Besides, NPY has been connected with several types of cardiovascular pathologies (McDermott & Bell 2007).

The studies in this thesis investigated both calcium signaling and NPY, as well as the potential of exploiting calcium cycling enhancing gene therapy in the framework of particular types of cardiac pathologies. First, doxorubicin (DOX) is one of the most efficient cytotoxic drugs used in clinical practice to treat various types of cancers. The main adverse effect of DOX is cardiotoxicity, leading to cardiomyopathy and HF. Furthermore, major epidemic-scale health challenges, obesity and type 2 diabetes, associate strongly with pathological changes in the heart, and eventually lead to HF, though the exact nature of these associations is not completely clear.

This work employs animal models and viral mediated gene therapy, which are useful tools in unravelling the underlying disease mechanisms and for assessing new treatment methods, since the initiation of clinical trials requires convincing evidence of efficacy and safety from preclinical research. With increasing knowledge, we are able to gain a deeper understanding about the molecular mechanisms behind HF and to help to clarify the possibilities of calcium cycling -targeted gene therapy.

2 Review of the Literature

2.1 Heart failure

The classic definition of HF describes it as the inability of the heart to provide sufficient perfusion to organs for filling the requirements of the body (Reddy & Borlaug 2016). Rather than a uniform disease, this inability emerges in the spectrum of symptoms, which create a common syndrome. HF is diagnosed by its symptoms, a physical examination and diagnostic testing of the patients, and the underlying causes consist of several pathophysiological factors and comorbidities complicating both diagnosis and treatment (Metra & Teerlink 2017, Snipelisky*, et al.* 2019). HF may emanate for example from defects in the myocardium, coronary arteries, pericardium, heart valves, conduction system, or from a combination of these defects (Mazurek & Jessup 2017, Snipelisky*, et al.* 2019). The HF syndrome is advancing; the activated neurohormonal regulation and an upregulated sympathetic nervous system (SNS) initially assist the heart to maintain cardiac output by boosting heart rate (HR) and stroke volume, but in the long term, these alterations permanently damage the heart (Mazurek & Jessup 2017).

Heart dysfunction has traditionally been categorized as systolic or diastolic HF, however, according to present knowledge, HF is classified as heart failure with reduced ejection fraction (HFrEF) or heart failure with preserved ejection fraction (HFpEF) (Reddy & Borlaug 2016). In HFrEF, a cardiac injury leads to the development of myocardial dysfunction, and via a worsening of symptoms, to the end-stage heart failure (Oh*, et al.* 2019). The concept of HFpEF still raises some differing opinions and it may have been previously considered less harmful than HFrEF. However, HFpEF may account for nearly half of all HF diagnoses (Carbone*, et al.* 2019). In HFpEF, a systemic proinflammatory state and the production of reactive oxygen species have been hypothesized to result in hypertrophy of myocytes, increased fibrosis, and decreased left ventricular capabilities (Oh*, et al.* 2019). Treatment of HFpEF has been challenging, and there are no evidence-based therapies which are shown to improve outcomes in HFpEF, probably due to the vast heterogeneity of the HFpEF syndrome (Reddy & Borlaug 2016, Metra & Teerlink 2017, Oh*, et al.* 2019).

The view about how HF should be treated has shifted over the course of time. Looking back from year 1989, the first treatments were based on increasing inotropy and decreasing preload. Next, reducing afterload was demonstrated to relieve symptoms and prolong life. This was followed by an understanding of the importance of relaxation and treating HF by increasing lusitropy. Thereafter, the next strategy was to preserve the failing heart by reducing preload, afterload and inotropy (Katz 1989). During the past three decades, as knowledge about the pathophysiology of HF has accumulated, the treatment of HF, utilizing medical therapy, coronary revascularization and device therapy, has advanced significantly (Reddy & Borlaug 2016, Mazurek & Jessup 2017). Nonetheless, HF is still one of the main causes of hospitalization in the elderly population (Mazurek & Jessup 2017).

2.2 Calcium cycling in the heart

The contraction–relaxation cycle of the heart is controlled by a delicate balance in the intracellular regulation of calcium concentration in cardiomyocytes. In excitation–contraction coupling, as a result of membrane depolarization, a small amount of calcium entering the cell through L-type Ca^{2+} channels triggers the co-operation with the ryanodine receptor 2 (RyR2) stimulating the release of a higher calcium amount from the sarcoplasmic reticulum (Fig. 1) (Hajjar*, et al.* 2000). In this process, the intracellular calcium concentration rises tenfold, from 0.1 μm to 1 μm (Gianni*, et al.* 2005). The elevated cytosolic calcium concentration facilitates the interaction between actin and myosin in myofibrils, resulting in contraction (MacLennan & Kranias 2003). In the relaxation phase, calcium is extruded from the cytosol to the extracellular space by Na/Ca^{2+} exchanger and Ca^{2+} ATPase, and reaccumulated in the sarcoplasmic reticulum by sarcoplasmic reticulum Ca^{2+} ATPase (SERCA2a) (Fig. 1). In mammals, sarcoplasmic calcium uptake is the dominant cytosolic calcium removal process (Bers 1997). Phospholamban (PLN), in its non-phosphorylated form, inhibits SERCA2a (James*, et al.* 1989).

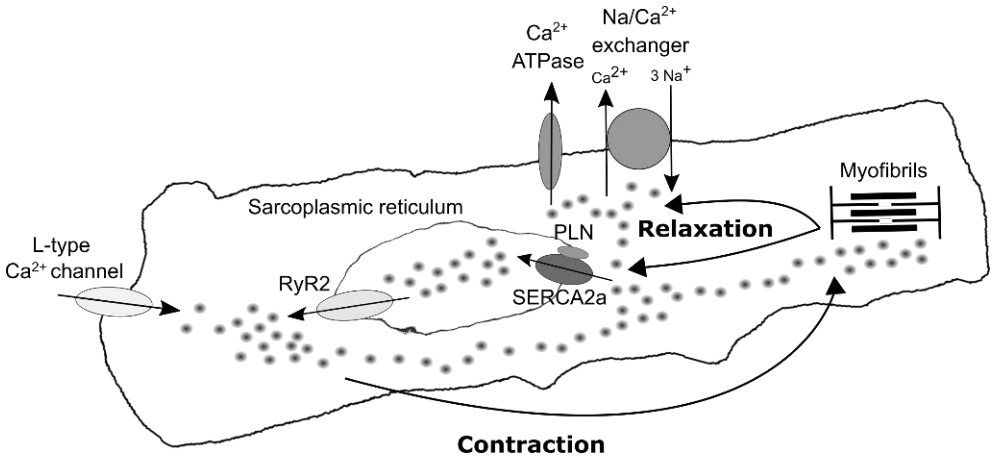

Figure 1. Calcium cycling in a cadiomyocyte. Calcium enters the cell through L-type Ca^{2+} channels and the ryanodine receptor 2 subsequently releases a greater amount of calcium from the sarcoplasmic reticulum, leading to contraction. During relaxation, calcium is reaccumulated into sarcoplasmic reticulum by SERCA2a and extruded from the cell by Na/Ca2+ exchanger and Ca2+ ATPase. Modified from Hajjar, et al. 2000, MacLennan 2003.

2.2.1 Sarcoplasmic reticulum Ca^{2+} ATPase 2a (SERCA2a)

2.2.1.1 General introduction

The mammalian genome harbors three different genes for SERCA; SERCA1*,* which is present in fast-twitching skeletal muscle, SERCA2, and SERCA3, which can be detected in several nonmuscle cell types (Gianni*, et al.* 2005). SERCA2 encodes a transcript for two separate isoforms, SERCA2a being expressed mainly in the cardiac muscle and SERCA2b in the smooth muscle (Martonosi & Pikula 2003).

The data available on the distribution of SERCA2a in the heart is scarce, and furthermore, the structure of SERCA2a remained a mystery until very recently when the first crystal structures, originating from pig heart, were published (Eisner*, et al.* 2017, Sitsel*, et al.* 2019). SERCA2a, a 125 kDa protein, consists of three cytoplasmic domains regulating ATP binding, autophosphorylation and dephosphorylation, and a transmembrane domain controlling Ca^{2+} binding and translocation. Several proteins regulate SERCA2a, including PLN, S100A and Sumo1, however, PLN is the main regulatory protein and the only one known to be directly involved in the development of cardiac disease (Federico*, et al.* 2019, Zhihao*, et al.* 2019).

2.2.1.2 The role of SERCA2a in calcium signaling and therapeutics

SERCA2a has a key role in extruding calcium from cytosol, albeit the proportion of extruded calcium varies between the Na/Ca^{2+} exchanger and SERCA2a in a species-dependent manner (Bers 1997). In rodents, SERCA2a extrudes approximately 90–92% of cytosolic calcium while in humans, the corresponding proportion is 76% (Milani-Nejad & Janssen 2014). Moreover, the process of excitation–contraction coupling relies not only on the properties and amplitude of calcium channels and transporters, but also on their appropriate synchronization and spatial arrangement (Eisner*, et al.* 2017, Gambardella*, et al.* 2018).

As first reported in 1987, abnormal calcium handling was found in patients with end-stage HF (Gwathmey*, et al.* 1987). This provided the first direct evidence about the role of calcium in the function of the heart. Since then, the central role of SERCA2a in the process of maintaining intracellular calcium homeostasis in the heart has been clearly demonstrated. Moreover, diminished SERCA2a expression and activity in both human and experimental animal models of HF have been demonstrated (Schmidt*, et al.* 1998, Hajjar*, et al.* 2000, Olson 2004). In a recent review, post-translational modifications in SERCA2a and in the other main modulators of calcium cycling, PLN and RyR2, were highlighted to play an important role in regulating calcium homeostasis (Federico*, et al.* 2019). At present, abnormal sarcoplasmic calcium handling in failing cardiomyocytes is seen as the primary defect that causes contractile dysfunction (Zima*, et al.* 2014).

At the turn of the millennium, enhancing sarcoplasmic calcium transport was seen as a potential therapeutic modality (Hajjar*, et al.* 2000). SERCA2a gene transfer was studied in several experimental animal HF models utilizing viral gene delivery vectors and the results were rather promising with regard to restoring SERCA2a expression and improving systolic and diastolic function in failing hearts (Miyamoto*, et al.* 2000, Sakata*, et al.* 2007, Kawase*, et al.* 2008, Niwano*, et al.* 2008, Prunier*, et al.* 2008). In the field of clinical research, a phase 2 SERCA2a-mediated CUPID trial (Calcium Upregulation by Percutaneous Administration of Gene Therapy in Cardiac Disease) in patients with advanced HF reported very favorable results (Jessup*, et al.* 2011, Zsebo*, et al.* 2014), but unfortunately the subsequent phase 2b trial was a major disappointment (Greenberg, *et al.* 2014, Greenberg, *et al.* 2016). Another phase 2 trial, AGENT-HF, was terminated prematurely because of the CUPID trial results, and again, no improvements had been evident in the small number of patients treated (Hulot*, et al.* 2017). These failures could well be attributed to either inefficient delivery route or too low dose of the viral vector, and not because of the SERCA2a product itself. The CUPID trial and several other gene therapy trials utilized antegrade coronary artery infusion to deliver the viral vectors (Jessup*, et al.* 2011, Shareef*, et al.* 2014, Hayward*, et al.* 2015). Further analysis revealed that the transduction rate of the SERCA2a gene was much lower in the CUPID phase 2b trial

than in the previous phase 2 trial. Inadequate delivery by intracoronary route and lower transduction efficiency possibly due to a change in the proportion of empty viral capsid as compared to phase 1 have been discussed as being the main factors behind the negative results (Mingozzi*, et al.* 2013, Greenberg, *et al.* 2016, Gabisonia & Recchia 2018, Ishikawa*, et al.* 2018). However, in these clinical trials, the SERCA2a gene transfer was confirmed to be safe and feasible.

2.3 Neuropeptide Y (NPY)

2.3.1 General introduction

NPY is a 36 amino acid neurotransmitter, first isolated in the early 1980s (Tatemoto 1982). NPY is expressed in the central nervous system, being one of the most abundant peptides in the brain (Hirsch & Zukowska 2012). In the peripheral SNS, NPY is co-localized and co-released with catecholamines (i.e. adrenaline and noradrenaline). NPY has a 92% sequence homology in cartilaginous fish and mammals, suggesting that it serves important roles in physiology (Hirsch & Zukowska 2012). NPY certainly participates in a vast number of biological processes e.g. cortical neural excitability, stress response, food intake, circadian rhythms, and cardiovascular function (Yi*, et al.* 2018). In the central nervous system, NPY is known to mediate an orexigenic effect. When administered as a long-term central infusion, NPY leads to obesity by increasing food intake, fostering lipogenesis in the liver and white adipose tissue, as well as increasing plasma insulin, corticosterone and triglyceride levels (Zarjevski*, et al.* 1993). In the SNS, NPY is released primarily in conditions of prolonged activation of the sympathetic nerves as in stress conditions (Kuo*, et al.* 2007). In the central nervous system, NPY inhibits excessive activation of the stress response, whereas, in the periphery, NPY has been shown to amplify the stress response (Hirsch & Zukowska 2012). NPY is widely expressed in the periphery in a vast number of tissues including the nerve fibers innervating blood vessels (Ekblad*, et al.* 1984) and the heart (Gu*, et al.* 1984). In the heart, NPY is the most abundant neuropeptide (McDermott & Bell 2007).

2.3.2 NPY receptors and role in heart

The effects of NPY are mediated via the six identified G protein-coupled receptor subtypes (Y1, Y2, “Y3”, Y4, Y5, and y6). Five of the receptors have been cloned from mammals (Y1, Y2, Y4, Y5, and y6), of which Y1, Y2, Y4 and Y5 are functional in humans and have been cloned from human tissues in 1992–1996 (Brothers & Wahlestedt 2010, Yi*, et al.* 2018). Receptors Y1, Y2 and Y5 mediate the main functional responses in the heart (McDermott & Bell 2007).

In the heart, NPY has been demonstrated to participate in an extensive number of processes affecting neuronal control, the excitation–contraction coupling and the contractility of ventricular cardiomyocytes as well as cellular growth and blood supply (Fig. 2) (McDermott & Bell 2007, Dvorakova*, et al.* 2014). The net effect of NPY-activated pathways varies or even can be opposite between distinct cell types (Tan*, et al.* 2018). Concerning the cardiovascular system, receptor Y1 modulates calcium transients and increases the intracellular Ca^{2+} level in both cardiomyocytes and ventricular endocardial endothelial cells leading to a positive inotropic effect (Heredia*, et al.* 2005, Jacques & Abdel Samad 2007, Jacques*, et al.* 2017). In vascular smooth muscle cells, the activation of Y1-receptor stimulates protein degradation and mitogenesis (Zhu, *et al.* 2015, Tan*, et al.* 2018). In addition, Y1-receptor activation contributes to the sympathetic stimulation that potentiates noradrenaline-induced vasoconstriction (Tan*, et al.* 2018). Receptor Y2 takes part in the crosstalk between sympathetic and parasympathetic neurotransmission. The Y2-receptor modulates noradrenaline and NPY secretion in the myocardium at the presynaptic level, and mediates slowing of the HR (McDermott & Bell 2007, Brothers & Wahlestedt 2010). In addition, activation of Y2-receptor is involved in promoting angiogenesis (McDermott & Bell 2007). In comparison to the other NPY receptors, the Y-receptor 5 contains an additional 100 amino acid sequence (Tan*, et al.* 2018). The Y5-receptor contributes to protein turnover, and it has been shown to function synergistically with the Y1-receptor to modulate vasomotion and mitogenesis, and to promote vascular angiogenesis and arteriogenesis with Y2-receptor (Fig. 2) (Brothers 2010, Tan 2018). Taken together, the effects of NPY in the heart are multifaceted and mediated via SNS or via a direct interaction with receptors in the target cells.

Since the 1980s, the role of NPY in the pathophysiology of the heart has been the focus of intensive study. NPY has been linked, via diverse mechanisms, in different types of cardiovascular diseases with some conflicting evidence (McDermott & Bell 2007, Dvorakova*, et al.* 2014, Tan*, et al.* 2018). There is a consensus that elevated plasma NPY levels do correlate with the severity of HF (Ullman*, et al.* 1994, Persson*, et al.* 2002, Cuculi*, et al.* 2013, Shanks & Herring 2013, Dvorakova*, et al.* 2014, Ajijola*, et al.* 2019).

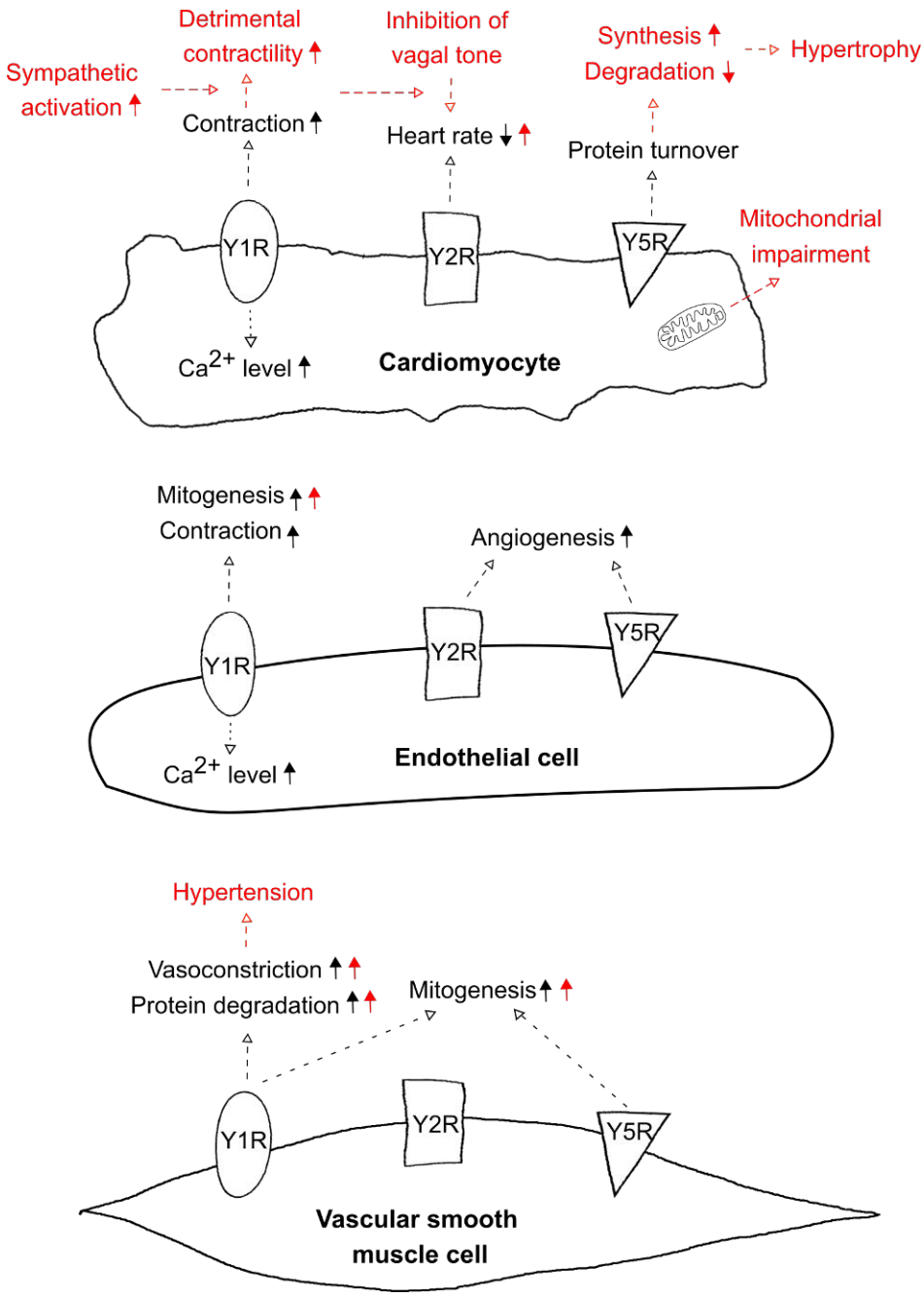

Figure 2. The physiological and pathophysiological role of neuropeptide Y in the heart. Neuropeptide Y acts in the heart via both the sympathetic nervous system and direct receptor signaling in a multifaceted way. Modified from McDermott 2007.

Deleterious effects of NPY in a compromised heart, marked with red colour in Fig. 2, include detrimental maintenance of contractile performance driven by increased sympathetic activity and inhibition of the vagally mediated parasympathetic response, together increasing HR (Ilebekk, *et al.* 2005, Tan, *et al.* 2018). Furthermore, the demonstrated direct unfavorable contribution of NPY involves also a reduced degradation and increased synthesis of proteins leading to an increased cardiac mass (Millar, *et al.* 1994, Bell, *et al.* 2002) and activation of cardiac fibroblasts promoting fibrosis (Zhu, *et al.* 2015). However, in vascular smooth muscle cells, the activation of receptor Y1 in pathological conditions has been reported to result in an elevated degradation of proteins (Tan, *et al.* 2018). The NPY-modulated remodeling effect in myocardial tissue may be beneficial in the short-term, but in the long run, it can lead to hypertrophy (McDermott & Bell 2007). In addition, NPY has been demonstrated to have an effect on cardiomyocyte mitochondria, impairing mitochondrial function and energy metabolism (Luo, *et al.* 2015, Hu, *et al.* 2017). At the receptor level, the gene expression of Y1 has been reported to decline in conjunction with the severity of hypertrophy while Y2 expression has been reported to increase in failing heart. These changes are believed to reflect a pathological role for Y1 in the development of cardiac hypertrophy and respectively, a compensatory role for Y2 as an angiogenic factor (Callanan, *et al.* 2007, Jacques & Abdel Samad 2007).

2.3.3 The model of transgenic NPY overexpression

The transgenic OE-NPY$^{D\beta H}$ mouse model, generated earlier in our laboratory, overexpresses *Npy* in the peripheral SNS system and in the noradrenergic system of the brain (Ruohonen, *et al.* 2008, Vähätalo, *et al.* 2015). In the OE-NPY$^{D\beta H}$ mouse model, *Npy* expression is driven under the dopamine-β-hydroxylase promoter (DβH) targeting the transgene expression to noradrenergic neurons with very little evidence for ectopic expression (Ruohonen, *et al.* 2008). A single nucleotide polymorphism NPY L7P, having highest allele frequencies in northern countries, has been recognized as a risk factor for type 2 diabetes and cardiovascular diseases (Pesonen 2008). The targeted overexpression of *Npy* in the OE-NPY$^{D\beta H}$ mouse model recapitulates situations of NPY excess in chronic mild stress and this kind of polymorphism of NPY in humans (Ruohonen, *et al.* 2012, Vähätalo, *et al.* 2016). Compared to normal wild-type (WT) mice, the homozygous OE-NPY$^{D\beta H}$ mice have been shown to express about a twofold elevated *Npy* level in the noradrenergic neurons of brain and a significantly higher expression in the adrenal glands (Vähätalo, *et al.* 2015). OE-NPY$^{D\beta H}$ mice have been shown to exhibit a metabolic syndrome -like phenotype with adult-onset obesity, dyslipidemia and impaired glucose tolerance (Ruohonen, *et al.* 2008, Vähätalo, *et al.* 2015, Vähätalo, *et al.*

2016). The mechanisms leading to OE-NPY$^{D\beta H}$ phenotype are mediated mainly via inhibition of adrenergic tone in metabolic tissues instead of NPY causing direct effects on adipose tissue and the liver (Vähätalo, *et al.* 2016). This is characterized by decreased expression of the rate-limiting enzyme in noradrenaline synthesis, tyrosine hydroxylase (*Th*) in the brain and the adrenal gland, changes in the expression of beta adrenergic receptor in the target tissue, and reduced urinary adrenaline levels (Ailanen, *et al.* 2017). In addition, the OE-NPY$^{D\beta H}$ mice have been shown to be more susceptible to endothelial damage-induced vascular wall hypertrophy, with an increased formation of the neointima (Ruohonen*, et al.* 2009).

2.4 Doxorubicin (DOX)

2.4.1 General introduction

Doxorubicin (DOX) is a member of the anthracycline family of drugs. It was first isolated in the early 1960s and incorporated into anticancer practice in the late 1960s. DOX is a nonselective class I agent and its principal mechanism of action is to inhibit topoisomerase I and II and interfere with the uncoiling of DNA, a process eventually resulting in programmed cell death (Tacar*, et al.* 2013). The efficacy of DOX was quickly noticed and it has been used to treat several types of cancers, including solid tumors, leukemia and lymphomas (Octavia*, et al.* 2012). The adverse effects include hematopoietic suppression, myelosuppression, nausea, vomiting, extravasation, alopecia and cardiotoxicity (Singal & Iliskovic 1998, Octavia*, et al.* 2012). In fact, the major limitation associated with the use of DOX is toxicity affecting the myocardium, leading to myocardial dysfunction, induction of dose-dependent cardiomyopathy and ultimately to congestive heart failure (Umlauf & Horký 2002, Chatterjee*, et al.* 2010, Renu*, et al.* 2018). DOX-induced toxicity may drive wall motion abnormalities and/or dilatation with HFpEF, though this may be a precursor state to HFrEF (Del Buono*, et al.* 2018). After treatment with DOX or its derivatives, cardiac complications will occur in about 10% of cancer patients within 10 years after the termination of the chemotherapy (Octavia*, et al.* 2012). In a recent registry study concerning various anticancer therapies, severe cardiotoxicity led to a 10-fold increase in total mortality when compared to patients with a milder form or without cardiotoxicity (Lopez-Sendon*, et al.* 2020). Among cancer survivors, anthracycline-induced heart disease has been shown to be a major cause of morbidity and mortality (Ghigo*, et al.* 2016). There are some strategies to reduce the adverse cardiovascular effects of DOX, such as modulating the dosage, liposomal formulation of DOX, administering erythropoietin due to apoptosis inhibition, or dexrazoxane due to free iron chelation, and utilizing beta-adrenergic antagonists or angiotensin-converting enzyme inhibitors (Octavia*, et al.* 2012, Wenningmann*, et al.* 2019, D'Oria*, et al.*

2020). Furthermore, synthetic flavonoids have been evaluated for their radical-scavenging and chelative properties with encouraging results (van Acker, *et al.* 2001, Octavia, *et al.* 2012). However, no prevention or complete treatment for the DOX-induced HF has been identified (Ghigo, *et al.* 2016). Nonetheless, DOX has still today a role in clinical practice as it is one of the most effective anticancer drugs ever developed.

2.4.2 Mechanism of DOX-induced cardiotoxicity

The knowledge of the causal mechanisms of DOX-induced cardiotoxicity still remains incomplete, however, in particular the cardiomyocytes might be susceptible to the long-term adverse effects as they do not regenerate to any significant extent (Kalyanaraman 2019). Putative mechanisms for cardiotoxicity include the formation of reactive oxygen species leading to oxidative stress, apoptosis, mitochondrial dysfunction and altered molecular signaling (Fig. 3) (Cappetta, *et al.* 2018). DOX-induced cardiotoxicity has been associated with increased SNS activity (Tong, *et al.* 1991, Bartoli, *et al.* 2011) as the increased reactive oxygen species level may elevate sympathetic tone (Renu, *et al.* 2018). Furthermore, reactive oxygen species activate matrix metalloproteinase enzymes that are responsible for the degradation of the extracellular matrix, which is an important platform for the cardiomyocytes to attach (D'Oria, *et al.* 2020). Oxidative stress might be a significant contributor in DOX-induced cardiotoxicity since the myocardium is a redox-sensitive target with an inadequate antioxidant defence mechanism (Kalyanaraman 2019, D'Oria, *et al.* 2020). Moreover, DOX and doxorubicinol, its metabolite formed in cardiac tissue, bind to the SERCA2a and alter its activity detrimentally (Fig. 3) (Hanna, *et al.* 2014). Furthermore, since it is more prone to damage than nuclear DNA, the disruption of mitochondrial DNA might play a significant role in developing HF (Chen, *et al.* 2019). DOX intercalates with DNA bases and mediates double-strand DNA breakage through blocking the activity of the topoisomerase II-beta (Fig. 3) (Renu, *et al.* 2018). In addition to decreasing the expression of SERCA2a and RyR2, DOX induces an inappropriate opening of the ryanodine receptors (Gambliel, *et al.* 2002, Octavia, *et al.* 2012, Tocchetti, *et al.* 2014).

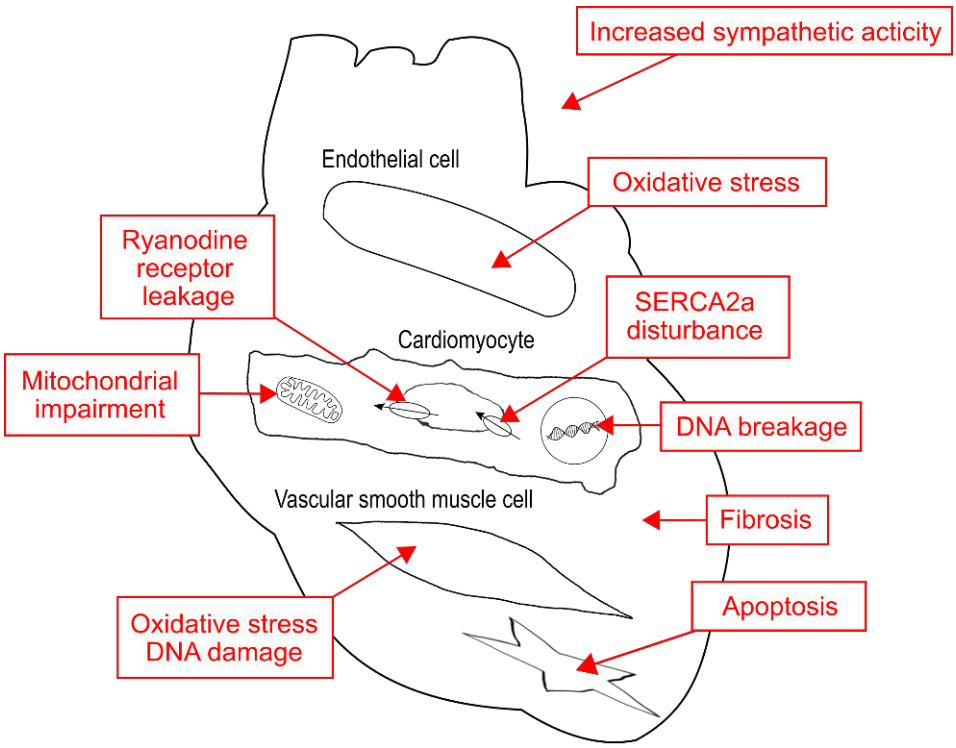

Figure 3. The effects of doxorubicin on the heart. Doxorubicin induces various pathological processes in the heart, including increased sympathetic activity, oxidative stress, damage in DNA, disturbances in calcium cycling and in mitochondria, and increased apoptosis and fibrosis. Modified from Cappetta et al. 2018.

2.4.3 The model of DOX-induced heart failure

DOX-induced HF has been studied in various experimental settings. The first mouse studies date back to the beginning of the current century. DOX has been typically administered by intraperitoneal injection (i.p.) either as one larger dose (usually 10–20 mg/kg) or as weekly dosing with the cumulative dose being in the same range. Furthermore, DOX-induced cardiotoxicity has been studied utilizing a vast number of genetically modified mouse models, seeking to unravel different aspects of cardiotoxicity, such as DOX metabolism, DNA damage, oxidative stress, apoptosis, necrosis, autophagy and mitophagy, as reviewed thoroughly by Chen *et al.* (2019). Here, the focus is limited to WT mouse models of HF. The characteristic findings of DOX-induced cardiotoxicity include repressed cardiac function, increased fibrosis and apoptosis, and decreased survival. In addition, numerous genes have been shown to be either upregulated or downregulated by DOX. The effects of DOX-induced cardiotoxicity on WT mice heart are summarized in Table 1.

Table 1. Doxorubicin-induced cardiotoxic effects on the heart of wild-type mice.

Dose + Strain	Functional changes	Other changes	Reference
20 mg/kg single i.p. Male C57BL/6J/129S6	Day 9: EF, FS ↓ LVEDD, LVESD ↑	Day 9: weight, survival ↓ Day 18: necrosis ↑	Olson, *et al.* 2003
20 mg/kg single i.p. Male C57BL/6	Day 5: FS ↓ LVEDD LVESD ↑	Day 5: apoptosis, cytokine production ↑ survival ↓	Nozaki *et al.* 2004
20 mg/kg single i.p. Male Balb/c	Day 6: FS, LVEDD ↓	Day 7: BW, survival ↓ apoptosis, myofibrillar loss ↑	Li *et al*. 2006
20 mg/kg single i.p. 4 mg/kg / week x 5 Male C57BL/6	Day 5: EF, FS, LVIDd ↓ Week 12/16: EF, FS ↓ LVIDd, LVIDs ↑	Day 1: apoptosis ↑ 6/12/16 weeks: survival ↓	Neilan *et al.* 2006
20 mg/kg single i.p. C57BL/10ScSn	Day 5: EF, LVpres ↓	TNF-α, apoptosis ↑	Riad*, et al.* 2008
15 mg/kg single i.p. Male C57BL/6		Day 2: *α-Mhc,Bnp,Serca2a* ↓ Day 28: HW/BW ↑ survival ↓	Ito*, et al*. 2009
18 mg/kg single i.p. Balb/c		Day 8: BW, HW/BW, survival ↓ Day 14: myofibrillar loss ↑	Zhu, *et al.* 2010
12/15/18 mg/kg single i.p. Balb/c		Day 7: IL-1β ↑ myofibrillar disorganization ↑	Zhu, *et al.* 2011
5 mg/kg / week x 5 i.p. 129/SvJae		Week 5: *Pgc-1α, Pgc-1β* ↑ ROS level, fibrosis ↑	Zhang, *et al.* 2012
3 mg/kg / week x 4 i.p. Male Balb/c		Week 4: BW, HW, HW/BW ↓ ROS level ↑	Chen *et al*. 2015
15 mg/kg single i.p. FWB	Day 6: FS ↓ LVEDD, LVESD ↑	LVmass/BW ↑ SERCA2a, PGC-1α ↓	Ge *et al*. 2016
6 mg/kg single i.p. Male C57BL/6	Day 10/20: N: EF n.s. OW: EF ↓ LVEDD ↑		Guenancia*,* *et al.* 2016
10 mg/kg D1+D4 i.p. Male C57BL/6	Day 8: EF, FS ↓ LVIDs ↑	ROS, apoptosis ↑ PGC-1α ↓	Liu*, et al.* 2018
4 mg/kg / week x 3 i.p. Male C57BL/6N	Week 8: n.s.	Week 3: BW, HW ↓ *Anp* ↑	Matsumura *et al*. 2018
20 mg/kg single i.p. C57BL/6J	Day 7: EF, FS ↓	BW, HW/TL ↓ β-MHC, ANP ↑	Willis*, et al.* 2019

ANP: Atrial natriuretic peptide; BW: Body weight; BNP: Brain natriuretic peptide; EF: Ejection fraction; FS: Fraction shortening; HW: Heart weight; IL-1β: Interleukin 1 beta; i.p.: Intraperitoneal; LVEDD: Left ventricular end-diastolic diameter; LVESD: Left ventricular end-systolic diameter; LVIDd: Left ventricular internal diameter in diastole; LVIDs: Left ventricular internal diameter in systole; LVmass: Left ventricular mass; LVpres: left ventricular pressure; α-MHC: Myosin heavy chain alpha; β-MHC: Myosin heavy chain beta; N: normal; n.s.: not significant; OW: overweight; PGC-1α: Peroxisome proliferator activated receptor gamma coactivator 1 alpha; PGC-1β: Peroxisome proliferator activated receptor gamma coactivator 1 beta; ROS: Reactive oxygen species; TNF-α: Tumor necrosis factor alpha.

2.5 Obesity and type 2 diabetes

2.5.1 General introduction

Overweight and obesity, conditions which influence harmfully on human health throughout the world, have reached a global epidemic scale as over one billion people worldwide are overweight (body mass index; BMI between 25 and 29.9 kg/m^2) or obese (BMI over 30 kg/m^2) (Singh*, et al.* 2018, Carbone*, et al.* 2020). This is alarming as obesity increases the risk of cardiovascular and metabolic diseases (Carbone*, et al.* 2020). Obesity may lead to hypertension, diabetes, HF, and major cardiovascular events (De Lorenzo*, et al.* 2019). According to the World Health Organization, in 2016, a significant proportion i.e. 39% of adults aged 18 years and over, were overweight, and 13% were obese (https://www.who.int/news-room/fact-sheets/detail/obesity-and-overweight, accessed April 26, 2020). The link between obesity and HF is notable, as depending on the demographics of the study, the proportion of HF patients being overweight or obese tends to be rather high, with percentages reaching 40% and 49%, respectively (Zhai & Haddad 2017, Horwich*, et al.* 2018). Obesity and metabolic syndrome are HFpEF-associated pathologies as the prevalence of overweight and obesity is over 80% in HF patients with HFpEF (Reddy & Borlaug 2016, Horwich*, et al.* 2018). Nonetheless, the overweight and mild to moderate obese patients diagnosed with HF may exhibit considerably improved survival as compared to normal weight patients (Horwich*, et al.* 2018). This phenomenon called the obesity paradox still remains unresolved though the increased lean mass and higher cardiorespiratory fitness in obese individuals may play a role in their improved prognosis of HF (Carbone*, et al.* 2020). Moreover, one explanation might be that obese patients are diagnosed earlier in life, thus explaining the improved prognosis (Turer*, et al.* 2012, Elagizi*, et al.* 2018).

Obesity associates strongly with the development of type 2 diabetes (T2D) (Zhai & Haddad 2017). The prevalence of T2D is increasing universally e.g. it has doubled over the last two decades driven by the obesity epidemic (Bugger & Abel 2014, Athithan*, et al.* 2019). T2D is now recognized as a global pandemic as it is included into the top ten causes of mortality and morbidity and in global terms, it represents a major medical and economic burden on the health services (Singh*, et al.* 2018, Athithan*, et al.* 2019). T2D accounts for 90-95% of all diabetes mellitus cases and it is a multifactorial metabolic disorder characterized by insulin resistance, impaired insulin secretion and elevated hepatic glucose production and release leading to chronic hyperglycemia (Singh*, et al.* 2018, Athithan*, et al.* 2019, Kenny & Abel 2019).

In numerous studies, diabetes has been shown to be a cardiovascular risk factor, with the cardiovascular complications representing the major cause of mortality and morbidity in diabetic patients (Bugger & Abel 2014). Diabetes accelerates atherosclerosis leading to coronary artery disease, and additionally evokes deleterious effects on the heart. The structural, functional and metabolic myocardial changes may lead to HF, which is the most common cardiovascular complication encountered in diabetes (Singh*, et al.* 2018, Athithan*, et al.* 2019, Evangelista*, et al.* 2019). The exact association of diabetes and HF is rather unclear but the relationship is bidirectional as it leads to an increased HF risk for diabetes patients and, conversely, diabetes worsens the HF outcome (Evangelista*, et al.* 2019). The Framingham study, started in 1974, was the first to identify the role of diabetes in HF; the risk of HF in diabetes patients was found to increase by twofold in men and by fivefold in women compared with age-matched controls (Kannel*, et al.* 1974). In the general population, the prevalence of diabetes is 10-15% whereas in hospitalized HF patients, the prevalence rises up to 44%, (Evangelista*, et al.* 2019, Kenny & Abel 2019).

2.5.2 Pathological role of obesity and type 2 diabetes in the heart

The precise mechanisms by which obesity induces HF are not entirely understood. Nevertheless, it is known that a western diet can further contribute to the activation of proinflammatory pathways, and obesity is also associated with alterations in hemodynamics, cardiac structure and neurohumoral regulation (Abel*, et al.* 2008, Carbone*, et al.* 2019). The obesity driven changes in the heart include left ventricle dilation, remodeling and hypertrophy, and furthermore, increased left ventricular end-diastolic pressure, right atrial pressure and pulmonary wedge pressure (Fig. 4) (Abel*, et al.* 2008, Lavie*, et al.* 2018, Carbone*, et al.* 2019). Moreover, weight gain is connected with increased blood pressure, resulting in arterial hypertension, which is a leading cause of HF (Carbone*, et al.* 2019). In obesity, increased SNS activity is a key mechanism for hypertension. Furthermore, suppressed parasympathetic activity is also associated with hypertension, and accounts for the elevated HR in obese humans (Hall*, et al.* 2015). In addition, obesity promotes insulin resistance, subsequently evolving into hyperglycemia (Turer*, et al.* 2012, Zhai & Haddad 2017).

The diabetes-associated changes in myocardial structure and function, called diabetic cardiomyopathy, were identified in 1972 (Rubler*, et al.* 1972). Diabetic cardiomyopathy has been recently defined by AHA (the American Heart Association), ESC (the European Society of Cardiology) and EASD (the European Association for the Study of Diabetes) as a clinical condition of ventricular dysfunction that occurs in the absence of coronary atherosclerosis and hypertension

in patients with diabetes (Evangelista, *et al.* 2019). At present, diabetic cardiomyopathy is considered as a progressive condition from an asymptomatic subclinical period advancing via hypertrophy to diastolic dysfunction, and finally to systolic dysfunction (Athithan, *et al.* 2019, Murtaza, *et al.* 2019). The diabetes-associated changes interfering with the heart and impairing cardiac function include altered lipid metabolism creating lipotoxicity, hyperglycemia, increased oxidative stress, mitochondrial disturbance, endothelial dysfunction, fibrosis, and increased stiffness (Fig. 4) (Poornima, *et al.* 2006, Abel, *et al.* 2008, Turer, *et al.* 2012, Bugger & Abel 2014, Singh, *et al.* 2018, Athithan, *et al.* 2019, Evangelista, *et al.* 2019). There is accumulating information that malfunctions in metabolic pathways play a role in developing diabetic cardimyopathy. Previous studies have revealed the role of calcium homeostasis as a relevant factor in diabetic cardiomyopathy, with data pointing to reduced SERCA2a expression, increased PLN expression, and ryanodine receptor defects leading to elevated resting Ca^{2+} levels in cytosol, and diastolic dysfunction (Fig. 4) (Poornima, *et al.* 2006, Pereira, *et al.* 2014, Singh, *et al.* 2018, Dillmann 2019). An excess of glycolytic intermediates, related to diabetic cardiomyopathy, has been shown to reduce SERCA2a expression (Young, *et al.* 2002). In addition, acute hyperglycemia may be responsible for diastolic Ca^{2+} leakage from sarcoplasmic reticulum in cardiomyocytes via RyR2 (Pereira, *et al.* 2014). Furthermore, in diabetes patients, oxidative damage impacting on the heart impairs the vulnerable RyR channels (Murtaza, *et al.* 2019). A recent review raises the phosphorylation of RyR2 and the subsequent increase of sarcoplasmic reticulum Ca^{2+} leakage as the main disturbance of Ca^{2+} handling in the prediabetic heart (Federico, *et al.* 2019). In the CUPID trial (introduced in section 2.2.1.2), almost half of the patients had diabetes, highlighting the connection between HF and diabetes, and the relevance of calcium signaling (Dillmann 2019).

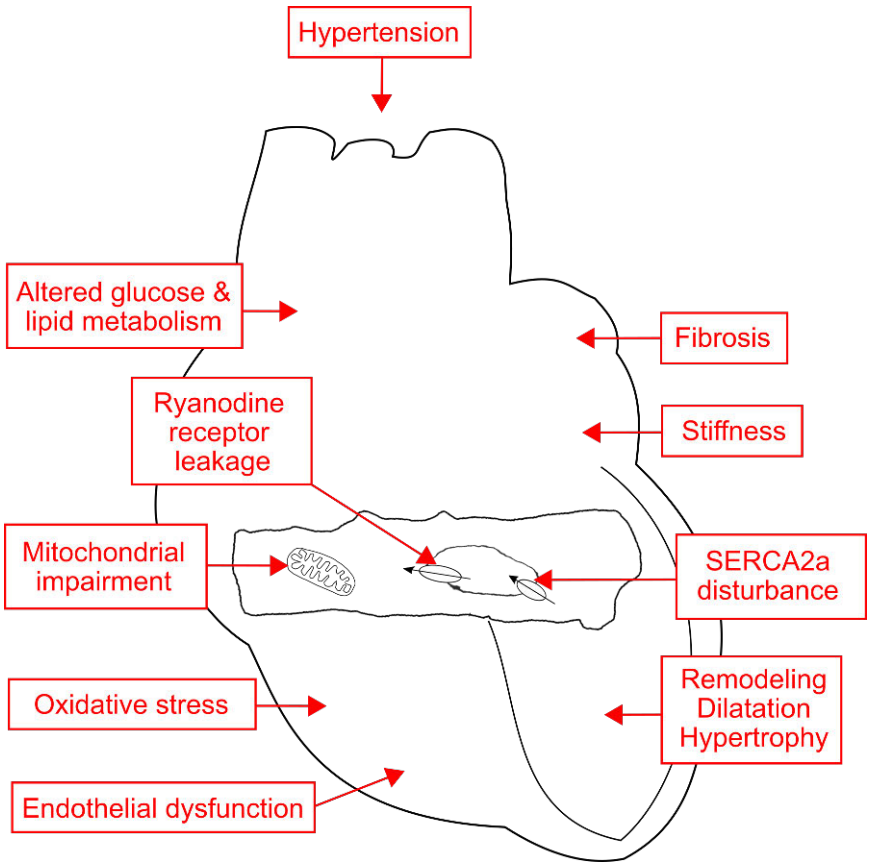

Figure 4. The effects of obesity and type 2 diabetes on the heart. Obesity and type 2 diabetes cause various detrimental changes impairing the heart including hypertension, lipotoxicity, hyperglycemia, oxidative stress, disturbances in mitochondria and calcium cycling, remodeling of the left ventricle and increased stiffness followed from increased fibrosis and endothelial dysfunction.

2.5.3 The models of obesity and type 2 diabetes

Obesity and T2D are most often studied using a mouse model of diet-induced obesity (DIO) or using monogenic mice, commonly ob/ob mice (Fuchs, *et al.* 2018). The ob/ob mouse model harbors a mutation in the leptin gene, resulting in a non-functional protein and hypoleptinemic mice have a nearly 3-fold higher weight than a normal mouse (da Silva Xavier & Hodson 2018). The ob/ob mouse model has played an important role in unraveling the key position of leptin in energy homeostasis, although the relevance of this mouse model for human obesity is not clear (da Silva Xavier & Hodson 2018).

The DIO mice exhibit many features of gradually developing human obesity, including the slowly advancing weight gain and the progression of insulin resistance

(Kleinert, *et al.* 2018). The feeding of the mice for 1-20 weeks with high fat diet (HFD) containing 40-60% of calories from fat seems to be the most widely used animal model for studying obesity (da Silva Xavier & Hodson 2018). Generally, male mice develop obesity in a shorter time and to a greater extent than female mice, indicating that male mice are more prone to DIO (Kleinert, *et al.* 2018). As well as obesity, the DIO mice usually exhibit hypertension, hyperglycemia, and hyperinsulinemia (da Silva Xavier & Hodson 2018). However, there is no single, standardized diet utilized to induce obesity, and the variation in nutrient compositions and energy densities, as well as the differences between separate mouse strains, lead to phenotype differences in DIO models (Barrett, *et al.* 2016). For example, the strain C57BL/6J is prone to develop severe obesity, elevated adiposity, glucose intolerance and moderate insulin resistance while the C57BL/6N mice have been found to develop hepatosteatosis, hyperglycaemia and hyper-insulinaemia (Kleinert, *et al.* 2018).

To model a more progressed state of T2D, a low dose streptozotocin (STZ) can be utilized as an additional stressor (Heydemann 2016). STZ is a cytotoxic glucose analogue targeting primarily pancreatic β-cells, having a damaging effect on their mitochondrial and genomic DNA; this eventually triggers a partial loss of β-cells, resulting in decreased insulin secretion (da Silva Xavier & Hodson 2018, Kleinert, *et al.* 2018). A common method is to combine DIO with the administration of a low dose STZ to recapitulate the transition from the pre-diabetic state to the actual state of T2D (Kleinert, *et al.* 2018).

Concerning cardiac effects, there are many discrepancies between different studies as some investigators have identified cardiomyopathy after a relatively short period of HFD whereas other do not report cardiomyopathy despite feeding HFD for over 6 months (Heydemann 2016). The effects of HFD-fed DIO model and STZ-induced T2D model on the mouse heart are summarized in Table 2.

Table 2. Cardiotoxic effects on the heart of wild-type mice in diet-induced obesity and streptozotocin-induced type 2 diabetic model.

Model	Functional changes	Other changes	Reference
HFD 16 months male C57BL/6	IVSs, LVPWs ↑	HW, HW/TL ↑ *β-Mhc*, *Col I* ↑ hypertrophy ↑	Calligaris, *et al.* 2013
HFD 20 weeks male FVB	FS ↓ LVESD, LVEDD ↑	HW, HW/TL ↑ hypertrophy ↑	Liang, *et al.* 2015
HFD 12 weeks male C57BL/6J	EF, FS ↓ LVESD, LVEDD ↑	HW, HW/BW ↑	Zhang, Y., *et al.* 2015
HFD 5 months 4–6 wo C57BL/6	FS ↓	IL-6, TNFα ↑ fibrosis ↑	Cao, *et al.* 2016
HFD 30 weeks 9 mo C57BL/6		*Bnp* ↑ cell area, fibrosis ↑	Lucas, *et al.* 2016
HFD 36 weeks 6 wo male C57BL/6J		Week 51: *Tnf-α, Tgf-β1* ↑ *Mmp9, Col1a1* ↑ fibrosis ↑	Daltro, *et al.* 2017
HFD 12 weeks 44 wo male C57BL/6J		cell size ↓ fibrosis ↑ cell−cell spaces ↑	Hung, *et al.* 2017
HFD 16 weeks 10 wo C57BL/6	EF, FS ↓ IVSs, LVPWs ↑	*Anp, Bnp, Tnf-α, IL-6, IL-1β* ↑ disorganized myofibers, collagen deposition ↑	Wang, *et al.* 2017
HFD 12 weeks 10 wo male CL57/B6		BW ↑ TNF-α, IL-10 ↑ fibrosis ↑	Kondo, *et al.* 2018
HFD 16 weeks (+ control viral injection) C57BL/6J	EF, FS ↓ LVESD, LVEDD ↑	BW ↑ *Tgf-β1*, C*ol I&III* ↑ collagen deposition ↑	Li, *et al.* 2018
HFD 6 weeks → STZ 80 mg/kg single i.p. 4 wo male C57BL/6	EF, FS ↓ LVESD, LVEDD ↑	HW, HW/BW ↑ TGF-β1, COL I&III ↑ hypertrophy, fibrosis ↑	Huang, *et al.* 2017
HFD 4w → 40mg/kg STZ for 5d → HFD 4w Male Mm. castaneus 4–6 wo		8 w: BW ↓ *Anp* ↑ hypertrophy, fibrosis ↑	Zhang, *et al.* 2018
HFD 8 weeks → STZ 120 mg/kg single i.p. 8–10 wo male	EF ↓	HW/BW ↑ *Tnf-α, IL-1β* ↑	Feng, *et al.* 2019
HFD 12 weeks → STZ 100 mg/kg single i.p. → HFD 12/24 weeks 8 wo male C57BL/6	EF, FS ↓	*Anp* ↑ TNF-α, PGC-1α, COL1A1 ↑ hypertrophy, fibrosis ↑	Sun, *et al.* 2020

ANP: Atrial natriuretic peptide; BNP: Brain natriuretic peptide; BW: Body weight; COL I: Collagen I; COL1A1: Collagen 1A1; COL III: Collagen III; EF: Ejection fraction; FS: Fraction shortening; HW: Heart weight; HFD: High fat diet; IL-1β: Interleukin 1 beta; IL-6: Interleukin 6; IL-10: Interleukin 10; i.p.: Intraperitoneal; IVSs: Intraventricular septum in systole; LVEDD: Left ventricular end-diastolic diameter; LVESD: Left ventricular end-systolic diameter; LVPWs: Left ventricular posterior wall in systole; MMP9: Matrix metalloproteinase 9; β-MHC: Myosin heavy chain beta; PGC-1α: Peroxisome proliferator activated -receptor gamma coactivator 1α alpha; STZ: Streptozotocin; TL: Tibia length; TGF-β1: Transforming growth factor beta 1, TNF-α: Tumor necrosis factor alpha; wo: week old.

2.6 Gene therapy

2.6.1 General introduction

The first attempts to treat patients with genetic disease using foreign DNA were recorded at the beginning of 1970s (Friedmann & Roblin 1972). By 1990, the technological advances had enabled the cloning of disease-related genes and efficient transfer of genes into mammalian cells, however, there were still no clinically useful applications for genetic modifications (Friedmann 1990). At the turn of the millennium, clinical trials utilizing gene therapy typically were targeted to treat common polygenic diseases such as cancer, atherosclerosis and Alzheimer's disease, and, on the other hand to rare and well defined genetic disorders such as cystic fibrosis and Duchenne muscular dystrophy (Selkirk 2004). By 2013, the field had developed with over 1800 approved gene therapy clinical trials (Wirth*, et al.* 2013), and according to the most recent data from September 2019, there were over 3000 registered clinical trials with the main indications being cancer, monogenic, infectious and cardiovascular diseases (http://www.abedia.com/wiley/indications.php, accessed April 10, 2020).

The methods to deliver transgene into the target tissue can be divided into non-viral and viral approaches. Non-viral vectors, for example, plasmid DNA, may enable high organ specificity, but they are able to achieve only a relatively low transduction efficiency and short-lasting gene expression (Muller*, et al.* 2007). Viral vectors are capable of a much more efficient delivery of the transgene, however, the immunogenic response limits the feasibility of adenovirus and adeno-associated virus (AAV) as approximately 97% of the population carry neutralizing antibodies against adenoviral vectors and against AAV the proportion is up to 40% (Muller*, et al.* 2007, Tilemann*, et al.* 2012). Due to neutralizing antibodies, adenoviral gene therapy has been demonstrated to lack long-lasting efficacy (Bradshaw & Baker 2013). The AAV vector has been shown to be safe, well-tolerated, longer lasting and less immunogenic than the adenovirus, although the host immune system may still be triggered (Naso*, et al.* 2017). Retroviruses, integrating the transgene complex into the host genome are capable of offering a lifetime expression of the transgene, but with the cost of a potential for insertional mutagenesis. The development of safer, lentiviral vectors has reduced the risk of insertional mutagenesis (Hayward*, et al.* 2015, High & Roncarolo 2019). The triggering of guaranteed long-term transgene expression and the lack of neutralizing antibodies make lentivirus an appealing vector choice (Tilemann*, et al.* 2012). Recently, two clinical trials, utilizing lentivirus reported the safety and benefits of lentiviral gene therapy, and the use of lentiviral vectors seems to be increasing (Hayward*, et al.* 2015). In 2019, adenovirus, AAV, retrovirus, and lentivirus together accounted for approximately 54% of gene

therapy trials while naked plasmid were being utilized in 15% of trials (http://www.abedia.com/wiley/vectors.php, accessed April 10, 2020). In the future, the creation of a gene transfer vector, which would enable the regulation of the transgene expression in a fine tuned manner by an external stimulus, would be a significant advance (Yla-Herttuala & Baker 2017).

The process of developing more efficient and safer vectors for gene transfer is a complex path and the utilization of preclinical animal models is one of the crucial steps towards success in clinical trials. Gene therapy is an area holding great promise, yet clinical trials have so far failed to provide large scale consistent results and the cost of successful therapies has been high (Yla-Herttuala 2017a, Gabisonia & Recchia 2018). Several clinical gene therapy trials have displayed promising results, including β-thalassemia in 2010, X-linked severe combined immunodeficiency (SCID-X1) in 2010, and hemophilia B in 2011 (Wirth*, et al.* 2013). In recent years, there have been some real success stories emerging from the clinical trials. In 2012, the first gene therapy product, AAV directed to lipoprotein lipase deficiency, was approved by EMA (the European Medicines Agency), followed by e.g. retroviral *ex vivo* gene therapy for adenosine deaminase-deficient SCID in 2016 and AAV directed to retinal dystrophy in 2018 (Yla-Herttuala & Baker 2017, High & Roncarolo 2019).

2.6.2 Cardiac gene therapy

Although there have been significant developments in the field of treating HF with pharmacological drugs, nevertheless, current treatment methods are clearly not sufficient (Wolfram & Donahue 2013, Shareef*, et al.* 2014). At the end of the 20th century, gene therapy became viewed as an intriguing prospective future method for treating HF (Chien*, et al.* 1997, Hajjar*, et al.* 2000). Since then, the prospects to employ gene therapy in the cardiovascular field have been extensively studied. Finally, during the recent five years, significant conceptual progress has been achieved as well in this field of gene therapy (Yla-Herttuala & Baker 2017).

The choice which vector to administer in cardiac gene therapy is important; besides adenovirus and AAV, lentivirus may represent an applicable option, as cardiomyocytes are virtually nonproliferative, limiting the safety risk posed by potential oncogenic transformation (Tilemann*, et al.* 2012). However, lentivirus has been reported to have a low cardiac transduction efficiency as compared to adenovirus and AAV, but on the other hand, lentivirus did not affect negatively cardiac function, whereas adenovirus led to dilatation and systolic dysfunction, and AAV led to diastolic dysfunction in mouse heart (Wolfram & Donahue 2013, Merentie*, et al.* 2016).

In vivo methods to deliver the gene therapy vector to the heart include an antegrade intracoronary infusion, an antegrade infusion with coronary artery balloon occlusion, a closed loop recirculation method, retrograde infusion through the coronary sinus, pericardial injection, and direct myocardial injection (Hayward*, et al.* 2015, Ishikawa*, et al.* 2018). Antegrade coronary artery infusion is considered to be a safe percutaneous gene delivery method and the recent gene therapy trials have used this route to deliver the viral vectors, but unfortunately, the viral transduction efficacy has been shown to be limited (Shareef*, et al.* 2014, Hayward*, et al.* 2015). Direct intramyocardial injection results in a high local concentration of the viral vector owing to an endothelial bypass, and allows minimal distribution of vector to off-target organs (Shareef*, et al.* 2014). However, with intramyocardial injection, the coverage of areas that can be reached by injection is limited in human patients (Ishikawa*, et al.* 2018). The needle track may cover 1/8 of the left ventricular wall in mouse, but only 1/200 of the human ventricular wall (Yla-Herttuala 2017b). In the human heart, the best transduction efficiency achieved with any given method is typically 10%-20% (Yla-Herttuala & Baker 2017). A peripheral intravenous injection and a vector selectively transducing only cardiomyocytes would be an ideal delivery choice, but it is a complicated equation in humans as their large blood volume causes a dilutional effect and, in addition, viruses may infect non-target organs (Hayward*, et al.* 2015). In general, regarding large animals, the greater transgene efficiency is associated with higher invasiveness, and therefore the balance between the efficacy and the safety needs to be considered depending on the gene of the interest, the patient population, and the desired transgene distribution (Ishikawa*, et al.* 2018).

In a recent review, Ylä-Herttuala discussed an important topic – pharmacological aspects in gene therapy. Low dose or inefficient delivery to the target cells may cause a failure. Beyond the classical ADME (Absorption, Distribution, Metabolism, Excretion) parameters, in gene therapy, STED (Spreading through and reaching appropriate cells in the target tissue, Transduction efficiency, Expression strength in the transduced cells, Duration of gene expression) parameters may be more useful in optimizing the therapeutic response (Yla-Herttuala 2017b). Furthermore, the translation from animal models to clinical trials may be challenging due to simpler preclinical models with quantifiable endpoints for therapeutic response, compared to more variable disease process with functional and, additionally, subjective goals for improvement in clinical trials (Lahteenvuo & Yla-Herttuala 2017). Moreover, the restoration of myocardial force and contractility is a feasible target in patients with the early stage of HF, however, in more severe HF conditions, increased fibrosis, apoptosis and arrhythmias pose severe difficulties for any therapy to cure (Yla-Herttuala & Baker 2017).

Today, there are still many issues to be resolved, including physiologic target validation of the myocyte, optimal strategies for gene target manipulation, vector selection, correct vector dose, as well as an efficient and safe delivery route suitable for the clinic, before gene therapy will be ready to be implemented (Fargnoli*, et al.* 2017, Ishikawa*, et al.* 2018). One innovation is to target gene therapy precisely to the most appropriate areas of myocardium using electromechanical mapping together with radiowater positron emission tomography (PET) imaging, a method called NOGA mapping (Hassinen*, et al.* 2016). So far, the majority of gene therapy trials have aimed at increasing blood flow to ischaemic tissue by therapeutic angiogenesis e.g. utilizing vascular endothelial growth factor (VEGF), and fibroblast growth factor (FGF), however, research interest has broadened from solely protein-coding genes towards oligonucleotides and RNA regulation, especially in the field of vascular therapy (Lahteenvuo & Yla-Herttuala 2017, Yla-Herttuala & Baker 2017). In the future, gene therapy is anticipated to represent a new horizon for, inter alia, myocardial protection, repair and regeneration (Ginn*, et al.* 2018). It is unclear whether the clinical trials have failed because of technical problems or because of failures in the pharmacological properties of transgene products (Yla-Herttuala & Baker 2017). However, after some struggles in the past, there have been also successes in clinical trials in the cardiovascular field. A trial utilizing an adenoviral NOGA-mediated intramyocardial gene transfer of VEGF reported safe and well-tolerated gene transfer and increased myocardial perfusion in refractory angina patients (Hartikainen*, et al.* 2017).

3 Aims of the study

The aim of this thesis was to investigate selected mouse models of heart failure to gain a better understanding of the molecular and functional changes in pathological processes of heart failure, focusing on calcium signaling and neuropeptide Y. The experimental heart failure models studied were doxorubicin-induced cardiotoxicity, diet-induced obesity and type 2 diabetes. Furthermore, this thesis aimed at studying the potential of the lentiviral gene therapy vector as a way of enhancing the calcium cycling in a model of heart failure.

The specific aims were:

1. To set up a doxorubicin-induced mouse model of heart failure.
2. To produce a lentiviral vector expressing SERCA2a, to confirm the expressed protein product, and to validate the *in vivo* integration of the transgene carried by the gene delivery vector.
3. To evaluate the therapeutic potential of the SERCA2a-expressing lentiviral vector in the doxorubicin-induced heart failure model.
4. To study the effects of transgenic neuropeptide Y overexpression in the doxorubicin-induced heart failure model.
5. To assess the effects of transgenic neuropeptide Y overexpression in the diet-induced obesity and type 2 diabetes model.

4 Materials and Methods

4.1 Animals

Male C57BL/6N WT mice (Harlan, Horst, The Netherlands) were used in Study I. Male homozygous transgenic OE-NPY$^{D\beta H}$ from homozygous breeders, and WT mice from WT breeders originating from the same heterozygous breedings maintained on a C57BL/6N inbred background were used in Studies II and III. Mice were housed in the Central Animal Laboratory of University of Turku, individually in a ventilated cage system (Scanbur, Karlslunde, Denmark) at 22±1°C (Studies I & II) or group-housed at 21±3ºC (Study III), under a fixed 12:12 h dark/light cycle with free access to water *ad libitum* and regular chow feed (irradiated standard pellets) unless stated otherwise in the dietary *in vivo* intervention of Study III (see section 4.2.1.3).

4.1.1 Ethical aspects

Animal care was in accordance with the guidelines of the International Council of Laboratory Animal Science (ICLAS). The experimental procedures were approved by the National Animal Experimental Board (Eläinkoelautakunta, ELLA). The studies were designed and performed according to ethical 3R's (Reduction, Replacement, Refinement) principles. The sample size was minimized to a number of mice sufficient to detect statistically significant and physiologically relevant differences. Excessive stress and suffering of the mice were avoided and the welfare of the mice was monitored during the experiments via their weight gain, food intake and visual condition. Any mice showing signs of serious illness were removed from the study.

4.2 *In vivo* interventions

4.2.1 Heart failure models

4.2.1.1 DOX-induced heart failure model (I & II)

Cardiac toxicity was induced by doxorubicin (Caelyx 2 mg/ml; Janssen Pharmaceutica NV, Geel, Belgium) which was administered to mice as a single intraperitoneal injection at a dose of 20 mg/kg. The well-being of the mice was monitored carefully after DOX injection. The protocol to induce cardiotoxicity by DOX was based on earlier comparable studies (Nozaki*, et al.* 2004, Li, *et al.* 2006, Neilan*, et al.* 2006). Cardiotoxicity was assessed by monitoring weight, body composition, gene and protein expression, and by echocardiography.

4.2.1.2 OE-NPY$^{D\beta H}$ transgene model (II & III)

The generation of the transgenic OE-NPY^{DBH} mouse model has been described in detail by Ruohonen *et al.* (2008) and Vähätalo *et al.* (2015). This mouse model overexpresses NPY in noradrenergic neurons in the brain and also in the peripheral sympathetic nerves via the dopamine-beta-hydroxylase (DβH) gene promoter. OE-NPY^{DBH} mice has been shown to exhibit increased fat mass and body weight, which cause impairments of glucose metabolism and hyperinsulinaemia with age (Vähätalo, *et al.* 2015). To verify that the current cohorts resampled the previously published cohorts, body weight, body composition (Studies II & III) and blood glucose measured with a glucose meter (Precision Xtra Glucose Monitoring Device, Abbott Diabetes Care, Abbot Park, IL, USA) (Study III) were used as markers of the metabolic phenotype.

4.2.1.3 Diet-induced obesity and type 2 diabetes models (III)

For DIO, mice were placed on high caloric Western type diet (WD) containing 40% kcal fat, 43% kcal carbohydrate, 17% kcal protein (D12079B, Research Diets, New Brunswick, NJ, USA) for 12–15 weeks. To induce type 2 diabetes (i.e. insulin resistance and hypoinsulinemia), WD-fed mice were administered low-dose of STZ intraperitoneally (40 mg/kg in 7.5 mg/ml Na-Citrate solution, pH 4.5, Sigma-Aldrich, St. Louis, MO, USA) for 3 consecutive days. A single dose of STZ was re-administered every 4.5 weeks to maintain hyperglycemia (Gilbert*, et al.* 2011).

4.2.2 Lentiviral vectors (I)

4.2.2.1 Generation and analysis of lentiviral vectors (I)

The human SERCA2a gene and green fluorescent protein (GFP) reporter gene containing lentiviral vector (LV-SERCA2a-GFP) and the control vector containing GFP gene (LV-GFP) were constructed. The human SERCA2a cDNA was subcloned into a bicistronic pWPI plasmid (Tronolab, Écolé Polytechnique Fédérale de Lausanne, Switzerland) allowing simultaneous expression of the SEFCA2a gene and the GFP gene. Subsequently, the lentiviral construct plasmid pWPI, the packaging plasmid pR8.91, and the envelope coding plasmid pMD2G were co-transfected by using the calcium phosphate protocol into human embryonic kidney 293T (HEK293T) cells cultured in Dulbecco's modified Eagle's medium supplemented with 10 % fetal bovine serum, 2 mM L-glutamine, non-essential amino acids and 100 U/ml penicillin/streptomycin. The cells were incubated at 37°C with 5% CO_2. Supernatant containing viral particles were harvested at 24 and 48 h after transfection, centrifuged at 2300 g for 5 min at 4°C, filtered through a 0.45 μm filter (Millipore, Bedford, MA, USA) and concentrated using ultracentrifugation settings of 130000 g for 2 h at 4°C. The viral pellet was resuspended in cold phosphate-buffered saline (PBS) (Sigma-Aldrich, St Louis, MO, USA) and stored frozen at -150°C. The viral vector titers (transducing units/ml, TU/ml) were analyzed by flow cytometry based on the relative amounts of infected, GFP-expressing cells in a diluted series of transduction on HEK293T cells. The cells were fixed for 15 min in 4% paraformaldehyde. The flow cytometry analysis was performed at the Turku Centre for Biotechnology Cell Imaging Core facility on a LSRII machine using Cyflogic FACS analysis software (CyFlo Ltd, Turku, Finland).

4.2.2.2 Lentiviral injection (I)

Prior to the lentivirus injection, mice were anesthetized by inhalation of 4.5% isoflurane with anaesthesia maintained by 1.5% isoflurane. The mice were immobilized on a warm plate, and HR, respiration rate and body temperature were monitored. The intramyocardial injections were performed via 30-gauge needle using a 50-μl syringe (Hamilton, Reno, NV, USA) and micromanipulator (VisualSonics, Toronto, Canada). Injections were visualized by ultrasound and documented as video clips. A total volume of 30 μl (3 × 10 μl) was injected at a dose of LV-SERCA2a-GFP 1.39×10^8 TU/ml and LV-GFP 9.18×10^8 TU/ml to three distinct areas in the anterior wall of the left ventricle. Saline injection was performed as a sham control procedure.

4.3 *In vivo* and *ex vivo* methods

4.3.1 Body composition (II & III)

Body composition (fat and lean mass) was measured with an EchoMRI-700 quantitative nuclear magnetic resonance (qNMR) whole body composition analyzer (Echo Medical Systems, Houston, TX) from conscious mice. Each animal was scanned twice in order to minimize the error caused by the minor movements of the animal. Average values for fat mass and lean mass, and fat and lean mass percentage relative to body weight were calculated from two separate scans. The weight of the mice was recorded once a week during the study.

4.3.2 Echocardiography (I–III)

Echocardiography was performed with the VisualSonics Vevo 2100 ultrasound system (VisualSonics, Toronto, Canada) equipped with a 30-MHz transducer. Mice were anesthetized by inhalation of 4.5% isoflurane. Anaesthesia was maintained by 1.5% isoflurane (Studies I & III) or by 1.5–2.5% isoflurane gating the HR between 400 and 500 beats per minute (Study II). Chemical hair remover (Veet; Reckitt Benckiser, Slough, UK) was rubbed onto the chests of the mice and gel (Eco Supergel; Ceracarta, Forlì, Italy) was applied before the placement of the probe. The mice were kept on a heating pad to maintain normothermia. HR, respiration rate and body temperature were monitored. Functional parameters and the dimensions of the left ventricle, and HR were analyzed in a short-axis view (Studies II & III) and, additionally, in a parasternal long-axis view (Study I) using VisualSonics Vevo 2100 software version 1.2.0 (VisualSonics, Toronto, Canada).

4.3.3 Hemodynamic measurements (III)

The hemodynamic properties were studied *in vivo* in conscious freely moving mice conducting carotid artery measurements via radiotelemetry as previously described by Rinne *et al.* (2008). Briefly, mice were anesthetized with 2% isoflurane and a polyethylene catheter was inserted into the left carotid artery and the transmitter probe was positioned subcutaneously on the flank of the animal. Mean arterial pressure (MAP) and HR were monitored. To assess the control of the autonomic nervous system on the hemodynamics, the response to sympathetic activation was studied by injecting mice with different doses of phenylephrine (PE, 2-32 µg/kg, i.v.) and to study the parasympathetic activity, the anticholinergic drug, atropine, was administered (2 mg/kg, i.p.).

4.3.4 Vascular reactivity analysis (III)

Wire micromyography was conducted *ex vivo* as previously described by Rinne *et al.* (2013). Briefly, mouse thoracic aortae and small mesenteric arteries were excised and arterial rings were mounted in a microvessel myograph for isometric tension recording. When assessing vasoconstrictor responses, concentration-response curves to PE were constructed. To invoke endothelium-dependent or endothelium-independent relaxation, cumulative doses of either acetylcholine (ACh) or sodium nitroprusside (SNP) were added to the chambers, respectively. Vasorelaxation was studied in arterial rings precontracted with PE. The contribution of vasodilator nitric oxide (NO) to ACh-induced relaxation was determined by the inhibitory effect of a nitric oxide synthase inhibitor L-NNA (100 μM).

4.3.5 Tissue collection & sample preparation (I–III)

In Study I, the mice were sedated with CO_2 before blood collection and sacrificed by cervical dislocation. In Studies II and III, a terminal blood sample (0.5–1 ml) was collected by heart puncture or from the inferior vena cava. Prior to terminal blood sampling, the mice were anesthetized with inhaled isoflurane (induction 4.5%, maintenance 1.5%) (Study II) or, after a 4 h fast, with ketamine (75 mg/kg i.p. Ketaminol, Intervet Oy, Finland) combined with medetomidine (1 mg/kg i.p. Cepetor, ScanVet Oy, Finland) (Study III).

In Study I, the hearts were snap-frozen in liquid nitrogen immediately after collection and stored at -70°C or fixed for 24 hours in 4% paraformaldehyde and subsequently transferred to 70% ethanol and embedded in paraffin. In Study II, the hearts were cut in half after which the apex of the heart was frozen in liquid nitrogen immediately after collection, stored at -70°C and used later for RNA extraction, and the base of the heart was fixed for 24 hours in 4% paraformaldehyde and subsequently transferred to 70% ethanol and embedded in paraffin. In Study III, the hearts were halved and the apex of the heart was fixed for 24 hours in 10% formalin and subsequently transferred to 70% ethanol and embedded in paraffin. The base of the heart was stored for 24 hours in 4°C RNA Stabilization Reagent (RNAlater, Qiagen, Hilden, Germany) and subsequently transferred to -70°C. In addition, in Study II, the tibia was collected and its length was recorded.

4.3.6 Histology (I–III)

The frozen sections (8 μm) were prepared and transferred onto Superfrost plus slides (O. Kindler GmbH, Freiburg im Breisgau, Germany) and mounted (Study I) with VectaShield Hard Set Mounting Medium with DAPI (Vector Laboratories, Inc., Burlingame, CA, USA). Paraffin sections (5 μm) were prepared and the sections

were transferred onto Superfrost plus slides (O. Kindler GmbH, Germany). The paraffin sections were stained with hematoxylin and eosin as well as with Van Gieson's staining. In Study I, the sections were photographed using a microscope (frozen sections: Axiovert 200M, Carl Zeiss, Oberkochen, Germany; paraffin sections: BX60l, Olympus, Tokyo, Japan). In Study II, the sections were scanned using a Pannoramic 250F Flash III SlideScanner (3dHistech, Hungary) and in Study III using a Pannoramic 1000P slide scanner (3dHistech, Hungary). In Study I, the myocardial wall thickness was measured from the paraffin sections by assessing eight measuring points in the left ventricle. In addition, the sections were evaluated for tissue damage by a pathologist. In Studies II and III, myocardial degeneration, inflammation, fibrosis and nuclear atypia were analyzed and scored by two observers, a pathologist and the primary investigator. Histological scoring was carried out blinded as to the other investigator and to the treatment status of the mice. Myocardial degeneration, inflammation, fibrosis and nuclear atypia were scored on a scale from 0 to 3. In case of discrepancy, the investigators evaluated the samples together to gain consensus.

4.4 *In vivo* study design

The protocols for Studies I-III are described in Fig. 5. In Study I, DOX (n=14) or PBS (n=6) was administered to 9–11 week old WT mice as a single intraperitoneal injection. The mice were sacrificed on day 28 and the serum and the hearts were collected for analysis. For the gene transfer experiment, DOX was administered to 9–11 week old WT mice as a single intraperitoneal injection and the subsequent intramyocardial lentiviral injections (LV-SERCA2a-GFP/LV-GFP) or PBS (n=7/group) were performed under echocardiography surveillance two days later. The mice were weighed weekly, and echocardiography control was conducted and the mice were sacrificed 6 weeks after intramyocardial injection.

In Study II, DOX or saline was administered to 8–10 week old OE-NPY$^{D\beta H}$ and WT mice (n =7–9/group) as a single intraperitoneal injection. The mice were weighed weekly, and the body composition of the mice was measured on week 0 and 6 by qNMR. On week 6, cardiac structure and function were analyzed by echocardiography and the mice were sacrificed.

In Study III, OE-NPY$^{D\beta H}$ and WT mice were fed either with a chow diet (lean state) or with WD. To induce DIO or T2D, mice were fed with WD for 14 weeks starting at the age of 5 weeks, or for 16 weeks starting at age of 13 weeks, respectively. To induce T2D, 3 weeks after starting the WD, mice were administered STZ on 3 consecutive days and a single dose of STZ was re-administered every 4.5 weeks to maintain hyperglycemia. The mice were weighed weekly and the body composition was measured with qNMR at 9 weeks of age in lean state mice, and in

DIO mice, 5 and 11 weeks after induction of DIO (at 10 and 16 weeks of age). Echocardiography was conducted at the age of 18 weeks for both the lean and DIO state mice. 24 hour urine samples were collected in metabolic cages at the age of 19 weeks. The vascular reactivity was measured *ex vivo* by wire myography in lean and DIO mice (age 20 weeks, n=9–10/group). In addition, a cohort of T2D mice was included in wire myography (n=7/group), and their blood vessels were collected at 13 weeks after the induction of hyperglycemia. The hemodynamic properties in lean or DIO state were studied with a different cohort of mice utilizing radiotelemetry and, in addition, using PE or atropine.

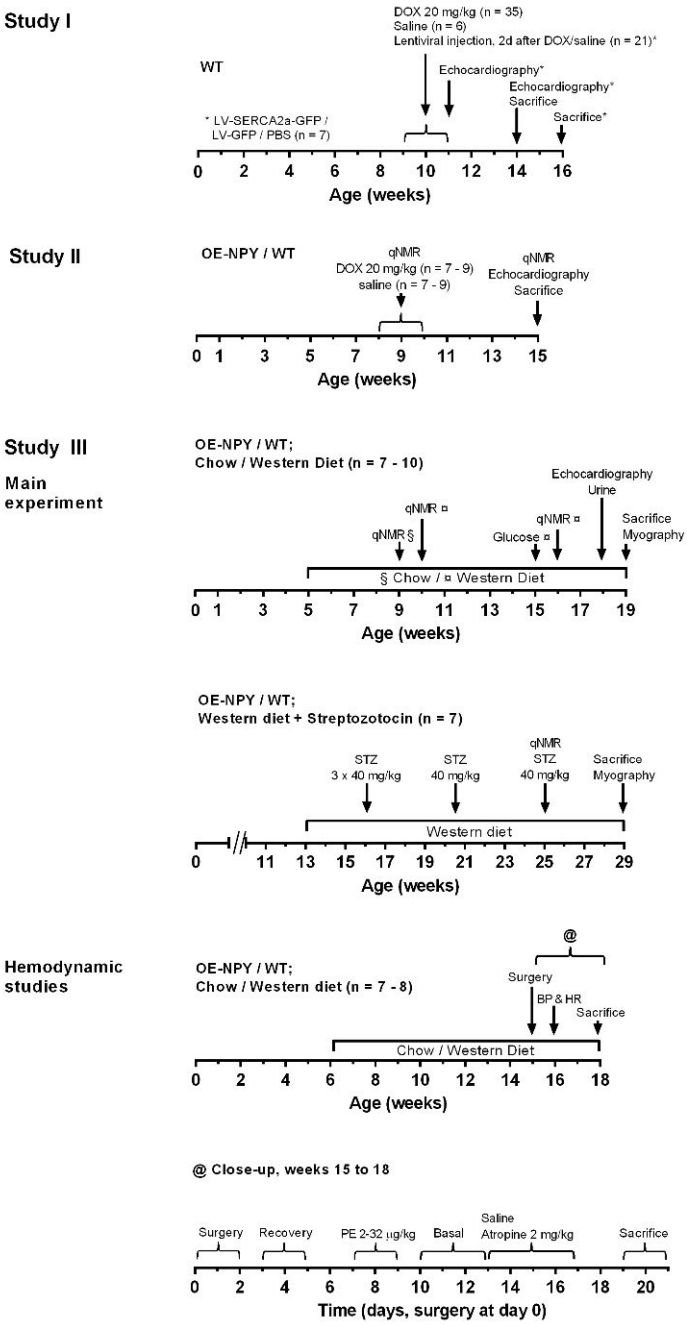

Figure 5. Experimental protocols of the interventions in Studies I-III. Wild-type (WT) mice (Studies I-III) and OE-NPY$^{D\beta H}$ (OE-NPY) mice (Studies II & III) were used. Mice were subjected to doxorubicin (DOX) in Studies I and II and to lentiviral injection in Study I. In Study III, mice consumed normal chow diet or a Western Diet (WD) and, additionally, WD-fed mice were administered a low dose of streptozotocin (STZ). BP = Blood pressure, HR = Heart rate, qNMR = Body composition measurement.

4.5 Biochemical analyses

4.5.1 Brain natriuretic peptide assay (I)

In the measurement of brain natriuretic peptide (BNP) levels, the serum was separated from the blood sample with Capiject T-MG serum collection tubes (Terumo, Tokyo, Japan). The sample was incubated for 20 minutes at room temperature prior to centrifugation (3000 g for 90 seconds). Serum was extracted from the collection tube, frozen in liquid nitrogen and stored at -80°C. BNP levels were determined with Brain Natriuretic Peptide EIA Kit (Sigma-Aldrich, St Louis, MO, USA) adhering to the manufacturer's instructions.

4.5.2 Biochemical markers in the urine (III)

After 24 hour of habituation to metabolic cages, 24 hour urine samples were collected. Noradrenaline was extracted with activated alumina and analyzed with high performance liquid chromatography and coulometric electrochemical detection. NO metabolites levels in urine were measured with commercially available colorimetric assay kit (Cayman Chemical, Ann Arbor, Michigan, USA).

4.5.3 Protein expression analysis (I)

HEK293T cells were infected with LV-SERCA2a-GFP lentiviral vector with a multiplicity of infection (MOI) of 2, 5 and 10. After 48 hours, uninfected control cells were counted (750 000 cell / well) and infected cells were lysed in a sample buffer. The samples were boiled for 5 minutes at 95°C and sodium dodecylsulfate-polyacrylamide gel electrophoresis was performed with a 6% separating gel for 2 hour at 110 V. The run samples were transferred onto polyvinylidene fluoride membranes by electroblotting for 1 hour at 400 mA. The membranes were blocked with 5% milk in PBS-Tween 20 for 1 hour and incubated overnight at 4°C in 2.5 ml of antibody working dilution (1 µl of Anti-SERCA2 ATPase Monoclonal Antibody, clone IID8; Thermo Scientific, Waltham, MA, USA). Horseradish peroxidase conjugated goat anti-mouse antibody 0.1 µg/ml working dilution (Dako, Glostrup, Denmark) was added onto the membranes and incubated for 50 minutes at room temperature. Light reaction was initiated by adding 4 ml of ECL mix (Pierce ECL Western Blotting Substrate; Thermo Scientific, Massachusetts, USA) onto the membranes which were then incubated for 2 minutes at RT, with X-ray film being exposed to the light reaction in the dark.

Proteins were extracted from mice heart by disrupting the tissue in RIPA buffer (radioimmunoprecipitation assay buffer, supplemented with protease and

phosphatase inhibitors cocktail) with Ultra-Turrax T25 Homogenizer (IKA®-Werke GmbH & Co. KG, Germany), transferring the solution to a shaker at 250 rpm 4°C for 1 hour and centrifuging 12 000 rpm 4°C for 20 minutes. Western blotting was conducted as described above using a dilution of 1:1000 polyclonal anti-SERCA2a antibody (sc-8095; Santa Cruz Biotechnology, Dallas, TX, USA) and a dilution of 1:10 000 horseradish peroxidase conjugated donkey anti-goat antibody. Actin was probed with a dilution of 1:5000 anti-actin antibody (A2066; Sigma-Aldrich, Missouri, USA) and a dilution of 1:20 000 horseradish peroxidase conjugated goat anti-rabbit antibody dilution. The membranes were imaged with LAS-3000 Imager (Fuji Photo Film Co., Tokyo, Japan). Images were quantified with ImageJ (National Institutes of Health, Bethesda, MD, USA) and normalized to mean control values.

4.5.4 Gene expression analysis (I–III)

RNA was extracted from frozen heart tissue with RNeasy mini kit including DNase treatment (Qiagen, Hilden, Germany) according to the manufacturer's instructions. The total RNA concentration and purity were determined with BioSpec-nano Microvolume UV-Vis Spectrophotometer (Shimadzu Scientific Instruments Columbia, MD, USA). Total RNA was transcribed to cDNA with High Capacity RNA-to-cDNA Kit (Applied Biosystems, Foster City, CA, USA) according to the manufacturer's instructions.

In Study I, reverse transcriptase polymerase chain reaction (PCR) was conducted using Pfu polymerase enzyme with an annealing temperature of 58°C, running 35 cycles and visualizing the product in 2.5% agarose gel with ethidium bromide. The list of the primers used in PCR analysis is presented in Table 3. In Studies II and III, quantitative reverse transcriptase PCR (qPCR) was performed using the SYBR Green method with Kapa Sybr Fast qPCR Kit (Kapa Biosystems, Woburn, MA, USA) and Applied Biosystems 7300 Real-Time PCR system according to the manufacturer's instructions for qPCR. Target gene expression was normalized to housekeeping gene, ribosomal protein S29, expression and the fold induction was calculated using the comparative ΔCt method and presented as relative transcript levels ($2^{-\Delta\Delta Ct}$). The list of the primers used in qPCR analysis is presented in Table 3.

Table 3. Primer sequences used in gene expression analyses.

Gene name	Sequence	Study
Adrenergic receptor, beta 1; *Adrb1* (*Beta1R*)	F: 5'-GTGGGTAACGTGCTGGTGAT -3' R: 5'-GAAGTCCAGAGCTCGCAGAA-3'	II
Atrial natriuretic peptide; *Nppa* (*Anp*)	F: 5'-GCTTCCAGGCCATATTGGAG-3 R: 5'-GGGGGCATGACCTCATCTT-3'	II
Brain natriuretic peptide; *Nppb* (*Bnp*)	F: 5'-CTGAAGGTGCTGTCCCAGAT-3' R: 5'-CCTTGGTCCTTCAAGAGCTG-3'	II, III
Collagen I alpha 2; *Col1a2*	F: 5′-TGCAGTAACTTCGTGCCTAGC-3′ R: 5′-ACGTGGTCCTCTGTCTCCA-3′	III
Green fluorescent protein; *GFP*	F: 5′-GTTCAGCGTGTCCGGCGAGG-3′ R: 5′-TCGGGGTAGCGGCTGAAGCA-3′	I
Interleukin 1 beta; *Il1b* (*Il-1β*)	F: 5'-TGTAATGAAAGACGGCACACC-3' R: 5'-TCTTCTTTGGGTATTGCTTGG-3'	II
Matrix metalloproteinase 2; *Mmp2*	F: 5'-GATGTCGCCCCTAAAACAGAC-3' R: 5'-CAGCCATAGAAAGTGTTCAGGT-3'	II
Matrix metalloproteinase 9; *Mmp9*	F: 5'-CTGGACAGCCAGACACTAAAG-3' R: 5'-CTGGCGGCAAGTCTTCAGAG-3'	II
Matrix metalloproteinase 13; *Mmp13*	F: 5'-ATCCCTTGATGCCATTACCA-3' R: 5'-AAGAGCTCAGCCTCAACCTG-3'	II
Myosin heavy chain alpha; *Myh6* (*Mhc-α*)	F: 5'-CCACTTCTCCTTGGTCCACTATG-3' R: 5'-ACAAACCCACCACCGTCTCA-3'	II
Myosin heavy chain beta; *Myh7* (*Mhc-β*)	F: 5'-AGGGTGGCAAAGTCACTGCT-3' R: 5'-CATCACCTGGTCCTCCTTCA-3'	II
Neuropeptide Y; *Npy*	F: 5'-CTCCGCTCTGCGACACTAC-3' R: 5'-GGAAGGGTCTTCAAGCCTTGT-3'	II, III
Peroxisome proliferative activated receptor gamma coactivator 1 alpha; *Ppargc1* (*Pgc-1α*)	F: 5'-TATGGAGTGACATAGAGTGTGCT-3' R: 5'-CCACTTCAATCCACCCAGAAAG-3'	II, III
Phospholamban; *Pln*	F: 5'-CACTGTGACGATCACCGAAG-3' R: 5'-CAGCATCTCGTTTCGCATTA-3'	II
Ribosomal protein S29; *Rps29* (*S29*)	F: 5'-ATGGGTCACCAGCAGCTCTA-3' R: 5'-AGCCTATGTCCTTCGCGTACT-3'	II, III
Ryanodine receptor 2; *RyR2*	F: 5'-CAGCATCTCGTTTCGCATTA-3' R: 5'-GGCTGTGTTCCACCTTCAAT-3'	II
Sarcoplasmic reticulum Ca2+ ATPase; *Atp2a2* (*Serca2a*)	F: 5′-GAGAACGCTCACACAAAGACC-3′ R: 5′-CAATTCGTTGGAGCCCCAT-3′	I
Serca2a	F: 5'-GAGAACGCTCACACAAAGACC-3' R: 5'-CTTCTTCAGCCGGCAATTCGTTG-3'	II
SERCA2a (Human)	F: 5′-GAACTCAACCCCTCCGCCCAGC-3′ R: 5′-ATTGCCCGCCCCTCCTCAACG-3′	I
Smooth muscle actin alpha; *Acta2* (*α-Sma*)	F: 5'-AGATTGTGCGCGACATCAAAG-3' R: 5'-GCAGACTCCATACCGATAAAGGA-3'	II
Transforming growth factor beta 1; *Tgfb1* (*Tgf-β1*)	F: 5'-TGGAGCAACATGTGGAACTC-3' R: 5'-CAGCAGCCGGTTACCAAG-3'	II, III
Tumor necrosis factor alpha*; Tnf* (*Tnf-α*)	F: 5'-CTGAACTTCGGGGTGATCGG-3' R: 5'-GGCTTGTCACTCGAATTTTGAGA-3'	II
Tyrosine hydroxylase; *Th*	F: 5'-CCCAAGGGCTTCAGAAGAG-3' R: 5'-GGGCATCCTCGATGAGACT-3'	II
NPY Y1 receptor; *Npy1R*	F: 5'-TCACAGGCTGTCTTACACGACT-3' R: 5'-TTTCTCCTTTTCAAGCGAATG-3'	II
NPY Y5 receptor; *Npy5R*	F: 5'-CAGATTAATCCAGCTGTTCTGC-3' R: 5'-GAAAACAGCCTTTATTTGACAATG-3'	II

4.6 Statistical analyses

GraphPad Prism 6 software (La Jolla, USA) was used in the statistical analyses. Statistical significance was accepted at the level of $P < 0.05$. Data are presented as the mean of absolute values, or as the mean percentage change of parameters over time ± standard error of the mean (SEM).

In Study I, normality of the populations and statistical significances were determined using the Kolmogorov–Smirnov test (a test which compares the observed distribution of two groups) or Student's t-test, respectively. In Study II, statistical significances were determined with unpaired Student's t-test, with two-way ANOVA using NPY overexpression and DOX as independent variables, or with ANOVA for repeated measures. In two-way ANOVA, multiple comparisons were analyzed and corrected with Bonferroni or Tukey post-hoc tests when the P-value for interaction of genotype and treatment effect was < 0.1. In study III, statistical significances were determined with two-way ANOVA using NPY overexpression and DIO as independent variables, with ANOVA for repeated measures, or with Students t-test. In two-way ANOVA, multiple comparisons were analyzed and corrected with Sidak or Bonferroni post-hoc test when the p-value for interaction of the genotype and diet effect was < 0.1.

5 Results and discussion

5.1 The effects of DOX-induced cardiotoxicity (Studies I & II)

5.1.1 Weight and body composition

In Study I, DOX decreased the weight of the WT mice (Fig. 6A, B). In Study II, DOX treatment resulted in a milder response (Fig. 6C), nevertheless, weight gain over time was significantly decreased in both WT and OE-NPY$^{D\beta H}$ mice (Fig. 6D), and cumulative weight gain and fat mass gain were significantly decreased when the genotypes were analyzed together (Fig. 6E, G). Lean mass gain was significantly decreased by DOX only in the OE-NPY$^{D\beta H}$ mice (Fig. 6F). In addition, DOX treatment tended to decrease the weight of the heart (P=0.061) and heart/tibia ratio (P=0.073) when the genotypes were analyzed together (Table 4). In summary, the weight gain and fat mass gain were significantly hampered by DOX, which fits with the previous results of studies using similar doses as in our experimental setting (15 to 20 mg/kg) including both single and cumulative dosing regimens (Li, *et al.* 2006, Zhu, *et al.* 2010, Zhang, W.*, et al.* 2015, Sahu*, et al.* 2016). The decreased heart weight in relation to body weight or tibia length has been reported in several studies (Li, *et al.* 2006, Zhu, *et al.* 2010, Chen, *et al.* 2015, Matsumura*, et al.* 2018). A possible cause for this might be impaired cardiac growth and cardiac atrophy (Matsumura*, et al.* 2018). The decreased weight gain after DOX treatment served as an indicator of a downturn in the general well-being of the mice.

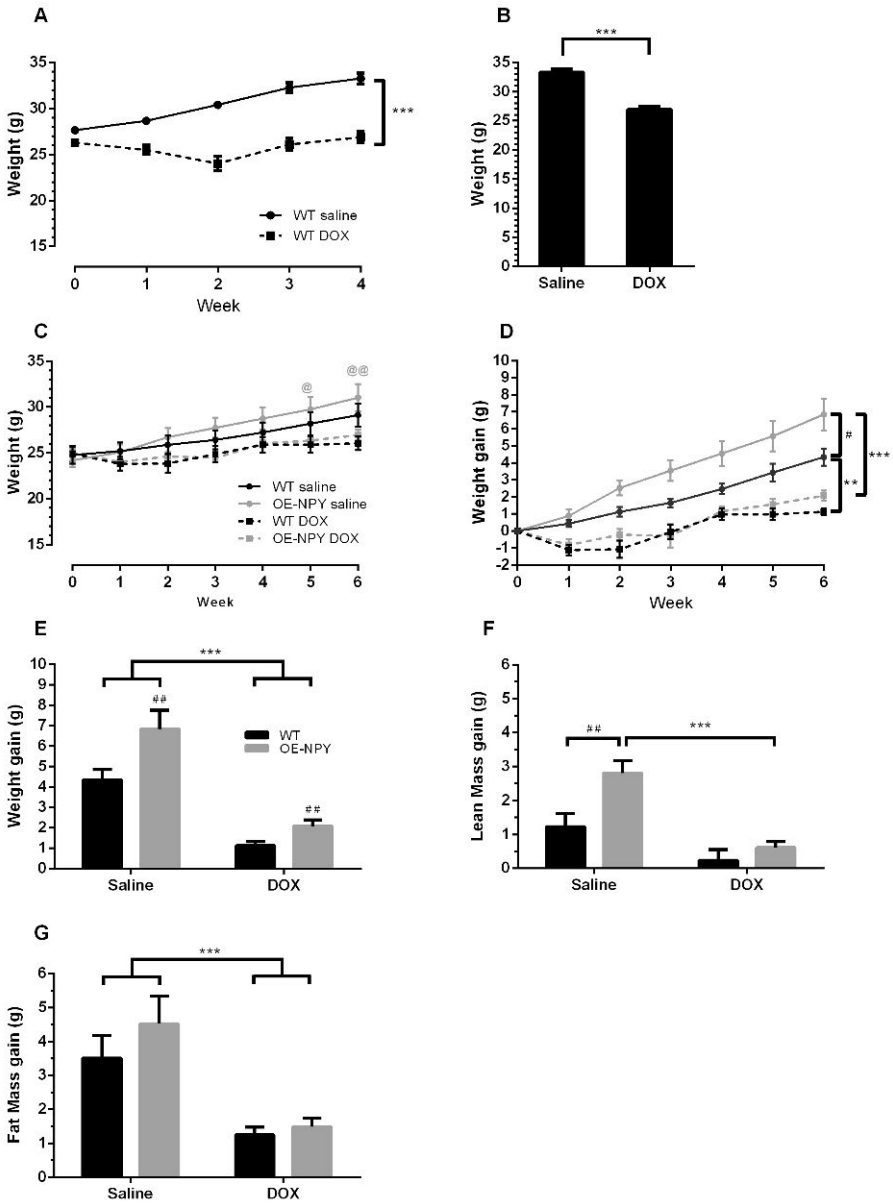

Figure 6. Body weight and composition in saline and doxorubicin (DOX) -treated mice. A) Body weight over 4 weeks and B) body weight at week 4 in wild-type (WT) mice (n=6-14/group). C) Body weight and D) weight gain change over 6 weeks, E) body weight gain, F) lean mass gain and G) fat mass gain at week 6 in WT and OE-NPY$^{D\beta H}$ (OE-NPY) mice (n =7–9/group). Values are presented as means ± SEM. A) *** P<0.001 ANOVA for repeated measures, B) *** P<0.001 Student's t-test, C) @ P<0.05, @@ P<0.01 OE-NPY DOX vs. OE-NPY saline with Bonferroni post-hoc test following two-way ANOVA, D) # P<0.05, ** P<0.01, *** P<0.001 Tukey post-hoc test following ANOVA for repeated measures, E),G) *** P<0.001 two-way ANOVA treatment effect, E) ** P<0.01 two-way ANOVA genotype effect, F) ## P<0.01, *** P<0.001 Tukey post-hoc test following two-way ANOVA.

Table 4. Organ weights and tibia lengths of the saline and doxorubicin-treated wild-type and NPY-OE$^{D\beta H}$ mice.

	WT saline	OE-NPY saline	WT DOX	OE-NPY DOX
Heart (mg)	148.5 ± 6.2	147.7 ± 4.1	133.6 ± 3.1	142.9 ± 5.4
Lungs (mg)	138.1 ± 8.0	144.9 ± 3.9	154.3 ± 8.8	157.0 ± 7.0
Liver (g)	1.45 ± 0.12	1.57 ± 0.09	1.47 ± 0.06	1.47 ± 0.04
Tibia (mm)	17.6 ± 0.05	17.5 ± 0.09	17.6 ± 0.04	17.6 ± 0.02
Heart/Tibia	8.39 ± 0.39	8.44 ± 0.25	7.60 ± 0.16	8.11 ± 0.31

WT wild-type mice, *OE-NPY* neuropeptide Y overexpressive mice, *saline* saline treatment, *DOX* doxorubicin treatment. Values are presented as mean ± SEM. Statistics were analyzed with two-way ANOVA (n=6-8/group). Reprinted with permission from Mattila et al. *Journal of Gene Medicine,* 2016:18*,*124–133.

5.1.2 Study I

5.1.2.1 SERCA2a protein expression

SERCA2a protein levels seemed to be lower in the hearts of the DOX-treated WT mice compared to saline-treated control mice 4 weeks after DOX treatment, though statistical significance was not reached (Fig. 7). Previous studies have addressed the decrease of the SERCA2a protein expression subsequent to DOX treatment, and the current result is in line with these previous findings, thus supporting in that respect the cardiotoxicity generated in the current study setting (Ge*, et al.* 2016, Llach*, et al.* 2019).

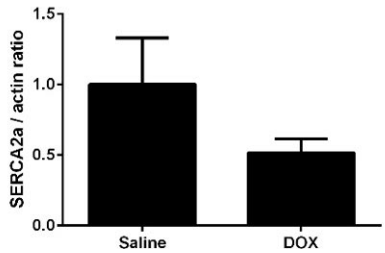

Figure 7. SERCA2a protein levels adjusted to actin levels in doxorubicin-treated (DOX, n=11) or saline-treated (n=6) wild-type mice heart. Modified from publication I.

5.1.2.2 Histological analysis

The histological findings of the hearts were examined at 4 weeks after DOX treatment in WT mice. Even though there were no statistically significant changes between the DOX-treated and saline-treated mice, the increasing observable degradation in myocardial tissue seen as lighter, more indistinctly defined area

(signified with arrow) was found to follow the higher heart/weight and lower SERCA2a/Actin protein ratio (unpublished data) (Fig. 8A–D). This suggests that there had been differences in the DOX response between individual animals as the observations are pointing coherently to either milder or stronger degradation, heart mass growth, and decrease in SERCA2a protein level. In previously published literature, a decreased heart weight has been a common finding in response to DOX, but also increased heart weight (Ito*, et al.* 2009) and left ventricular mass (Ge*, et al.* 2016) have been reported (see Table 2 for review).

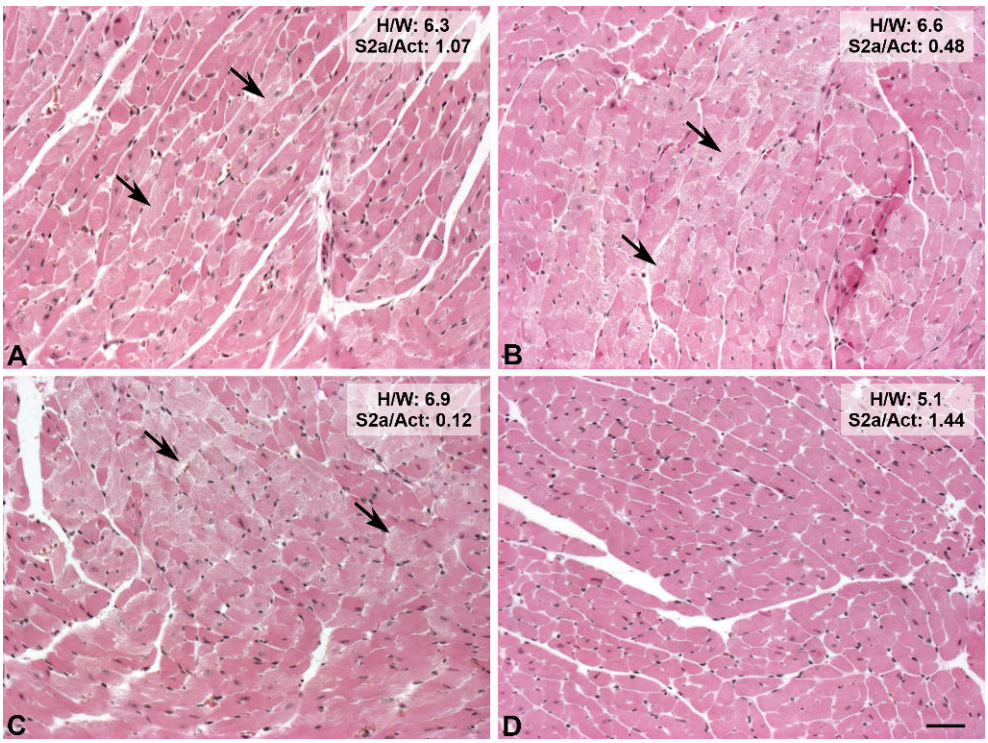

Figure 8. Examples of histological findings in the paraffin sections of the heart stained with hematoxylin/eosin. A)–C) Doxorubicin-treated mouse exhibited degradation indicated with arrow, D) saline-treated mouse with normal histological profile. H/W: heart mass / body weight ratio, S2a/Act: SERCA2a/Actin protein level ratio. Scale bar indicates 100 µm length.

5.1.3 Study II

5.1.3.1 Echocardiography analysis

Echocardiography was conducted six weeks after DOX administration in WT and NPY-OE$^{D\beta H}$ mice. DOX treatment tended to decrease ejection fraction (Fig. 9A) and

fractional shortening (Fig. 9B) when the genotypes were analyzed together. There were no differences in left ventricle internal diameter in diastole or systole or in interventricular septum in systole and diastole (II: Fig. 2C–F). Moreover, DOX tended to decrease the mass of the left ventricle when the genotypes were analyzed together (Fig. 9C), corresponding to a change seen also in heart weight measured at termination. The changes evident in the echocardiography analysis were quite moderate; ejection fraction and fractional shortening tended to be decreased in the DOX-treated mice. Previous studies have usually reported more markedly decreased ejection fraction and/or decreased fractional shortening in comparable research settings (Li 2006, Zhu 2010, Ge, 2016, Llach 2019). Nevertheless, these findings support the larger picture of DOX-induced cardiotoxicity.

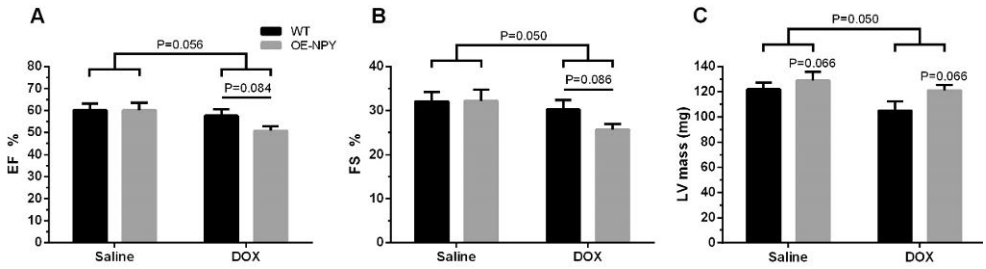

Figure 9. Echocardiography data in saline and doxorubicin (DOX) -treated wild-type (WT) and OE-NPY$^{D\beta H}$ (OE-NPY) mice (n=7-8/group). A) Ejection fraction (EF), B) fractional shortening (FS), C) left ventricle mass (LV mass). Values are presented as means ± SEM. A)-C) P=0.056, P=0.050 two-way ANOVA treatment effect; P=0.084, P=0.086 DOX-treated OE-NPY vs. WT t-test; P=0.066 two-way ANOVA genotype effect. Modified from publication II.

5.1.3.2 Histological analysis

The histological analysis was performed at 6 weeks after DOX treatment in WT and OE-NPY$^{D\beta H}$ mice. Saline-treated hearts appeared to be histologically normal as no nuclear atypia, changes in nuclear size, fibrosis or perivascular inflammation were observed (Fig. 10A, B). In DOX-treated hearts of either genotype, as an example of abnormal findings, there were cytoplasmic degeneration of myocardial cells (Fig. 10C, arrow), hypertrophy of the myocardial cell nuclei (Fig. 10D, arrow), some extravasated red blood cells (Fig. 10C, asterisk) and mild fibrosis (Fig. 10E, arrow). Even though the statistical significance was inconclusive, these findings are in agreement with previous reports of DOX treatment leading to cardiomyocyte disorganization and myofibrillar loss (Arola*, et al.* 2000, Li, *et al.* 2006, Zhu, *et al.* 2010, Zhu, *et al.* 2011, Sahu*, et al.* 2016).

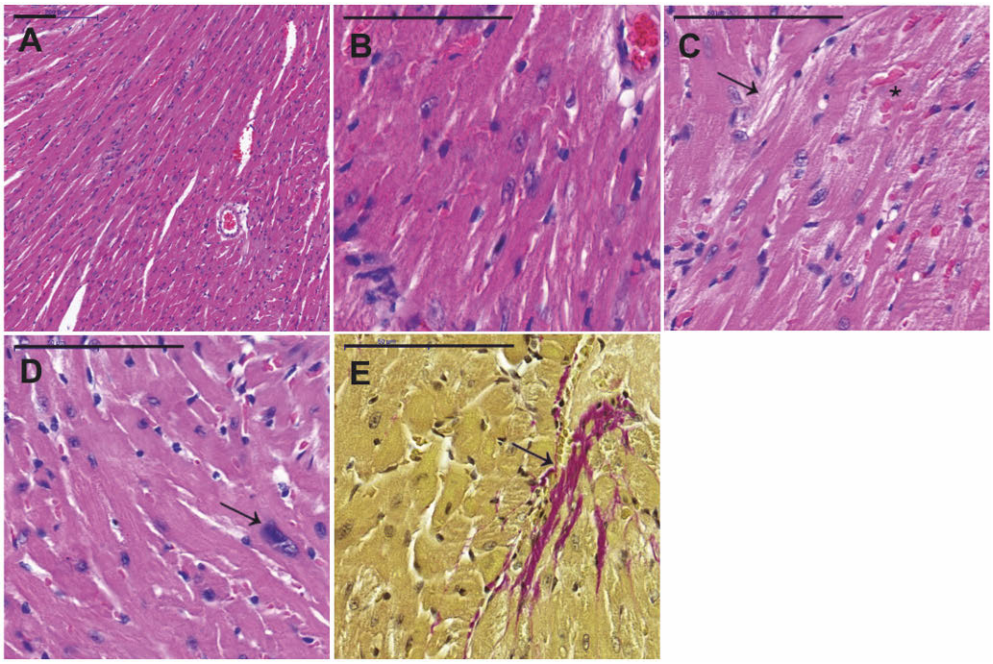

Figure 10. Examples of histological findings in the paraffin sections of the heart stained with hematoxylin/eosin and Van Gieson's staining. A)-B) Saline-treated mouse with normal histological profile, C)–E) doxorubicin-treated mouse. Arrows signify C) degeneration of myocardial cells, D) hypertrophy of the myocardial cell nuclei E) mild fibrosis and asterisk point C) extravasated red blood cells. Scale bar indicates 100 µm length. Reprinted with permission from Mattila et al. *Cardiovascular Toxicology*, 2020; 20: 328–33.

5.1.3.3 Gene expression analysis

Genes modifying calcium cycling

Gene expression related to cardiac calcium cycling was studied 6 weeks after DOX treatment in WT and NPY-OE$^{D\beta H}$ mice. DOX treatment resulted in significantly lower *Serca2a* (Fig. 11A) and *RyR2* (Fig. 11B) expression when the genotypes were analyzed together. These are well-described effects of DOX-induced cardiotoxicity on intracellular calcium metabolism and the present results parallel those reported previously (Boucek*, et al.* 1999, Hanna*, et al.* 2014, Tocchetti*, et al.* 2014). Markedly decreased *Serca2a* and *RyR2* expression levels represent strong molecular level evidence of the disturbed calcium cycling in the present HF model.

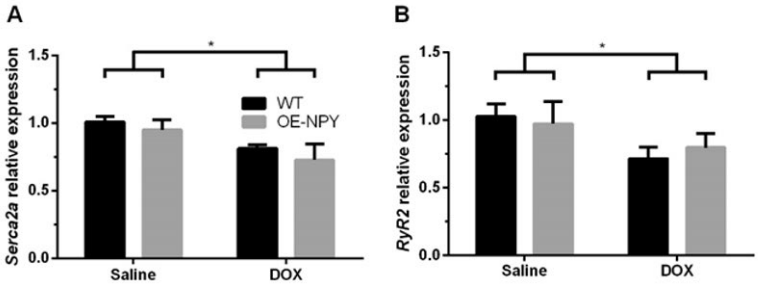

Figure 11. Relative expression levels of genes modifying calcium cycling system in the heart of saline and doxorubicin (DOX)-treated wild-type (WT) and OE-NPY$^{D\beta H}$ (OE-NPY) mice (n = 5–8/group). A) Sarcoplasmic reticulum Ca^{2+} ATPase (*Serca2a*) level, B) ryanodine receptor 2 (*RyR2*) level. Values are presented as means ± SEM. * P<0.05 two-way ANOVA treatment effect. Modified from publication II.

Marker genes of cardiomyopathy

Several genes involved in cardiomyopathy, inflammation, structural integrity and fibrosis were studied. Atrial natriuretic peptide *(Anp)* expression levels were significantly higher in DOX-treated mice when the genotypes were analyzed together (Fig. 12A), though there were no differences in *Bnp* expression (Fig. 12B). DOX altered also the expression of two genes involved in the degradation of proteins; matrix metalloproteinase 2 *(Mmp2)* expression was increased (Fig. 12C) and matrix metalloproteinase 9 *(Mmp9)* tended to be increased (Fig. 12D) by DOX when the genotypes were analyzed together. There were no differences in the expression levels of matrix metalloproteinase 13 *(Mmp13)* (Fig. 12E) or in those of the measured cytokines including interleukin-1β *(IL-1β)*, transforming growth factor beta 1 *(Tgf-β1)* and tumor necrosis factor-α *(Tnf-α)* (Fig. 12F–H). With respect to fibrosis, no significant changes were seen in the myofibroblast marker, α-smooth muscle actin (*α-Sma*) (Fig. 12I).

Based on reports on animal models with the corresponding setup, DOX was expected to upregulate both *Anp* and *Bnp*, as well as the marker genes of inflammation and fibrosis (Prathumsap*, et al.* 2020). Furthermore, in previous studies, DOX has been shown to upregulate matrix metalloproteinases, which participate in the degradation of sarcomeric and cytoskeletal proteins (Octavia*, et al.* 2012, Chen, *et al.* 2014, Tocchetti*, et al.* 2014, Polegato*, et al.* 2015). Here, the changes in gene expression regarding the cardiomyopathy markers were rather modest pointing to fairly mild cardiotoxicity. However, the increased *Anp* level indicates that the cellular mechanisms driving hypertrophy had been recruited and the increase in *Mmp2* expression points to activation of degradation of structural proteins, with the changes being consistent with observations evident in human HF (Meyer*, et al.* 1995, Polyakova*, et al.* 2011, Volpe*, et al.* 2014, Acsai*, et al.* 2016).

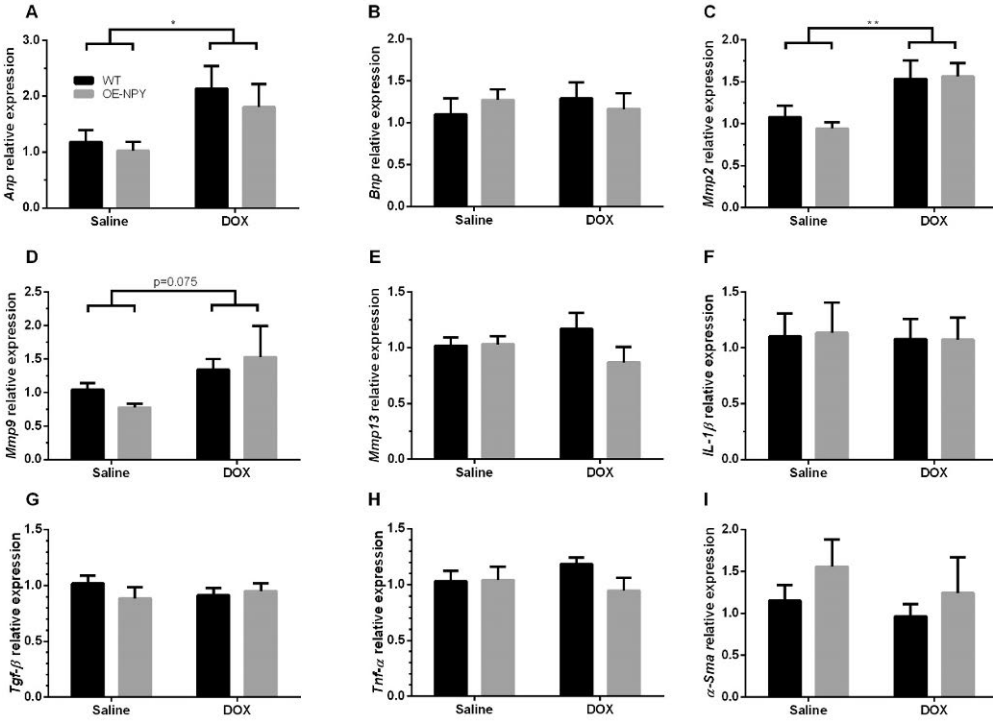

Figure 12. Relative expression levels of cardiomyopathy marker genes in the heart of saline and doxorubicin (DOX) -treated wild-type (WT) and OE-NPY$^{D\beta H}$ (OE-NPY) mice (n=5–8/ group). A) Atrial natriuretic peptide (*Anp*), B) B-type natriuretic peptide (*Bnp*), C) matrix metalloproteinase 2 (*Mmp2*), D) matrix metalloproteinase 9 (*Mmp9*), E) matrix metalloproteinase 13 (*Mmp13*) I, F) interleukin-1β (*Il-1β*), G) transforming growth factor-β (*Tgf-β*), H) Tumor necrosis factor-α (*Tnf-α*), I) α-smooth muscle actin (*α-Sma*) level. Values are presented as means ± SEM. * P<0.05, ** P<0.01, P=0.075 two-way ANOVA treatment effect. Modified from publication II.

Genes modifying sympathetic activity and mitochondrial biogenesis

The rate-limiting enzyme in noradrenaline synthesis, *Th,* tended to be increased by DOX treatment when the genotypes were analyzed together (Fig. 13A), while there were no differences in beta-1 adrenergic receptor expression, *Beta1R* (Fig. 13B) or in mitochondrial biogenesis regulator peroxisome proliferator-activated receptor gamma coactivator-1α (*Pgc-1α*) (Fig. 13C) expression. The higher expression of *Th* suggested that cardiac SNS activity was increased in DOX-treated mice, which is consistent with previous studies reporting that DOX upregulates the TH protein level thus linking DOX-induced cardiomyopathy to increased SNS activity (Tong*, et al.* 1991, Bartoli*, et al.* 2011, Jin*, et al.* 2014). *Beta1R* has previously been shown to be downregulated by DOX while in the current study there was no significant change between the saline and DOX-treated animals (Jin*, et al.* 2014). Similarly, the PGC-1α protein level has been previously shown to be decreased by DOX (Yin*,*

et al. 2018), but there was no change in the gene expression levels in the current study.

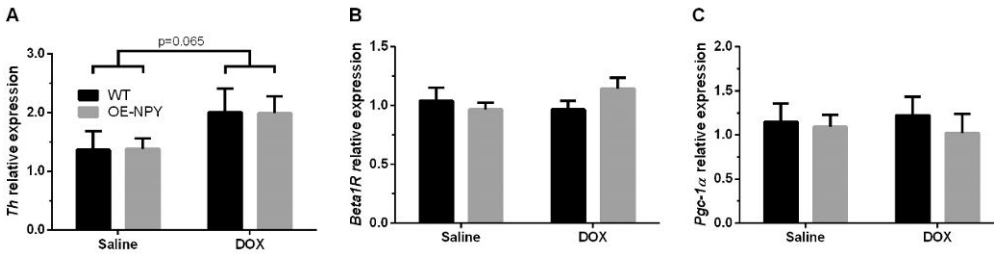

Figure 13. Relative expression levels of the genes modifying sympathetic activity and mitochondrial biogenesis in the heart of saline and doxorubicin (DOX) -treated wild-type (WT) and OE-NPY$^{D\beta H}$ (OE-NPY) mice (n=5-8/group). A) Tyrosine hydroxylase (*Th*) level, B) beta-1 adrenergic receptor (*Beta1R*) level, C) peroxisome proliferator-activated receptor gamma coactivator-1α (*Pgc-1a*) level. Values are presented as means ± SEM, P=0.065 two-way ANOVA treatment effect. Modified from publication II.

5.1.4 Overview of DOX-induced cardiotoxicity

DOX significantly decreased weight gain and the expression level of the genes modifying calcium cycling, and increased the expression level of marker genes of cardiomyopathy. In addition, some effects on heart weight, SERCA2a protein level and histology were seen, even though statistical significance was inconclusive in those respects. With regard to the functional parameters of the heart, in study II, the response to DOX was rather mild, however, when the WT and OE-NPY$^{D\beta H}$ genotypes were analyzed together, there was a trend in the treatment effect suggesting slight decrease in both EF and FS by DOX. The functional effects of DOX in Study I were present and are discussed in the gene therapy section below (see 5.2.3 Echocardiography analysis). Overall, DOX evoked less harsh response than expected based on the previous literature, and instead of severe heart failure, rather a state of cardiotoxicity was evident. As a part of the rationale behind Study I was to examine if the detrimental effects of DOX on the function of the heart could be overcome by viral gene therapy aimed at enhancing calcium cycling.

5.2 Lentiviral SERCA2a gene therapy (Study I)

5.2.1 The validity of lentiviral vector

5.2.1.1 SERCA2a protein expression analysis

The ability of lentiviral vector LV-SERCA2a-GFP to generate the correct SERCA2a protein product was tested in HEK293T cells, which were infected with the LV-SERCA2a-GFP lentiviral vector with a MOI 2, 5 and 10. The expression of SERCA2a protein product (110 kDa) produced by the lentiviral vector was confirmed by Western blot analysis, demonstrating increased levels of SERCA2a protein with higher MOIs (Fig. 14).

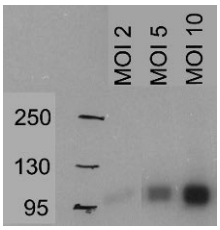

Figure 14. Western blot image of SERCA2a expression induced by LV-SERCA2a-GFP lentiviral vector in human embryonic kidney 293T cells with multiplicity of infection 2, 5 and 10.

5.2.1.2 Validation of transgene integration

As the lentiviral vector used in this study integrates its transgenes into the host genome, the integration of human *SERCA2a* gene and reporter gene GFP into mouse heart was validated by reverse transcriptase PCR. The analysis showed transgene expression in LV-SERCA2a-GFP and LV-GFP injected hearts, confirming that the human *SERCA2a* gene and the GFP gene had been successfully integrated into the mouse genome after viral injections (Fig. 15). In addition, endogenous mouse *Serca2a* levels were analyzed and there were no overt differences between the groups. As a positive control, HEK293T cells were infected by LV-SERCA2a-GFP. The documented integration of the *SERCA2a* gene into the mouse genome provided a solid base from which to initiate a study investigating the therapeutic effect of the LV-SERCA2a-GFP virus vector in the DOX-induced HF model.

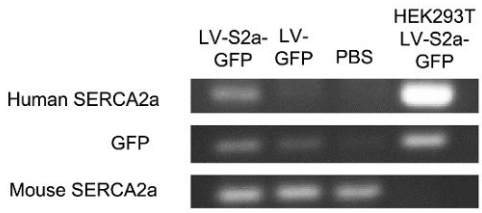

Figure 15. *SERCA2a* and *GFP* gene integration into mouse heart. Reverse transcriptase PCR analysis from LV-SERCA2a-GFP (LV-S2a-GFP), LV-GFP and saline (PBS) injected mouse heart. PCR analysis from LV-SERCA2a-GFP transduced human embryonic kidney 293T cells (HEK293T LV-S2a-GFP) are shown as a positive control. Reprinted with permission from Mattila et al. *Journal of Gene Medicine,* 2016:*18,*124-133.

5.2.2 Lentiviral injection

In the SERCA2a gene therapy study, lentiviral vectors were injected into the anterior wall of the hearts under ultrasound guidance. Intramyocardial injections were well tolerated with no mice dying from the operation. The integration of the lentiviral transgene into the mouse genome and the location of the infected area in the mouse heart were determined by analyzing reporter protein GFP fluorescence from frozen heart sections. Robust GFP expression in the LV-SERCA2a-GFP injected hearts was clearly distinguishable from the background (Fig. 16A, B; asterisk). As expected, there was no GFP expression in the saline injected hearts (Fig. 16C).

As shown in figure 7, the SERCA2a protein level seemed to be reduced in response to DOX, and the rationale was to increase the SERCA2a level with lentiviral gene transfer. Lentiviral gene therapy was successfully applied as the correct lentiviral SERCA2a protein product was confirmed, the transgene integrations into the host genome were confirmed and the cardiac tissue was confirmed to be transduced by the lentiviral vector. In a previous study, the human *SERCA2* gene was successfully transferred lentivirally into the rat heart by intracoronary delivery, achieving a notable area of infected cells (Niwano*, et al.* 2008). In this study, the infected area in the anterior wall of the left ventricle was moderate in size, stretching approximately 200 μm away from the needle track.

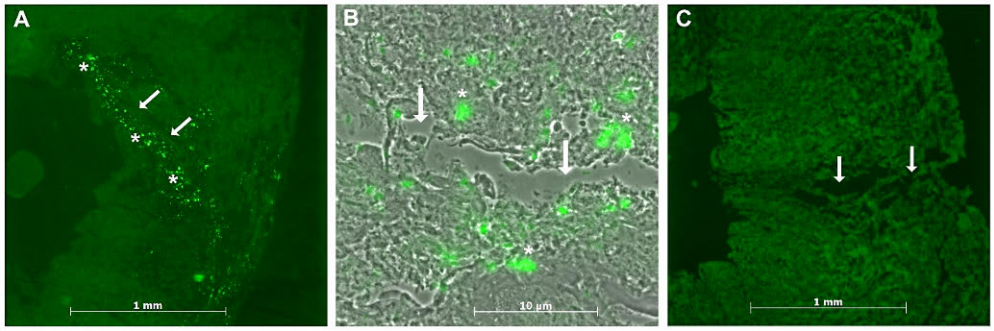

Figure 16. Frozen sections from intramyocardial injection of the LV-SERCA2a-GFP lentiviral vector into the left ventricular wall of the mouse heart. A–B) LV-SERCA2a-GFP injected heart, C) control heart injected with saline. Reporter protein GFP expression is indicated with an asterisk and the needle track of intramyocardial injection is indicated with arrows. Modified from publication I.

5.2.3 Echocardiography analysis

On the injection day (day 0), that is two days after DOX administration, there were no differences in echocardiography parameters between the groups (Fig. 17A, C, E). However, EF had already declined from the normal level, i.e. the level of the saline-treated WT control mice in Study II, 60.2 ± 3.1% (n=8) (Fig. 9) or the control animals in the similar studies (Riad*, et al.* 2008, Guenancia*, et al.* 2016). On day 28, absolute EF values were significantly higher in LV-SERCA2a-GFP (SERCA2a) injected mice compared to control virus LV-GFP (GFP) injected mice or saline (PBS) injected mice (Fig. 17A). From injection day to day 28, EF demonstrated a significant improvement in SERCA2a injected mice compared to GFP injected mice (Fig. 17B) and there was a marked increase in both the changes in end-systolic volume (ESV) and end-diastolic volume (EDV) change in the GFP and PBS injected mice in comparison to SERCA2a injected mice (Fig. 17C, D, F). Thus SERCA2a gene therapy enhanced notably the function of the heart and reduced left ventricular dilatation as EF increased and ESV decreased, despite the compact viral transduction area. Comparable results regarding changes in EF and cardiac volumes have been obtained in previous SERCA2a gene therapy reports exploiting ischemic heart failure models (del Monte*, et al.* 2001, Niwano*, et al.* 2008).

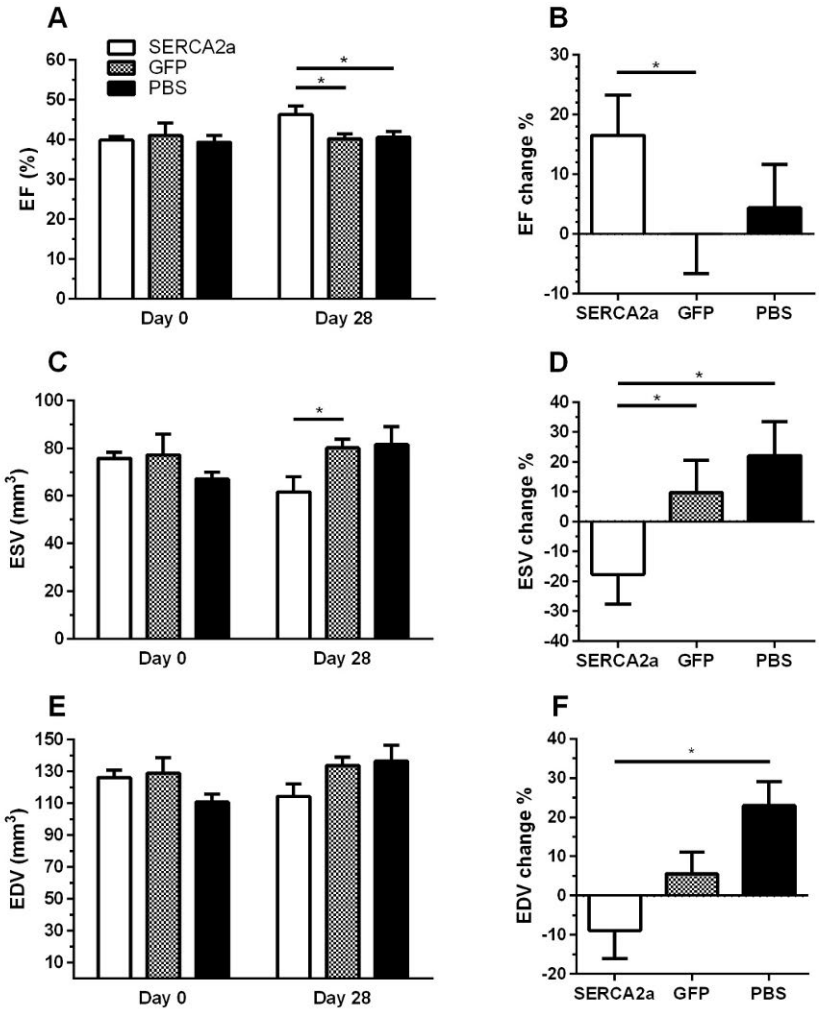

Figure 17. Echocardiography analyses of LV-SERCA2a-GFP (SERCA2a; n=5), LV-GFP (GFP; n=6) and saline (PBS; n=6) injected mice, treated with doxorubicin, on injection day (day 0) and on day 28. A) Ejection fraction (EF), B) EF percentual change from day 0 to day 28, C) end-systolic volume (ESV), D) ESV percentual change from day 0 to day 28, E) end-diastolic volume (EDV), F) EDV percentual change from day 0 to day 28. * P<0.05 Kolmogorov-Smirnov test (SERCA2a vs GFP; SERCA2a vs PBS). Modified from publication I.

5.2.4 Brain natriuretic peptide level in serum

Six weeks after DOX administration, the BNP levels seemed to be lowest in LV-SERCA2a-GFP (SERCA2a) injected mice, followed by the saline (PBS) and LV-GFP (GFP) injected mice (Fig. 18), although the differences were not statistically significant. In a previous SERCA2a gene therapy study, the BNP level was reported to decrease significantly after administration of the SERCA2a

containing AAV vector (Kawase*, et al.* 2008) and the BNP levels in the current study were comparable with that previous study.

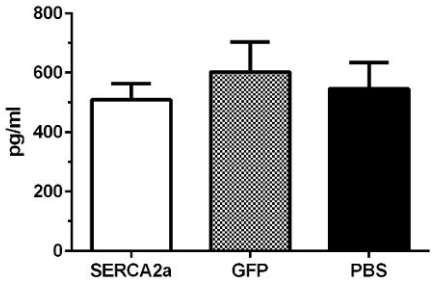

Figure 18. Serum brain natriuretic peptide (BNP) levels in LV-SERCA2a-GFP (SERCA2a; n=5), LV-GFP (GFP; n=6) and saline (PBS; n=6) treated mice. Modified from publication I.

5.2.5 Histological analysis

The paraffin sections of the hearts were measured 6 weeks after DOX treatment from eight points in the left ventricle to analyze the myocardial wall thickness. The analysis suggested that the average myocardium in LV-SERCA2a-GFP injected heart (Fig. 18B) was thicker than that in the LV-GFP injected heart (Fig 18A) and resembled an untreated heart (Fig. 18C), although no definitive conclusions could be drawn because of the small sample size. No differences in fibrosis or inflammation were observed between treatment groups.

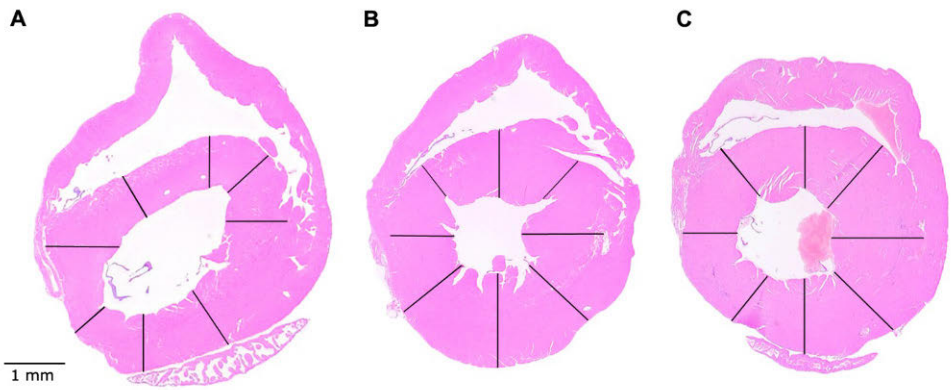

Figure 19. Histology images from hematoxylin and eosin stained paraffin sections of mouse heart. A) LV-GFP injected heart, B) LV-SERCA2a-GFP injected heart, C) Normal untreated heart as a control (n=1/group). Reprinted with permission from Mattila et al. *Journal of Gene Medicine,* 2016:*18,*124-133.

5.3 The effects of NPY overexpression on the DOX-induced cardiotoxicity (Study II)

5.3.1 Weight and body composition

The absolute body weight of the OE-NPY$^{D\beta H}$ mice had declined at weeks 5 and 6 after DOX treatment, an effect that was not evident in WT mice (Fig. 6C). In OE-NPY$^{D\beta H}$ mice, DOX significantly decreased lean mass gain whereas in WT mice there was no statistically significant difference in lean mass gain between saline and DOX treatment (Fig. 6F). Taken together, the body weight and gain in fat mass were decreased in DOX-treated mice regardless of the genotype while the lean mass gain was reduced significantly only in the OE-NPY$^{D\beta H}$ mice, suggesting that the OE-NPY$^{D\beta H}$ mice were more severely affected by DOX.

5.3.2 Gene expression analysis

5.3.2.1 NPY-related genes

Npy expression in the heart was overall low, as evidenced by the low Ct values in qPCR, but the expression level was found to be over ten times higher in OE-NPY$^{D\beta H}$ mice than in WT mice (Fig. 20A). DOX treatment did not alter *Npy* expression. There were no differences in neuropeptide Y 1 receptor expression levels (Fig. 20B) and the expression level of neuropeptide Y 5 receptor was below the reliable qPCR detection level. In the transgenic OE-NPY$^{D\beta H}$ model, in addition to neuronal tissue, heart is the only tissue where *Npy* gene expression has been quantified and found to be upregulated. Nonetheless, the higher expression observed in this study more likely represents the expression in the intracardiac noradrenergic neurons rather than cardiac myocytes (McDermott & Bell 2007). In the OE-NPY$^{D\beta H}$ mice, *Npy* expression is driven under the dopamine-β-hydroxylase promoter (DβH) targeting the transgene expression to noradrenergic neurons and showing very little ectopic expression (Ruohonen*, et al.* 2008). As the gene expression in heart was assumed to be low on an absolute scale, the direct effects on cardiac tissue are likely to have originated from the SNS-derived NPY. The increase of *Npy* gene expression in the heart tissue might represent the increase during mild chronic stress, but most likely, it is not equivalent to elevated NPY levels measured from plasma of human patients that have been associated with poor survival in HF (Hulting*, et al.* 1990).

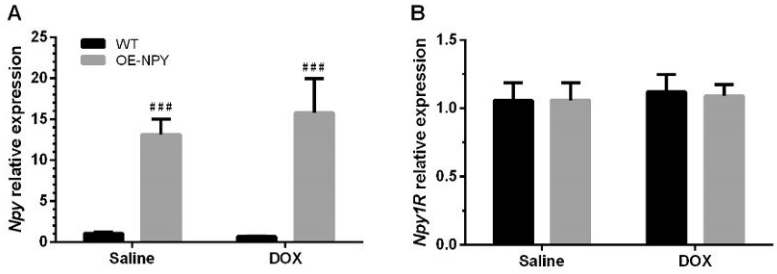

Figure 20. Relative expression levels of NPY-related genes in the heart of saline and doxorubicin (DOX) -treated wild-type (WT) and OE-NPY$^{D\beta H}$ (OE-NPY) mice (n=7–8/group). A) Neuropeptide Y (*Npy*) and B) neuropeptide Y 1 receptor (*Npy1R*) level. Values are presented as means ± SEM, ### P<0.001 two-way ANOVA genotype effect. Reprinted with permission from Mattila et al. *Cardiovascular Toxicology*, 2020; 20: 328–33.

5.3.2.2 Genes involved in calcium cycling and contractility

Concerning calcium cycling, there were no differences between the OE-NPY$^{D\beta H}$ and WT genotypes in *Serca2a* and *RyR2* expression (Fig. 11A, B). Interestingly, in the OE-NPY$^{D\beta H}$ mice, *Pln* expression tended to be decreased (Fig. 21A) and β-myosin heavy chain *(Mhc-β)* expression was significantly decreased when the treatment groups were analyzed together (Fig. 21B). There were no differences in the expression level of the α-myosin heavy chain *(Mhc-α)* (Fig. 21C). In previous studies, DOX has been reported to increase the *Mhc-β* expression (Boucek*, et al.* 1999, Umlauf & Horký 2002, Kucerova*, et al.* 2015, Doka*, et al.* 2017) but here, no response to DOX was seen. The reductions in *Mhc-β* and *Pln* have been associated with improved contractility (Abraham*, et al.* 2002, Iwanaga*, et al.* 2004, Tsuji*, et al.* 2009, Kucerova*, et al.* 2015, Doka*, et al.* 2017), which could fit with the known effects of NPY on cardiac contractility (McDermott & Bell 2007). However, this is not supported by the echocardiography results, as DOX-induced reductions in both EF and FS tended to be larger in OE-NPY$^{D\beta H}$ mice (Fig. 9A, B). Thus, these alterations in *Mhc-β* and *Pln* expression may rather point to a compensation caused by NPY overexpression that render the mice more susceptible to the DOX-induced cardiotoxicity. There were no significant changes in myofibroblast marker *α-Sma*, though the expression level seemed to be higher in the OE-NPY$^{D\beta H}$ mice (Fig. 12I).

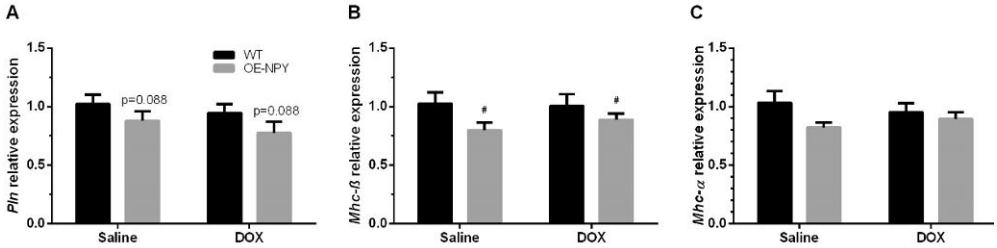

Figure 21. Relative expression levels of genes involved in calcium cycling and contractility in the heart of saline and doxorubicin (DOX) -treated wild-type (WT) and OE-NPY$^{D\beta H}$ (OE-NPY) mice (n=5–8/group). A) Phospholamban (*Pln*), B) β-myosin heavy chain (*Mhc-β*), C) α-myosin heavy chain (*Mhc-α*) level. Values are presented as means ± SEM. # P<0.05, P=0.088 two-way ANOVA genotype effect. Modified from publication II.

5.3.3 Overview of the effects of NPY on the DOX-induced cardiotoxicity

Previous studies have shown a diverse role of NPY in different types of pathological processes in the heart, involving also DOX-induced cardiotoxicity (Ananda*, et al.* 2012, Matyal*, et al.* 2013, Shanks & Herring 2013, Herring 2015, Özkaramanli Gür*, et al.* 2017, Tan*, et al.* 2018). However, in the current study, transgenic NPY overexpression had very little effect on the heart on its own, even when the expression level of *Npy*, measured on a relative scale, was notably higher in the OE-NPY$^{D\beta H}$ mice. As the effects of NPY overexpression were evaluated with respect to DOX-induced cardiotoxicity, the significantly reduced lean mass gain and the likelihood to larger declines in EF and FS, as evidenced by a tendency, suggested that DOX had affected the OE-NPY$^{D\beta H}$ mice more severely.

5.4 The effects of NPY overexpression on diet-induced obesity and type 2 diabetes models (Study III)

5.4.1 Metabolic phenotype

Both WD-fed genotypes demonstrated DIO compared to chow-fed lean mice, evidenced by increased body weight, white adipose tissue mass and fasting blood glucose levels ($P < 0.001$, diet effect, two-way ANOVA). Body weight did not differ between OE-NPY^{DBH} and WT mice, however, the blood glucose levels were higher in the OE-NPY^{DBH} genotype in lean and DIO mice when the treatment groups were analyzed together ($P < 0.05$, genotype effect, two-way ANOVA. The metabolic phenotype of T2D mice in the current study has been published previously (Ailanen, *et al.* 2017). WD combined with low-dose STZ resulted in fasting hyperglycemia

(blood glucose > 13 mmol/L) in OE-NPY^{DBH} but not in WT mice, thus suggesting that the overexpression of NPY had increased the susceptibility of the OE-NPY^{DBH} mice to develop a T2D-like state.

5.4.2 Echocardiography analysis

The echocardiography assessment was conducted 13 weeks after the onset of WD. In DIO WT mice, the internal diameter of the left ventricle in diastole was decreased in comparison to lean mice of the same genotype, a difference that was not present in OE-NPY^{DBH} mice (Fig. 22A). Moreover, DIO mice displayed a decreased left ventricle internal diameter in systole when the genotypes were analyzed together (Fig. 22B). The echocardiography-based measurement revealed a reduced left ventricular mass (Fig. 22C), and the weight of heart was also decreased in DIO mice (Fig. 22D) when the genotypes were analyzed together. No genotype differences were witnessed in left ventricular mass or heart weight, nor were there any differences in the EF between the diets or genotypes.

Despite the demonstrated DIO state, in the current study, WD of 13 weeks may not have been sufficiently severe to provoke functional changes in the heart, although some studies reported a decline of functional parameters within a comparable HFD period (Zhang, Y*., et al.* 2015, Wang, *et al.* 2017, Li, *et al.* 2018). Furthermore, studies utilizing a comparable diet setting (Zhang, Y*., et al.* 2015), or longer diets (Calligaris*, et al.* 2013, Liang*, et al.* 2015) have reported hypertrophy and increased heart weight in HFD, while no prior study could be located where a decreased heart weight had been reported.

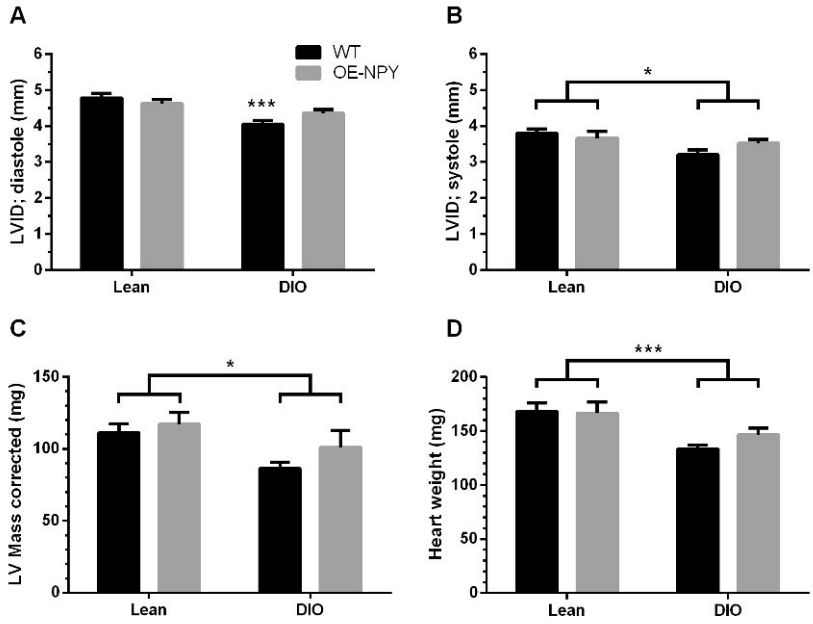

Figure 22. Echocardiography data and heart weight of lean and diet-induced obese (DIO) wild-type (WT) and OE-NPY^{DBH} (OE-NPY) mice (n=7–10/group). A) Left ventricle internal diameter; diastole (LVID; diastole), B) left ventricle internal diameter; systole (LVID; systole), C) left ventricle mass corrected (LV mass corrected), D) heart weight. Data is presented as mean ± SEM. A) *** P<0.001 Sidak post-hoc test following two-way ANOVA, diet effect within genotype, B)–D) * P<0.05 and *** P<0.001 two-way ANOVA diet effect. Modified from publication III.

5.4.3 Hemodynamic properties

Hemodynamics were studied *in vivo* by telemetry from carotid artery in lean state and DIO mice. The average of 48 hours recording revealed elevated MAP during both light and dark period in OE-NPY^{DBH} mice compared to WT mice, without any difference between the diets (Fig. 23A, B). Lean mice displayed no difference between the genotypes in MAP in their response to the alpha1-receptor agonist PE. In both genotypes, in the DIO state, the response to PE was augmented, with the MAP being higher in WT than in OE-NPY^{DBH} mice (Fig. 23C). In lean state, atropine increased HR less in OE-NPY^{DBH} mice compared to WT mice, while in the DIO state, the atropine-induced increase in HR was abolished in WT mice (Fig. 23D). To further evaluate whether the changes in MAP and HR resulted from increase in sympathetic activity, the noradrenaline levels were analyzed. DIO increased noradrenaline levels as compared to lean state, with OE-NPY^{DBH} mice having lower levels compared to WT mice in DIO state (III: Fig. 7A).

Vascular reactivity was studied *ex vivo* by wire myography from lean, DIO and T2D state mice. The maximal vasoconstrictive response of the mesenteric artery to PE was augmented in DIO and T2D as compared to lean state, especially in WT mice (Fig. 23E). In the PE-response curve, the contraction response in the mesenteric artery was reduced in OE-NPY^{DBH} genotype compared to WT mice in both DIO and T2D (III: Fig. 4C, E). With respect to vasorelaxation, the maximal response of the aorta to ACh was decreased in DIO and T2D compared to the lean state ($P < 0.01$, diet effect, two-way ANOVA). When inhibiting the NO production with L-NNA prior to the ACh treatment, the ACh response was less effectively blunted in the OE-NPY^{DBH} DIO state mice (III: Fig. 6E) showing that the contribution of NO to vasorelaxation was reduced in OE-NPY^{DBH} mice. The relaxation response to the NO-donor SNP was attenuated in OE-NPY^{DBH} mice in lean state as compared to WT mice (III: Fig. 6G) suggesting that endothelium-independent vasodilatation was impaired in OE-NPY^{DBH} mice aorta.

Taken together, the results of the hemodynamic studies showed that the overexpression of *Npy* led to a cardiovascular phenotype to some extent resembling DIO. Nonetheless, the mechanisms behind the changes are somewhat different. *Npy* overexpression and DIO both suppressed parasympathetic control of the heart, as evidenced by the suppressed response to atropine. Thus, the life-long transgenic NPY excess may provide a mechanism for elevated risk of cardiovascular disease linked with NPY. Only DIO (and not excess of *Npy*) increased sympathetic activity, as reflected in the higher *in vivo* MAP increase and *ex vivo* arterial vasoconstriction in response to PE, and the elevated urine noradrenaline level. Against our hypothesis, the overexpression of *Npy* had no synergistic effect with DIO. This could be explained by the attenuated increase in sympathetic activity and the vascular responses by NPY. The arterial vasoconstriction was similarly attenuated in response to PE in DIO and T2D state OE-NPY^{DBH} mice. However, in the ACh-induced vasodilation, the genotype difference in the NO-component evident in DIO was abolished by T2D. NPY excess did not aggravate the vascular function in T2D state.

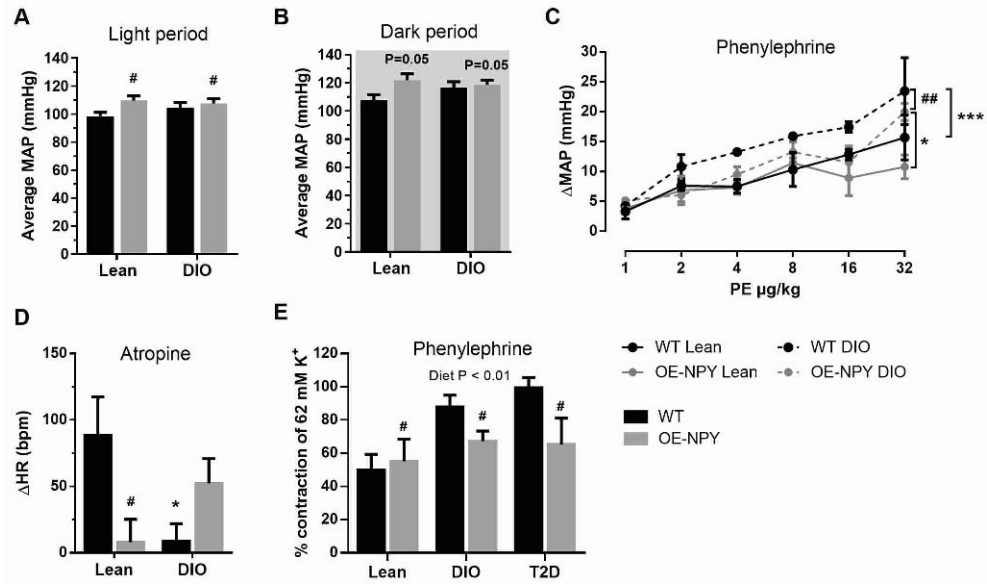

Figure 23. Hemodynamic properties of wild-type (WT) and OE-NPY$^{D\beta H}$ (OE-NPY) mice. Properties in lean state, in diet-induced obesity (DIO) (A-D) and in type 2 diabetic (T2D) state (E), studied by telemetry (A-D) or by myography (E). A-B) Average mean arterial pressure (MAP) on A) light and B) dark period, n=7–8/group, # P<0.05; P=0.05 comparing different genotypes with two-way ANOVA. C) MAP response to phenylephrine (PE, 2-32 µg/kg, doses in randomized order, i.v.), n=3-4/group, ## P<0.01 comparing different genotypes in DIO and * P<0.05 and *** P<0.001 comparing different diets with two-way ANOVA within a genotype. D) Heart rate (HR) response to atropine (2 mg/kg, i.p.), n=7/group, # P<0.05 comparing different genotypes on lean state and * P< 0.05 comparing different diets within WT mice with Bonferroni post-hoc test following two-way ANOVA. E) Maximal response to PE in mesenteric arteries, n=5-7/group, # P<0.05 comparing different genotypes and P<0.01 comparing different diets with two-way ANOVA. Data is presented as mean ± SEM. Modified from publication III.

5.4.4 Histological analysis

When the hearts were assessed histologically, lean mice displayed normal hearts with no nuclear atypia or changes in nuclear size (Fig. 24A, B). In DIO mice, hypertrophy of the myocardial cell nuclei (Fig. 24C, arrow) and some perivascular oedema (Fig. 24D, arrows) were evident. In T2D cohort, OE-NPY^{DBH} mice showed signs of cytoplasmic degeneration (Fig. 24E, arrows). In the T2D cohort, 71% of both genotypes displayed myocardial degeneration of tissue (scale 1/3) whereas 22% of lean and 33% of DIO OE-NPY^{DBH} mice, but none of the lean and DIO WT mice exhibited signs of degeneration (n=7–10/group).

Several studies have reported disorganization of myofibers in HFD, but in most cases, the length of the diet has been at least double compared to our study (Cao*, et al.* 2016, Lucas*, et al.* 2016, Daltro*, et al.* 2017) or the mice were notably older (Lucas*, et al.* 2016, Hung*, et al.* 2017). However, with a comparable diet duration to

ours, histological damage has been reported in some studies (Wang, *et al.* 2017, Kondo, *et al.* 2018). On the other hand, regarding STZ-induced T2D model, less than half of our diet period has been reported to lead to detrimental findings (Huang, *et al.* 2017).

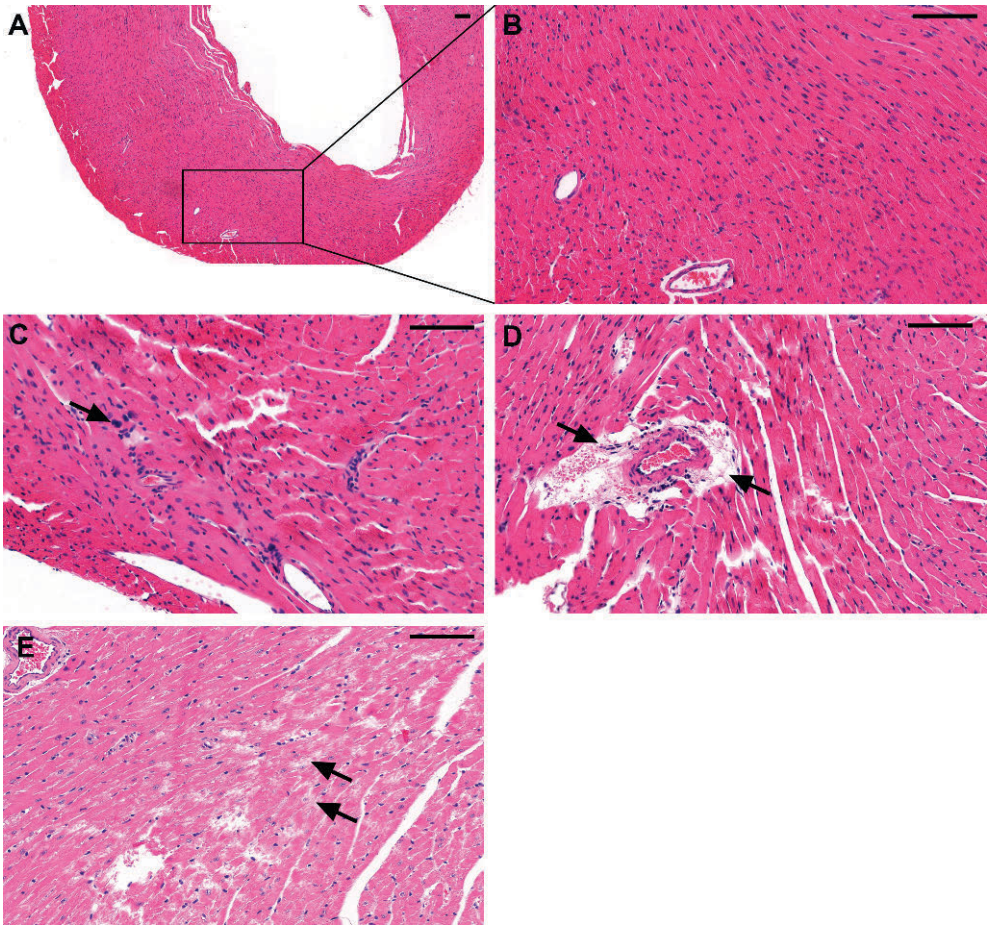

Figure 24. Histological findings in the paraffin sections of the heart stained with hematoxylin/eosin. A–B) Wild-type mouse in lean state and C) in diet-induced obesity (DIO), D) OE-NPY^{DBH} mouse in DIO, E) OE-NPY^{DBH} mouse in type 2 diabetic state. Arrows indicate C) hypertrophy of the myocardial cell nuclei, D) perivascular oedema, and E) cytoplasmic degeneration. Scale bar indicates 100 µm length. From publication III.

5.4.5 Gene expression analysis

Interestingly, the expression of collagen I alpha 2 (*Col1a2*), a fibrosis marker, was lower in the hearts of DIO mice as compared to lean mice when the genotypes were analyzed together (Fig. 25A). There were no differences in the expression levels of

the cytokine marker, transforming growth factor beta 1 (*Tgf-β1*) or mitochondrial marker, peroxisome proliferator-activated receptor gamma coactivator 1 alpha (*Pgc-1α*) (Fig. 25B, C).

A study utilizing a comparable research set-up (Li, *et al.* 2018), as well as studies where the mice have consumed longer HFD (Calligaris, *et al.* 2013, Daltro, *et al.* 2017) have reported increased *Tgf-β1* and *Col1* expression in HFD. In the current study, no explanation was found for the lower *Col1a2* fibrosis marker expression in the hearts of DIO mice.

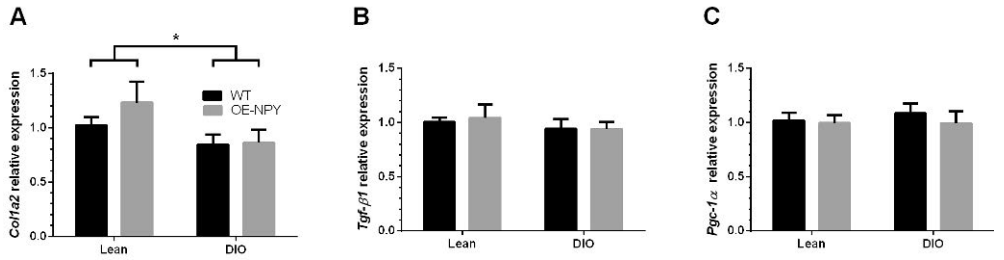

Figure 25. Relative gene expression level in the heart of lean and diet-induced obese (DIO) wild-type (WT) and OE-NPY^{DBH} (OE-NPY) mice (n=9–10/group). A) Collagen 1 a 2 (*Col1a2*), B) Transforming growth factor beta 1 (*Tgf-β1*) C) Peroxisome proliferator-activated receptor gamma coactivator 1 alpha (*Pgc-1α*) level. Data is presented as mean ± SEM. * P<0.05 two-way ANOVA diet effect. Modified from publication III.

5.5 Methodological considerations

5.5.1 Animals

The C57BL/6 mouse strain is the most well-known inbred mouse strain utilized in animal studies (Mekada, *et al.* 2009). The two main substrains of C57BL/6 are C57BL/6J and C57BL/6N, and the latter is used in all of the Studies I-III. In Studies II and III, an additional cohort of OE-NPY$^{D\beta H}$ mice, originating from the same C57BL/6N background was used. Male mice were used in order to eliminate the effects of the oestrus cycle.

The C57BL/6 strain has been reported to be prone to develop atherosclerosis when fed with a high fat diet (Schreyer, *et al.* 1998). Furthermore, there are various noteworthy genotypic and phenotypic differences between the C57BL/6 substrains, but not all the studies have reported which of the substrains was used (Fontaine & Davis 2016). The substrain C57BL/6N has maintained its stability well as no genetic variation was found in genotyping panels after 30 years of extensive breeding (Mekada, *et al.* 2009). C57BL/6N mice have been found to develop hyperglycaemia and hyperinsulinaemia after three 3 weeks of HFD (Kleinert, *et al.* 2018), however,

the substrain C57BL/6J is more commonly used in metabolic research as it is more susceptible to diabetes and DIO (Fontaine & Davis 2016). In the DOX-induced cardiotoxicity studies that have been reviewed in this thesis (see Table 2), only one had utilized C57BL/6N mice with certainty (many of the reviewed studies did not specify the substrain of the mice), and the results of that study were in line with ours, with only minor functional changes (Matsumura *et al.* 2018).

Single housing versus group housing of mice is a much debated issue. While single housing may predispose mice to stress due to the lack of social contacts, group housed mice may be predisposed to aggressive behavior between the males (Gonder & Laber 2007). In a previously published study, it was concluded that no general recommendations could be made, as mice seem to respond in a context-dependent manner, and thus the housing protocol needs to be considered individually in each case (Kappel*, et al.* 2017). In studies I and II, the mice were single-housed to ensure the proper recovery from the DOX administration. In study III, the mice were housed in groups.

5.5.2 Heart failure models

In Studies I and II, the dose of DOX was carefully considered on the basis of previous studies (Li, *et al.* 2006, Neilan*, et al.* 2006). The intraperitoneal dosing was performed under anaesthesia, thus the injection site could be determined in a very fine-tuned manner as the mice were unconscious and not moving. The response to DOX was slightly milder than would have been expected based on the literature, yet signs of cardiotoxicity were evident and marked differences were found in DOX-treated mice in comparison to the control animals.

In Study II, the hypothesis was that OE-NPY$^{D\beta H}$ genotype would be expected to exacerbate the DOX-induced cardiotoxicity. The OE-NPY$^{D\beta H}$ mouse model displays a metabolic syndrome-like phenotype rather similar to the human NPY L7P polymorphism, which has been found to be a risk factor for type 2 diabetes and cardiovascular diseases (Pesonen 2008). In addition, the OE-NPY$^{D\beta H}$ mice have been reported to be more susceptible to vascular damage-induced endothelial hypertrophy (Ruohonen*, et al.* 2009). Instead, here, the effects seemed to be rather minor. This might be because of moderate DOX-response or the limited *Npy* overexpression in the heart, i.e. the actual absolute level was low even although the expression was many times higher than in WT mice.

In study III, in order to obtain DIO, a high caloric rodent diet was used to mimic the highly processed Western type foods that many humans are consuming. The DIO state was reached independently of the genotype, which is in line with previous results (Vähätalo, *et al.* 2015, Ailanen, *et al.* 2018). To induce T2D, the DIO state mice were administered a low dose of streptozotocin. Previously published results

have verified this model in terms of the metabolic phenotype (Ailanen, *et al.* 2017). Based on our findings in Study III, parasympathetic control of the heart was suppressed by both DIO and NPY, but only DIO increased sympathetic activity. Contrary to the original hypothesis, overexpression of NPY did not augment the effects of DIO, and this may be mediated to some extent by the attenuated increase in sympathetic activity and vascular responses by NPY. The findings concerning decreased *Col1a2* expression and lower weight of heart in DIO mice, and decreased left ventricular end-diastolic diameter in DIO WT mice were contradictory to previous research, and no explanation was found with respect to technical research settings. However, the comparison between these results and the other studies should be conducted with caution since a strong genetic component has been shown to exist in the cardiac structure and function (Wang, *et al.* 2016).

5.5.3 Gene therapy

Lentiviral-mediated gene transfer is a well-established method (Selkirk 2004, Ly 2007, Niwano*, et al.* 2008). The lentiviral vector is a very suitable choice for HF gene therapy as it is capable of infecting non-dividing cardiomyocyte cells and it offers long-term overexpression by integrating into the host genome. The lentiviral vector used in this study represents a second-generation viral construct in which the possibility of a multi-recombination event has been eliminated, preventing the generation of a self-replicative vector. The lentiviral dose was determined by quantifying the GFP protein expression produced by the viral vector in the *in vitro* infected cells. In the bicistronic vector backbone, the *GFP* gene is located downstream from the *Serca2a* gene, the IRES (internal ribosome entry site) separating these two genes. IRES is known to affect the expression of the downstream gene, the expression range being 6-100% and the typical expression 20-50% compared to the upstream gene which is located next to the promoter (Mizuguchi*, et al.* 2000, Chinnasamy*, et al.* 2006). Thus, the *in vivo* expression of SERCA2a is comparable to GFP expression or probably somewhat higher. In study I, the expression of the *Serca2a* gene was not quantified using qPCR. There were no antibodies suitable at the time for the quantification of SERCA2a protein in the tissue samples as every antibody available was produced in mice, and thus inapplicable for histological samples derived from mice. As the viral injection area in the heart was narrow, the local protein isolation, limited to the exact injection site, was not an option and the Western blot analysis was not sensitive enough to detect transgenic SERCA2a overexpression. In addition, although the valid SERCA2a protein product was confirmed *in vitro*, however, the biological activity of the protein product was not evaluated.

By performing ultrasound-guided intramyocardial injection, the viral vectors can be delivered directly into the wall of the left ventricle, without the need for invasive open chest surgery. Direct injection caused only a minor needle track without any observed deleterious effects on cardiac function. The area covered by gene transfer in the anterior wall of the left ventricle was not extensive (comprising a few hundred micrometers along the needle track). It is unclear whether strong transgene expression in a smaller number of cells produces a similar therapeutic effect as lower expression in a greater number of cells (Yla-Herttuala 2017b). In addition, as SERCA2a is a membrane protein of the sarcoplasmic reticulum, each cardiomyocyte is required to be transduced by the viral vector in order to achieve a therapeutic response in the cardiomyocyte, and in this respect it differs from a paracrine gene therapy product (such as VEGF) which is able to affect also the nearby cells. However, in this model, the relatively limited number of SERCA2a overexpressing cells did occasion a clinically meaningful result as a marked improvement of cardiac function was observed. The delivery method chosen in this thesis, intramyocardial injection, is viewed as being much more efficient in animal models than intra-arterial delivery, and it has also been utilized in many recent clinical trials, especially with the help of the injection targeting method NOGA mapping (Hassinen*, et al.* 2016, Hartikainen*, et al.* 2017, Yla-Herttuala & Baker 2017).

5.5.4 Physiological aspects of study methods

The *in vivo* and *ex vivo* study methods and the biochemical analyses conducted in this thesis have been previously published and the results can be considered as reliable. In preclinical research set-up, the equipment, the protocols and the study conditions are not completely standardized and the sample size is relatively small, and these factors may introduce some variation. Thus, comparing the results between different independent studies must be performed with caution.

There are some aspects of study methods to be considered. Recording the body composition by qNMR required immobilization of the conscious mice during the measurement protocol. Each mouse was measured twice and the mean values were used as a way of enhancing the accuracy. In echocardiography, the level of anaesthesia was monitored by the HR and was set at a level not to dampen the function of the heart. The handling of mice and dosing of substances may have induced some stress, but there was a habituation period before the actual studies aimed at minimizing the stress-induced effects that may have occurred. Furthermore, to avoid stress, intraperitoneal administration of substances was performed under anaesthesia when possible (in Studies I and II).

6 Summary and conclusions

Studies I and II demonstrated that DOX generated cardiotoxicity, which subsequently could be ameliorated with lentiviral-mediated *SERCA2a* gene therapy. Studies II and III showed that life-long overexpression of NPY may worsen the DOX-induced cardiotoxicity and lead to cardiovascular alterations resembling DIO. The main findings and conclusions from the studies conducted in this thesis, as reflected in the original aims were:

1. DOX induced cardiotoxicity as demonstrated by a decline in myocardial function and mass, and a decline in the general condition of the mice. In addition, harmful alterations of expression levels in the genes modifying calcium cycling as well as in the marker genes of cardiomyopathy were observed, indicating that cellular mechanisms driving detrimental changes in the heart had been recruited.
2. The lentiviral vector expressing *SERCA2a* gene was shown to produce the correct SERCA2a protein, and the integration of *SERCA2a* into the host genome after intramyocardial injection was confirmed.
3. The therapeutic effect of the *SERCA2a*-expressing lentiviral vector was proven in the DOX-induced HF model, as evidenced by the improvements in cardiac function.
4. *Npy* expression was shown to be upregulated in the heart of transgenic OE-NPY$^{D\beta H}$ mouse model. The impaired lean mass accumulation and the tendency towards a larger decrease in the heart function may imply that neuropeptide Y overexpression increased the susceptibility to cardiotoxicity in DOX-induced HF model.
5. *Npy* overexpression suppressed parasympathetic activity while increasing sympathetic activity. DIO elevated sympathetic activity, but the effect was attenuated by overexpression of *Npy*. The vascular disturbances caused by *Npy* and DIO appeared, but were not further aggravated by T2D. The current model of DIO did not lead to any harmful effects on the heart, but signs of tissue degradation were seen, especially in T2D heart.

Acknowledgements

The work of this thesis was carried out in the Department of Pharmacology, Drug Development and Therapeutics, Institute of Biomedicine at the University of Turku. I am highly grateful to Professors Risto Huupponen, Markku Koulu, Mika Scheinin, Ullamari Pesonen, Olli Pentikäinen and Aleksi Tornio for providing the research facilities and equipment. I also appreciate the opportunity to teach, it has been a very rewarding part of my work. I warmly thank the Drug Research Doctoral Program (DRDP) for scientific and financial support, and especially its coordinator, Eeva Valve, for the outstanding assistance along the way. The other financial supporters, Turku University Hospital Research Fund, Turku University Foundation, Finnish Cultural Foundation Varsinais-Suomi Regional fund, Finnish Foundation for Cardiovascular Research, Orion Research Foundation, Aarne Koskelo Foundation and Ida Montin Foundation are also acknowledged.

I am deeply grateful to my supervisors Docent Mikko Savontaus and Associate Professor Eriika Savontaus. Mikko gave me the opportunity to become familiar and work with gene therapy and heart-related issues when I was finishing my master's degree. Later on, Eriika provided me with the new NPY-related perspective and also the new physical framework for conducting research. I admire the positivity of both of my supervisors, and their ability to inspire faith in students in every situation, even when performing scientific experimentation seems to be a long and a winding road.

I am much indebted to the reviewers of this thesis, Professor Anna-Liisa Levonen and Docent Johanna Magga for their constructive comments, which really helped me to improve the thesis manuscript and opened new insights into my work. In addition, I sincerely thank Docent Heli Forssell for valuable remarks, Dr. Ewen MacDonald for the linguistic revision, and Anne for the Finnish grammar check. I want to acknowledge all my co-authors for their contributions: Mirva Söderström, Juha Koskenvuo, Kim Eerola, Liisa Ailanen, Laura Vähätalo, Anna-Maija Penttinen, Petteri Rinne, Suvi Ruohonen and Saku Ruohonen. The members of the supervisory board, Associate Professor Antti Saraste and Professor Hannu Järvelainen are acknowledged for providing advice and feedback.

I want to express huge thanks to NPY/MSH group into which I was adopted, and to all the people with whom I had the privilege to share a room: Henriikka, Laura, Liisa, Milka, Satu, Kim, Raine, Salla, Anna, Anni, Aya, James and Keshaw. I want to acknowledge the whole Farmis crew, and especially Elina Kahra, Maarit Nikula and Sanna Bastman are acknowledged for skillful technical support. Anja Similä, Pia Tahvanainen and Virpi Aaltonen are acknowledged for secretarial assistance.

I thank all my fellow PhD students for peer support; my special thanks belong to Liisa, Maria, Milka and Noora for the late stage reinforcement. Jenni, Jonna and Niina, thank you for being by my side all the way from genetics studies until today. I am incredibly grateful for having so many dear friends also outside of academia. Some of you have traveled this road with me for over 20 years and others have known me only in the past few stressful years. You bring such a joy and off-work perspectives into my life. Extra thanks for all the companionship in our many adventures in the nature.

Viimeisenä mutta ei vähäisimpänä, rakas perheeni. Lämmin kiitos siskolleni Kirsille ja puolisolleen Eskolle myötäelämisestä ja rinnalla kulkemisesta. Äiti ja isä, Pirkko ja Pekka, olen valtavan kiitollinen läpi koko elämäni jatkuneesta tuestanne ja rakkaudestanne.

Turku, September 2020

Minttu Mattila

References

Abel ED, Litwin SE, Sweeney G (2008). Cardiac remodeling in obesity. *Physiological Reviews,* 88(2), 389–419.

Abraham WT, Gilbert EM, Lowes BD, Minobe WA, Larrabee P, Roden RL, Dutcher D, Sederberg J, Lindenfeld JA, Wolfel EE, Shakar SF, Ferguson D, Volkman K, Linseman JV, Quaife RA, Robertson AD, Bristow MR (2002). Coordinate changes in Myosin heavy chain isoform gene expression are selectively associated with alterations in dilated cardiomyopathy phenotype. *Molecular medicine,* 8(11), 750–760.

Acsai K, Ördög B, Varró A, Nánási P (2016). Role of the dysfunctional ryanodine receptor – Na(+)-Ca(2+)exchanger axis in progression of cardiovascular diseases: What we can learn from pharmacological studies? *European journal of pharmacology,* 779, 91–101.

Ailanen L, Ruohonen S, Vähätalo L, Tuomainen K, Eerola K, Salomäki Myftari H, Röyttä M, Laiho A, Ahotupa M, Gylling H, Savontaus E (2017). The metabolic syndrome in mice overexpressing neuropeptide Y in noradrenergic neurons. *Journal of Endocrinology,* 234(1), 57–72.

Ailanen L, Vahatalo LH, Salomaki-Myftari H, Makela S, Orpana W, Ruohonen ST, Savontaus E (2018). Peripherally Administered Y2-Receptor Antagonist BIIE0246 Prevents Diet-Induced Obesity in Mice With Excess Neuropeptide Y, but Enhances Obesity in Control Mice. *Frontiers in pharmacology,* 9, 319.

Ajijola OA, Chatterjee NA, Gonzales MJ, Gornbein J, Liu K, Li D, Paterson DJ, Shivkumar K, Singh JP, Herring N (2019). Coronary Sinus Neuropeptide Y Levels and Adverse Outcomes in Patients With Stable Chronic Heart Failure. *JAMA cardiology*.

Ananda S, Wang Y, Zhu S, Wang R, Zhou X, Zhuo L, Sun T, Ren L, Liu Q, Dong H, Liu Y, Liu L (2012). Role of neuropeptide Y and peroxisome proliferator-activated receptor γ coactivator-1α in stress cardiomyopathy. *Journal of Huazhong University of Science and Technology (Medical Science),* 32(6), 823–828.

Arola OJ, Saraste A, Pulkki K, Kallajoki M, Parvinen M, Voipio Pulkki LM (2000). Acute doxorubicin cardiotoxicity involves cardiomyocyte apoptosis. *Cancer research,* 60(7), 1789–1792.

Athithan L, Gulsin G, McCann G, Levelt E (2019). Diabetic cardiomyopathy: Pathophysiology, theories and evidence to date. *World Journal of Diabetes,* 10(10), 490–510.

Barrett P, Mercer JG, Morgan PJ (2016). Preclinical models for obesity research. *Disease models & mechanisms,* 9(11), 1245–1255.

Bartoli C, Brittian K, Giridharan G, Koenig S, Hamid T, Prabhu S (2011). Bovine model of doxorubicin-induced cardiomyopathy. *Journal of Biomedicine and Biotechnology,* 2011 758736–758736.

Bell D, Allen A, Kelso E, Balasubramaniam A, McDermott B (2002). Induction of hypertrophic responsiveness of cardiomyocytes to neuropeptide Y in response to pressure overload. *The Journal of pharmacology and experimental therapeutics,* 303(2), 581–591.

Bers DM (1997). Ca transport during contraction and relaxation in mammalian ventricular muscle. *Basic research in cardiology,* 92 Suppl 1 1–10.

Boucek RJ, Miracle A, Anderson M, Engelman R, Atkinson J, Dodd DA (1999). Persistent effects of doxorubicin on cardiac gene expression. *Journal of Molecular and Cellular Cardiology,* 31(8), 1435–1446.

Bradshaw A & Baker A (2013). Gene therapy for cardiovascular disease: perspectives and potential. *Vascular pharmacology,* 58(3), 174–181.

Brothers SP & Wahlestedt C (2010). Therapeutic potential of neuropeptide Y (NPY) receptor ligands. *EMBO molecular medicine,* 2(11), 429–439.

Bugger H & Abel ED (2014). Molecular mechanisms of diabetic cardiomyopathy. *Diabetologia,* 57(4), 660–671.

Callanan E, Lee E, Tilan J, Winaver J, Haramati A, Mulroney S, Zukowska Z (2007). Renal and cardiac neuropeptide Y and NPY receptors in a rat model of congestive heart failure. *AJP-Renal Physiology,* 293(6), F1811–F1817.

Calligaris SD, Lecanda M, Solis F, Ezquer M, Gutierrez J, Brandan E, Leiva A, Sobrevia L, Conget P (2013). Mice long-term high-fat diet feeding recapitulates human cardiovascular alterations: an animal model to study the early phases of diabetic cardiomyopathy. *PloS one,* 8(4), e60931.

Cao L, Qin X, Peterson MR, Haller SE, Wilson KA, Hu N, Lin X, Nair S, Ren J, He G (2016). CARD9 knockout ameliorates myocardial dysfunction associated with high fat diet-induced obesity. *Journal of Molecular and Cellular Cardiology,* 92, 185–195.

Cappetta D, Rossi F, Piegari E, Quaini F, Berrino L, Urbanek K, De Angelis A (2018). Doxorubicin targets multiple players: A new view of an old problem. *Pharmacological research,* 127, 4–14.

Carbone S, Canada J, Billingsley H, Siddiqui M, Elagizi A, Lavie C (2019). Obesity paradox in cardiovascular disease: where do we stand? *Vascular health and risk management,* 15, 89–100.

Carbone S, Lavie C, Elagizi A, Arena R, Ventura H (2020). The Impact of Obesity in Heart Failure. *Heart failure clinics,* 16(1), 71–80.

Chatterjee K, Zhang J, Honbo N, Karliner J (2010). Doxorubicin cardiomyopathy. *Cardiology,* 115(2), 155–162.

Chen C, Wang Z, Hsu C, Lin H, Chen J (2015). In Vivo Protective Effects of Diosgenin against Doxorubicin-Induced Cardiotoxicity. *Nutrients,* 7(6), 4938–4954.

Chen X, Guo Z, Wang P, Xu M (2014). Erythropoietin modulates imbalance of matrix metalloproteinase-2 and tissue inhibitor of metalloproteinase-2 in doxorubicin-induced cardiotoxicity. *Heart, lung and circulation,* 23(8), 772–777.

Chen Y, Huang T, Shi W, Fang J, Deng H, Cui G (2019). Potential targets for intervention against doxorubicin-induced cardiotoxicity based on genetic studies: a systematic review of the literature. *Journal of Molecular and Cellular Cardiology,* 138, 88–98.

Chien KR, Shimizu M, Hoshijima M, Minamisawa S, Grace AA (1997). Toward molecular strategies for heart disease – past, present, future. *Japanese circulation journal,* 61(2), 91–118.

Chinnasamy D, Milsom MD, Shaffer J, Neuenfeldt J, Shaaban AF, Margison GP, Fairbairn LJ, Chinnasamy N (2006). Multicistronic lentiviral vectors containing the FMDV 2A cleavage factor demonstrate robust expression of encoded genes at limiting MOI. *Virology journal,* 3, 14-422X-3-14.

Cuculi F, Herring N, De Caterina AR, Banning AP, Prendergast BD, Forfar JC, Choudhury RP, Channon KM, Kharbanda RK (2013). Relationship of plasma neuropeptide Y with angiographic, electrocardiographic and coronary physiology indices of reperfusion during ST elevation myocardial infarction. *Heart (British Cardiac Society),* 99(16), 1198–1203.

da Silva Xavier G & Hodson DJ (2018). Mouse models of peripheral metabolic disease. *Best practice & research.Clinical endocrinology & metabolism,* 32(3), 299–315.

Daltro PS, Barreto BC, Silva PG, Neto PC, Sousa Filho PHF, Santana Neta D, Carvalho GB, Silva DN, Paredes BD, de Alcantara AC, Freitas LAR, Couto RD, Santos RR, Souza BSF, Soares MBP, Macambira SG (2017). Therapy with mesenchymal stromal cells or conditioned medium reverse cardiac alterations in a high-fat diet-induced obesity model. *Cytotherapy,* 19(10), 1176–1188.

De Lorenzo A, Gratteri S, Gualtieri P, Cammarano A, Bertucci P, Di Renzo L (2019). Why primary obesity is a disease? *Journal of Translational Medicine,* 17(1), 169–169.

Del Buono MG, Buckley L, Abbate A (2018). Primary and Secondary Diastolic Dysfunction in Heart Failure With Preserved Ejection Fraction. *The American Journal of Cardiology,* 122(9), 1578–1587.

del Monte F, Williams E, Lebeche D, Schmidt U, Rosenzweig A, Gwathmey JK, Lewandowski ED, Hajjar RJ (2001). Improvement in survival and cardiac metabolism after gene transfer of sarcoplasmic reticulum Ca(2+)-ATPase in a rat model of heart failure. *Circulation,* 104(12), 1424–1429.

Dillmann W (2019). Diabetic Cardiomyopathy. *Circulation research,* 124(8), 1160–1162.

Doka G, Malikova E, Galkova K, La Rocca G, Kruzliak P, Adamek M, Rodrigo L, Krenek P, Klimas J (2017). Downregulation of myogenic microRNAs in sub-chronic but not in sub-acute model of daunorubicin-induced cardiomyopathy. *Molecular and cellular biochemistry,* 432(1–2), 79–89.

D'Oria R, Schipani R, Leonardini A, Natalicchio A, Perrini S, Cignarelli A, Laviola L, Giorgino F (2020). The Role of Oxidative Stress in Cardiac Disease: From Physiological Response to Injury Factor. *Oxidative medicine and cellular longevity,* 2020, 5732956.

Dvorakova M, Kruzliak P, Rabkin S (2014). Role of neuropeptides in cardiomyopathies. *Peptides,* 61 1–6.

Eisner DA, Caldwell JL, Kistamas K, Trafford AW (2017). Calcium and Excitation-Contraction Coupling in the Heart. *Circulation research,* 121(2), 181–195.

Ekblad E, Edvinsson L, Wahlestedt C, Uddman R, Håkanson R, Sundler F (1984). Neuropeptide Y co-exists and co-operates with noradrenaline in perivascular nerve fibers. *Regulatory peptides,* 8(3), 225–235.

Elagizi A, Kachur S, Lavie C, Carbone S, Pandey A, Ortega F, Milani R (2018). An Overview and Update on Obesity and the Obesity Paradox in Cardiovascular Diseases. *Progress in cardiovascular diseases,* 61(2), 142–150.

Evangelista I, Nuti R, Picchioni T, Dotta F, Palazzuoli A (2019). Molecular Dysfunction and Phenotypic Derangement in Diabetic Cardiomyopathy. *International journal of molecular sciences,* 20(13).

Fargnoli AS, Katz MG, Bridges CR, Hajjar RJ (2017). Gene Therapy in Heart Failure. *Handbook of Experimental Pharmacology,* 243, 395–421.

Federico M, Valverde C, Mattiazzi A, Palomeque J (2019). Unbalance Between Sarcoplasmic Reticulum Ca2 + Uptake and Release: A First Step Toward Ca2 + Triggered Arrhythmias and Cardiac Damage. *Frontiers in physiology,* 10, 1630–1630.

Feng W, Lei T, Wang Y, Feng R, Yuan J, Shen X, Wu Y, Gao J, Ding W, Lu Z (2019). GCN2 deficiency ameliorates cardiac dysfunction in diabetic mice by reducing lipotoxicity and oxidative stress. *Free radical biology & medicine,* 130, 128–139.

Fontaine DA & Davis DB (2016). Attention to Background Strain Is Essential for Metabolic Research: C57BL/6 and the International Knockout Mouse Consortium. *Diabetes,* 65(1), 25–33.

Friedmann T & Roblin R (1972). Gene therapy for human genetic disease? *Science,* 175(4025), 949–955.

Friedmann T (1990). The evolving concept of gene therapy. *Human Gene Therapy,* 1(2), 175–181.

Fuchs T, Loureiro MP, Macedo LE, Nocca D, Nedelcu M, Costa-Casagrande TA (2018). Animal models in metabolic syndrome. *Revista do Colegio Brasileiro de Cirurgioes,* 45(5), e1975-6991e-20181975.

Gabisonia K & Recchia F (2018). Gene Therapy for Heart Failure: New Perspectives. *Current Heart Failure Reports,* 15(6), 340–349.

Gambardella J, Trimarco B, Iaccarino G, Santulli G (2018). New Insights in Cardiac Calcium Handling and Excitation-Contraction Coupling. *Advances in Experimental Medicine and Biology,* 1067, 373–385.

Gambliel H, Burke B, Cusack B, Walsh G, Zhang Y, Mushlin P, Olson R (2002). Doxorubicin and C-13 deoxydoxorubicin effects on ryanodine receptor gene expression. *Biochemical and biophysical research communications,* 291(3), 433–438.

Ge W, Yuan M, Ceylan AF, Wang X, Ren J (2016). Mitochondrial aldehyde dehydrogenase protects against doxorubicin cardiotoxicity through a transient receptor potential channel vanilloid 1-mediated mechanism. *Biochimica et biophysica acta,* 1862(4), 622–634.

Ghigo A, Li M, Hirsch E (2016). New signal transduction paradigms in anthracycline-induced cardiotoxicity. *Biochimica et biophysica acta,* 1863(7), 1916–1925.

Gianni D, Chan J, Gwathmey JK, del Monte F, Hajjar RJ (2005). SERCA2a in heart failure: role and therapeutic prospects. *Journal of Bioenergetics and Biomembranes,* 37(6), 375–380.

Gilbert ER, Fu Z, Liu D (2011). Development of a nongenetic mouse model of type 2 diabetes. *Experimental diabetes research,* 2011, 416254.

Ginn SL, Amaya AK, Alexander IE, Edelstein M, Abedi MR (2018). Gene therapy clinical trials worldwide to 2017: An update. *The journal of gene medicine,* 20(5), e3015.

Gonder JC & Laber K (2007). A renewed look at laboratory rodent housing and management. *ILAR journal,* 48(1), 29–36.

Greenberg B, Yaroshinsky A, Zsebo K, Butler J, Felker GM, Voors A, Rudy J, Wagner K, Hajjar R (2014). Design of a phase 2b trial of intracoronary administration of AAV1/SERCA2a in patients with advanced heart failure: the CUPID 2 trial (calcium up-regulation by percutaneous administration of gene therapy in cardiac disease phase 2b). *JACC Heart Fail,* 2(1), 84–92.

Greenberg B, Butler J, Felker GM, Ponikowski P, Voors AA, Desai AS, Barnard D, Bouchard A, Jaski B, Lyon AR, Pogoda JM, Rudy JJ, Zsebo KM (2016). Calcium upregulation by percutaneous administration of gene therapy in patients with cardiac disease (CUPID 2): a randomised, multinational, double-blind, placebo-controlled, phase 2b trial. *Lancet (London, England),* 387(10024), 1178–1186.

Gu J, Polak JM, Allen JM, Huang WM, Sheppard MN, Tatemoto K, Bloom SR (1984). High concentrations of a novel peptide, neuropeptide Y, in the innervation of mouse and rat heart. *The journal of histochemistry and cytochemistry: official journal of the Histochemistry Society,* 32(5), 467–472.

Guenancia C, Hachet O, Aboutabl M, Li N, Rigal E, Cottin Y, Rochette L, Vergely C (2016). Overweight in mice, induced by perinatal programming, exacerbates doxorubicin and trastuzumab cardiotoxicity. *Cancer chemotherapy and pharmacology,* 77(4), 777–785.

Gwathmey JK, Copelas L, MacKinnon R, Schoen FJ, Feldman MD, Grossman W, Morgan JP (1987). Abnormal intracellular calcium handling in myocardium from patients with end-stage heart failure. *Circulation research,* 61(1), 70–76.

Hajjar RJ, del Monte F, Matsui T, Rosenzweig A (2000). Prospects for gene therapy for heart failure. *Circulation research,* 86(6), 616–621.

Hall JE, do Carmo JM, da Silva AA, Wang Z, Hall ME (2015). Obesity-induced hypertension: interaction of neurohumoral and renal mechanisms. *Circulation research,* 116(6), 991–1006.

Hanna A, Lam A, Tham S, Dulhunty A, Beard N (2014). Adverse effects of doxorubicin and its metabolic product on cardiac RyR2 and SERCA2A. *Molecular pharmacology,* 86(4), 438–449.

Hartikainen J, Hassinen I, Hedman A, Kivela A, Saraste A, Knuuti J, Husso M, Mussalo H, Hedman M, Rissanen TT, Toivanen P, Heikura T, Witztum JL, Tsimikas S, Yla-Herttuala S (2017). Adenoviral intramyocardial VEGF-DDeltaNDeltaC gene transfer increases myocardial perfusion reserve in refractory angina patients: a phase I/IIa study with 1-year follow-up. *European heart journal,* 38(33), 2547–2555.

Hassinen I, Kivela A, Hedman A, Saraste A, Knuuti J, Hartikainen J, Yla-Herttuala S (2016). Intramyocardial Gene Therapy Directed to Hibernating Heart Muscle Using a Combination of Electromechanical Mapping and Positron Emission Tomography. *Human Gene Therapy,* 27(10), 830–834.

Hayward C, Banner NR, Morley-Smith A, Lyon AR, Harding SE (2015). The Current and Future Landscape of SERCA Gene Therapy for Heart Failure: A Clinical Perspective. *Human Gene Therapy,* 26(5), 293–304.

Heidenreich PA, Albert NM, Allen LA, Bluemke DA, Butler J, Fonarow GC, Ikonomidis JS, Khavjou O, Konstam MA, Maddox TM, Nichol G, Pham M, Pina IL, Trogdon JG, American Heart Association Advocacy Coordinating Committee, Council on Arteriosclerosis, Thrombosis and Vascular Biology, Council on Cardiovascular Radiology and Intervention, Council on Clinical Cardiology, Council on Epidemiology and Prevention, Stroke Council (2013). Forecasting the impact of heart failure in the United States: a policy statement from the American Heart Association. *Circulation.Heart failure,* 6(3), 606–619.

Heredia MdP, Delgado C, Pereira L, Perrier R, Richard S, Vassort G, Bénitah J, Gómez A (2005). Neuropeptide Y rapidly enhances [Ca2+]i transients and Ca2+ sparks in adult rat ventricular myocytes through Y1 receptor and PLC activation. *Journal of Molecular and Cellular Cardiology,* 38(1), 205–212.

Herring N (2015). Autonomic control of the heart: going beyond the classical neurotransmitters. *Experimental physiology,* 100(4), 354–358.

Heydemann A (2016). An Overview of Murine High Fat Diet as a Model for Type 2 Diabetes Mellitus. *Journal of diabetes research,* 2016, 2902351.

High K & Roncarolo M (2019). Gene Therapy. *The New England journal of medicine,* 381(5), 455–464.

Hirsch D & Zukowska Z (2012). NPY and stress 30 years later: the peripheral view. *Cellular and molecular neurobiology,* 32(5), 645–659.

Horwich T, Fonarow G, Clark A (2018). Obesity and the Obesity Paradox in Heart Failure. *Progress in cardiovascular diseases,* 61(2), 151–156.

Hu J, Xu X, Zuo Y, Gao X, Wang Y, Xiong C, Zhou H, Zhu S (2017). NPY Impairs Cell Viability and Mitochondrial Membrane Potential Through Ca2+ and p38 Signaling Pathways in Neonatal Rat Cardiomyocytes. *Journal of cardiovascular pharmacology,* 70(1), 52–59.

Huang R, Shi Z, Chen L, Zhang Y, Li J, An Y (2017). Rutin alleviates diabetic cardiomyopathy and improves cardiac function in diabetic ApoEknockout mice. *European journal of pharmacology,* 814, 151–160.

Hulot JS, Salem JE, Redheuil A, Collet JP, Varnous S, Jourdain P, Logeart D, Gandjbakhch E, Bernard C, Hatem SN, Isnard R, Cluzel P, Le Feuvre C, Leprince P, Hammoudi N, Lemoine FM, Klatzmann D, Vicaut E, Komajda M, Montalescot G, Lompre AM, Hajjar RJ, AGENT-HF Investigators (2017). Effect of intracoronary administration of AAV1/SERCA2a on ventricular remodelling in patients with advanced systolic heart failure: results from the AGENT-HF randomized phase 2 trial. *European journal of heart failure,* 19(11), 1534–1541.

Hulting J, Sollevi A, Ullman B, Franco Cereceda A, Lundberg JM (1990). Plasma neuropeptide Y on admission to a coronary care unit: raised levels in patients with left heart failure. *Cardiovascular research,* 24(2), 102–108.

Hung CL, Pan SH, Han CL, Chang CW, Hsu YL, Su CH, Shih SC, Lai YJ, Chiang Chiau JS, Yeh HI, Liu CY, Lee HC, Lam CSP (2017). Membrane Proteomics of Impaired Energetics and Cytoskeletal Disorganization in Elderly Diet-Induced Diabetic Mice. *Journal of proteome research,* 16(10), 3504–3513.

Ilebekk A, Bjorkman JA, Nordlander M (2005). Influence of endogenous neuropeptide Y (NPY) on the sympathetic-parasympathetic interaction in the canine heart. *Journal of cardiovascular pharmacology,* 46(4), 474–480.

Ishikawa K, Weber T, Hajjar RJ (2018). Human Cardiac Gene Therapy. *Circulation research,* 123(5), 601–613.

Ito T, Muraoka S, Takahashi K, Fujio Y, Schaffer SW, Azuma J (2009). Beneficial effect of taurine treatment against doxorubicin-induced cardiotoxicity in mice. *Advances in Experimental Medicine and Biology,* 643, 65–74.

Iwanaga Y, Hoshijima M, Gu Y, Iwatate M, Dieterle T, Ikeda Y, Date M, Chrast J, Matsuzaki M, Peterson K, Chien K, Ross J (2004). Chronic phospholamban inhibition prevents progressive cardiac dysfunction and pathological remodeling after infarction in rats. *Journal of Clinical Investigation,* 113(5), 727–736.

Jacques D, D'Orléans Juste P, Magder S, Bkaily G (2017). Neuropeptide Y and its receptors in ventricular endocardial endothelial cells. *Canadian journal of physiology and pharmacology,* 95(10), 1224–1229.

Jacques D & Abdel Samad D (2007). Neuropeptide Y (NPY) and NPY receptors in the cardiovascular system: implication in the regulation of intracellular calcium. *Canadian journal of physiology and pharmacology,* 85(1), 43–53.

James P, Inui M, Tada M, Chiesi M, Carafoli E (1989). Nature and site of phospholamban regulation of the Ca2+ pump of sarcoplasmic reticulum. *Nature,* 342(6245), 90–92.

Jessup M, Greenberg B, Mancini D, Cappola T, Pauly D, Jaski B, Yaroshinsky A, Zsebo K, Dittrich H, Hajjar R (2011). Calcium Upregulation by Percutaneous Administration of Gene Therapy in Cardiac Disease (CUPID): a phase 2 trial of intracoronary gene therapy of sarcoplasmic reticulum Ca2+-ATPase in patients with advanced heart failure. *Circulation,* 124(3), 304–313.

Jessup M & Brozena S (2003). Heart failure. *The New England journal of medicine,* 348(20), 2007–2018.

Jin W, Qiao Z, Zheng C, Li S, Chen H (2014). [Protein interacting with kinase Cα mediates the down-regulation of myocardial norepinephrine transporter expression in mice with adriamycin-induced congestive heart failure]. *中华心血管病杂志,* 42(3), 219–224.

Kalyanaraman B (2019). Teaching the basics of the mechanism of doxorubicin-induced cardiotoxicity: Have we been barking up the wrong tree? *Redox Biology,* 29, 101394–101394.

Kannel WB, Hjortland M, Castelli WP (1974). Role of diabetes in congestive heart failure: the Framingham study. *The American Journal of Cardiology,* 34(1), 29–34.

Kappel S, Hawkins P, Mendl MT (2017). To Group or Not to Group? Good Practice for Housing Male Laboratory Mice. *Animals: an open access journal from MDPI,* 7(12), 10.3390/ani7120088.

Katz AM (1989). Changing strategies in the management of heart failure. *Journal of the American College of Cardiology,* 13(3), 513–523.

Kawase Y, Ly H, Prunier F, Lebeche D, Shi Y, Jin H, Hadri L, Yoneyama R, Hoshino K, Takewa Y, Sakata S, Peluso R, Zsebo K, Gwathmey J, Tardif J, Tanguay J, Hajjar R (2008). Reversal of cardiac dysfunction after long-term expression of SERCA2a by gene transfer in a pre-clinical model of heart failure. *Journal of the American College of Cardiology,* 51(11), 1112–1119.

Kenny H & Abel ED (2019). Heart Failure in Type 2 Diabetes Mellitus. *Circulation research,* 124(1), 121–141.

Kleinert M, Clemmensen C, Hofmann SM, Moore MC, Renner S, Woods SC, Huypens P, Beckers J, de Angelis MH, Schurmann A, Bakhti M, Klingenspor M, Heiman M, Cherrington AD, Ristow M, Lickert H, Wolf E, Havel PJ, Muller TD, Tschop MH (2018). Animal models of obesity and diabetes mellitus. *Nature reviews.Endocrinology,* 14(3), 140–162.

Kondo H, Abe I, Gotoh K, Fukui A, Takanari H, Ishii Y, Ikebe Y, Kira S, Oniki T, Saito S, Aoki K, Tanino T, Mitarai K, Kawano K, Miyoshi M, Fujinami M, Yoshimura S, Ayabe R, Okada N, Nagano Y, Akioka H, Shinohara T, Akiyoshi K, Masaki T, Teshima Y, Yufu K, Nakagawa M, Takahashi N (2018). Interleukin 10 Treatment Ameliorates High-Fat Diet-Induced Inflammatory Atrial Remodeling and Fibrillation. *Circulation. Arrhythmia and electrophysiology,* 11(5), e006040.

Kucerova D, Doka G, Kruzliak P, Turcekova K, Kmecova J, Brnoliakova Z, Kyselovic J, Kirchhefer U, Müller F, Krenek P, Boknik P, Klimas J (2015). Unbalanced upregulation of ryanodine receptor 2 plays a particular role in early development of daunorubicin cardiomyopathy. *American journal of translational research,* 7(7), 1280–1294.

Kuo LE, Kitlinska JB, Tilan JU, Li L, Baker SB, Johnson MD, Lee EW, Burnett MS, Fricke ST, Kvetnansky R, Herzog H, Zukowska Z (2007). Neuropeptide Y acts directly in the periphery on

fat tissue and mediates stress-induced obesity and metabolic syndrome. *Nature medicine,* 13(7), 803–811.

Lahteenvuo J & Yla-Herttuala S (2017). Advances and Challenges in Cardiovascular Gene Therapy. *Human Gene Therapy,* 28(11), 1024–1032.

Lavie C, Laddu D, Arena R, Ortega F, Alpert M, Kushner R (2018). Healthy Weight and Obesity Prevention: JACC Health Promotion Series. *Journal of the American College of Cardiology,* 72(13), 1506–1531.

Li K, Sung RYT, Huang W, Yang M, Pong N, Lee S, Chan W, Zhao H, To M, Fok T, Li C, Wong Y, Ng P (2006). Thrombopoietin protects against in vitro and in vivo cardiotoxicity induced by doxorubicin. *Circulation,* 113(18), 2211–2220.

Li C, Li X, Chang Y, Zhao L, Liu B, Wei S, Xu F, Zhang Y, Chen Y (2018). Aldehyde Dehydrogenase-2 Attenuates Myocardial Remodeling and Contractile Dysfunction Induced by a High-Fat Diet. *Cellular physiology and biochemistry: international journal of experimental cellular physiology, biochemistry, and pharmacology,* 48(5), 1843–1853.

Liang L, Shou XL, Zhao HK, Ren GQ, Wang JB, Wang XH, Ai WT, Maris JR, Hueckstaedt LK, Ma AQ, Zhang Y (2015). Antioxidant catalase rescues against high fat diet-induced cardiac dysfunction via an IKKbeta-AMPK-dependent regulation of autophagy. *Biochimica et biophysica acta,* 1852(2), 343–352.

Liu D, Ma Z, Di S, Yang Y, Yang J, Xu L, Reiter RJ, Qiao S, Yuan J (2018). AMPK/PGC1alpha activation by melatonin attenuates acute doxorubicin cardiotoxicity via alleviating mitochondrial oxidative damage and apoptosis. *Free radical biology & medicine,* 129, 59–72.

Llach A, Mazevet M, Mateo P, Villejouvert O, Ridoux A, Rucker-Martin C, Ribeiro M, Fischmeister R, Crozatier B, Benitah JP, Morel E, Gomez AM (2019). Progression of excitation-contraction coupling defects in doxorubicin cardiotoxicity. *Journal of Molecular and Cellular Cardiology,* 126, 129–139.

Lopez-Sendon J, Alvarez-Ortega C, Zamora Aunon P, Buno Soto A, Lyon AR, Farmakis D, Cardinale D, Canales Albendea M, Feliu Batlle J, Rodriguez Rodriguez I, Rodriguez Fraga O, Albaladejo A, Mediavilla G, Gonzalez-Juanatey JR, Martinez Monzonis A, Gomez Prieto P, Gonzalez-Costello J, Serrano Antolin JM, Cadenas Chamorro R, Lopez Fernandez T (2020). Classification, prevalence, and outcomes of anticancer therapy-induced cardiotoxicity: the CARDIOTOX registry. *European heart journal,* 41(18), 1720–1729.

Lucas E, Vila-Bedmar R, Arcones AC, Cruces-Sande M, Cachofeiro V, Mayor F,Jr, Murga C (2016). Obesity-induced cardiac lipid accumulation in adult mice is modulated by G protein-coupled receptor kinase 2 levels. *Cardiovascular diabetology,* 15(1), 155-016-0474-6.

Luo G, Xu X, Guo W, Luo C, Wang H, Meng X, Zhu S, Wei Y (2015). Neuropeptide Y damages the integrity of mitochondrial structure and disrupts energy metabolism in cultured neonatal rat cardiomyocytes. *Peptides (New York, NY : 1980),* 71 162–169.

Ly H (2007). Gene therapy in the treatment of heart failure. *Physiology,* 22(Bethesda), 81–96.

MacLennan D & Kranias E (2003). Phospholamban: a crucial regulator of cardiac contractility. *Nature Reviews Molecular Cell Biology,* 4(7), 566–577.

Martonosi AN & Pikula S (2003). The structure of the Ca2+-ATPase of sarcoplasmic reticulum. *Acta Biochimica Polonica,* 50(2), 337–365.

Matsumura N, Zordoky BN, Robertson IM, Hamza SM, Parajuli N, Soltys CM, Beker DL, Grant MK, Razzoli M, Bartolomucci A, Dyck JRB (2018). Co-administration of resveratrol with doxorubicin in young mice attenuates detrimental late-occurring cardiovascular changes. *Cardiovascular research,* 114(10), 1350–1359.

Matyal R, Sakamuri S, Wang A, Mahmood E, Robich M, Khabbaz K, Hess P, Sellke F, Mahmood F (2013). Local infiltration of neuropeptide Y as a potential therapeutic agent against apoptosis and fibrosis in a swine model of hypercholesterolemia and chronic myocardial ischemia. *European journal of pharmacology,* 718(1–3), 261–270.

Mazurek J & Jessup M (2017). Understanding Heart Failure. *Heart failure clinics,* 13(1), 1–19.

McDermott BJ & Bell D (2007). NPY and cardiac diseases. *Current topics in medicinal chemistry,* 7(17), 1692–1703.

Mekada K, Abe K, Murakami A, Nakamura S, Nakata H, Moriwaki K, Obata Y, Yoshiki A (2009). Genetic differences among C57BL/6 substrains. *Experimental animals,* 58(2), 141–149.

Merentie M, Lottonen-Raikaslehto L, Parviainen V, Huusko J, Pikkarainen S, Mendel M, Laham-Karam N, Karja V, Rissanen R, Hedman M, Yla-Herttuala S (2016). Efficacy and safety of myocardial gene transfer of adenovirus, adeno-associated virus and lentivirus vectors in the mouse heart. *Gene therapy,* 23(3), 296–305.

Metra M & Teerlink JR (2017). Heart failure. *Lancet (London, England),* 390(10106), 1981–1995.

Meyer M, Schillinger W, Pieske B, Holubarsch C, Heilmann C, Posival H, Kuwajima G, Mikoshiba K, Just H, Hasenfuss G (1995). Alterations of sarcoplasmic reticulum proteins in failing human dilated cardiomyopathy. *Circulation,* 92(4), 778–784.

Milani-Nejad N & Janssen PM (2014). Small and large animal models in cardiac contraction research: advantages and disadvantages. *Pharmacology & therapeutics,* 141(3), 235–249.

Millar BC, Schlüter KD, Zhou XJ, McDermott BJ, Piper HM (1994). Neuropeptide Y stimulates hypertrophy of adult ventricular cardiomyocytes. *American journal of physiology,* 266(5), C1271–C1277.

Mingozzi F, Anguela XM, Pavani G, Chen Y, Davidson RJ, Hui DJ, Yazicioglu M, Elkouby L, Hinderer CJ, Faella A, Howard C, Tai A, Podsakoff GM, Zhou S, Basner-Tschakarjan E, Wright JF, High KA (2013). Overcoming preexisting humoral immunity to AAV using capsid decoys. *Science translational medicine,* 5(194), 194ra92.

Miyamoto MI, del Monte F, Schmidt U, DiSalvo TS, Kang ZB, Matsui T, Guerrero JL, Gwathmey JK, Rosenzweig A, Hajjar RJ (2000). Adenoviral gene transfer of SERCA2a improves left-ventricular function in aortic-banded rats in transition to heart failure. *Proceedings of the National Academy of Sciences of the United States of America,* 97(2), 793–798.

Mizuguchi H, Xu Z, Ishii-Watabe A, Uchida E, Hayakawa T (2000). IRES-dependent second gene expression is significantly lower than cap-dependent first gene expression in a bicistronic vector. *Molecular therapy: the journal of the American Society of Gene Therapy,* 1(4), 376–382.

Muller OJ, Katus HA, Bekeredjian R (2007). Targeting the heart with gene therapy-optimized gene delivery methods. *Cardiovascular research,* 73(3), 453–462.

Murtaza G, Virk HUH, Khalid M, Lavie C, Ventura H, Mukherjee D, Ramu V, Bhogal S, Kumar G, Shanmugasundaram M, Paul T (2019). Diabetic cardiomyopathy – A comprehensive updated review. *Progress in cardiovascular diseases,* 62(4), 315–326.

Naso M, Tomkowicz B, Perry W, Strohl W (2017). Adeno-Associated Virus (AAV) as a Vector for Gene Therapy. *BioDrugs,* 31(4), 317–334.

Neilan T, Jassal D, Perez Sanz T, Raher M, Pradhan A, Buys E, Ichinose F, Bayne D, Halpern E, Weyman A, Derumeaux G, Bloch K, Picard M, Scherrer Crosbie M (2006). Tissue Doppler imaging predicts left ventricular dysfunction and mortality in a murine model of cardiac injury. *European heart journal,* 27(15), 1868–1875.

Niwano K, Arai M, Koitabashi N, Watanabe A, Ikeda Y, Miyoshi H, Kurabayashi M (2008). Lentiviral vector-mediated SERCA2 gene transfer protects against heart failure and left ventricular remodeling after myocardial infarction in rats. *Molecular therapy,* 16(6), 1026–1032.

Nozaki N, Shishido T, Takeishi Y, Kubota I (2004). Modulation of doxorubicin-induced cardiac dysfunction in toll-like receptor-2-knockout mice. *Circulation,* 110(18), 2869–2874.

Octavia Y, Tocchetti C, Gabrielson K, Janssens S, Crijns H, Moens A (2012). Doxorubicin-induced cardiomyopathy: from molecular mechanisms to therapeutic strategies. *Journal of Molecular and Cellular Cardiology,* 52(6), 1213–1225.

Oh A, Okazaki R, Sam F, Valero Muñoz M (2019). Heart Failure With Preserved Ejection Fraction and Adipose Tissue: A Story of Two Tales. *Frontiers in Cardiovascular Medicine,* 6, 110–110.

Olson E (2004). A decade of discoveries in cardiac biology. *Nature medicine,* 10(5), 467–474.

Olson LE, Bedja D, Alvey SJ, Cardounel AJ, Gabrielson KL, Reeves RH (2003). Protection from doxorubicin-induced cardiac toxicity in mice with a null allele of carbonyl reductase 1. *Cancer research,* 63(20), 6602–6606.

Özkaramanli Gür D, Sagbas M, Akyüz A, Güzel S, Alpsoy S, Güler N (2017). Role of sympathetic cotransmitter galanin on autonomic balance in heart failure: an active player or a bystander? *Anatolian journal of cardiology,* 18(4), 281–288.

Pereira L, Ruiz-Hurtado G, Rueda A, Mercadier JJ, Benitah JP, Gomez AM (2014). Calcium signaling in diabetic cardiomyocytes. *Cell calcium,* 56(5), 372–380.

Persson H, Andreasson K, Kahan T, Eriksson SV, Tidgren B, Hjemdahl P, Hall C, Erhardt L (2002). Neurohormonal activation in heart failure after acute myocardial infarction treated with beta-receptor antagonists. *European journal of heart failure,* 4(1), 73–82.

Pesonen U (2008). NPY L7P polymorphism and metabolic diseases. *Regulatory peptides,* 149(1–3), 51–55.

Polegato B, Minicucci M, Azevedo P, Carvalho R, Chiuso Minicucci F, Pereira E, Paiva SAR, Zornoff LAM, Okoshi M, Matsubara B, Matsubara L (2015). Acute doxorubicin-induced cardiotoxicity is associated with matrix metalloproteinase-2 alterations in rats. *Cellular physiology and biochemistry,* 35(5), 1924–1933.

Polyakova V, Loeffler I, Hein S, Miyagawa S, Piotrowska I, Dammer S, Risteli J, Schaper J, Kostin S (2011). Fibrosis in endstage human heart failure: severe changes in collagen metabolism and MMP/TIMP profiles. *International journal of cardiology,* 151(1), 18–33.

Poornima IG, Parikh P, Shannon RP (2006). Diabetic cardiomyopathy: the search for a unifying hypothesis. *Circulation research,* 98(5), 596–605.

Prathumsap N, Shinlapawittayatorn K, Chattipakorn SC, Chattipakorn N (2020). Effects of doxorubicin on the heart: From molecular mechanisms to intervention strategies. *European journal of pharmacology,* 866, 172818.

Prunier F, Kawase Y, Gianni D, Scapin C, Danik S, Ellinor P, Hajjar R, Del Monte F (2008). Prevention of ventricular arrhythmias with sarcoplasmic reticulum Ca2+ ATPase pump overexpression in a porcine model of ischemia reperfusion. *Circulation,* 118(6), 614–624.

Reddy YNV & Borlaug B (2016). Heart Failure With Preserved Ejection Fraction. *Current problems in cardiology,* 41(4), 145–188.

Renu K, V G A, P B TP, Arunachalam S (2018). Molecular mechanism of doxorubicin-induced cardiomyopathy – An update. *European journal of pharmacology,* 818, 241–253.

Riad A, Bien S, Gratz M, Escher F, Westermann D, Heimesaat MM, Bereswill S, Krieg T, Felix SB, Schultheiss HP, Kroemer HK, Tschope C (2008). Toll-like receptor-4 deficiency attenuates doxorubicin-induced cardiomyopathy in mice. *European journal of heart failure,* 10(3), 233–243.

Rinne P, Harjunpaa J, Scheinin M, Savontaus E (2008). Blood pressure regulation and cardiac autonomic control in mice overexpressing alpha- and gamma-melanocyte stimulating hormone. *Peptides,* 29(11), 1943–1952.

Rinne P, Nordlund W, Heinonen I, Penttinen AM, Saraste A, Ruohonen ST, Makela S, Vahatalo L, Kaipio K, Cai M, Hruby VJ, Ruohonen S, Savontaus E (2013). alpha-Melanocyte-stimulating hormone regulates vascular NO availability and protects against endothelial dysfunction. *Cardiovascular research,* 97(2), 360–368.

Rubler S, Dlugash J, Yuceoglu YZ, Kumral T, Branwood AW, Grishman A (1972). New type of cardiomyopathy associated with diabetic glomerulosclerosis. *The American Journal of Cardiology,* 30(6), 595–602.

Ruohonen S, Pesonen U, Moritz N, Kaipio K, Röyttä M, Koulu M, Savontaus E (2008). Transgenic mice overexpressing neuropeptide Y in noradrenergic neurons: a novel model of increased adiposity and impaired glucose tolerance. *Diabetes,* 57(6), 1517–1525.

Ruohonen S, Abe K, Kero M, Toukola L, Röyttä M, Koulu M, Pesonen U, Zukowska Z, Savontaus E (2009). Sympathetic nervous system-targeted neuropeptide Y overexpression in mice enhances

neointimal formation in response to vascular injury. *Peptides (New York, NY: 1980),* 30(4), 715–720.

Ruohonen S, Pesonen U, Savontaus E (2012). Neuropeptide Y in the noradrenergic neurons induces the development of cardiometabolic diseases in a transgenic mouse model. *Indian journal of endocrinology and metabolism,* 16(Suppl 3), S569–S576.

Sahu B, Kumar J, Kuncha M, Borkar R, Srinivas R, Sistla R (2016). Baicalein alleviates doxorubicin-induced cardiotoxicity via suppression of myocardial oxidative stress and apoptosis in mice. *Life Sciences,* 144, 8–18.

Sakata S, Lebeche D, Sakata N, Sakata Y, Chemaly E, Liang L, Tsuji T, Takewa Y, del Monte F, Peluso R, Zsebo K, Jeong D, Park W, Kawase Y, Hajjar R (2007). Restoration of mechanical and energetic function in failing aortic-banded rat hearts by gene transfer of calcium cycling proteins. *Journal of Molecular and Cellular Cardiology,* 42(4), 852–861.

Schmidt U, Hajjar RJ, Helm PA, Kim CS, Doye AA, Gwathmey JK (1998). Contribution of abnormal sarcoplasmic reticulum ATPase activity to systolic and diastolic dysfunction in human heart failure. *Journal of Molecular and Cellular Cardiology,* 30(10), 1929–1937.

Schreyer SA, Wilson DL, LeBoeuf RC (1998). C57BL/6 mice fed high fat diets as models for diabetes-accelerated atherosclerosis. *Atherosclerosis,* 136(1), 17–24.

Selkirk SM (2004). Gene therapy in clinical medicine. *Postgraduate medical journal,* 80(948), 560–570.

Shanks J & Herring N (2013). Peripheral cardiac sympathetic hyperactivity in cardiovascular disease: role of neuropeptides. *American journal of physiology.Regulatory, integrative and comparative physiology,* 305(12), R1411–R1420.

Shareef MA, Anwer LA, Poizat C (2014). Cardiac SERCA2A/B: therapeutic targets for heart failure. *European journal of pharmacology,* 724, 1–8.

Singal PK & Iliskovic N (1998). Doxorubicin-induced cardiomyopathy. *The New England journal of medicine,* 339(13), 900–905.

Singh RM, Waqar T, Howarth FC, Adeghate E, Bidasee K, Singh J (2018). Hyperglycemia-induced cardiac contractile dysfunction in the diabetic heart. *Heart failure reviews,* 23(1), 37–54.

Sitsel A, De Raeymaecker J, Drachmann ND, Derua R, Smaardijk S, Andersen JL, Vandecaetsbeek I, Chen J, De Maeyer M, Waelkens E, Olesen C, Vangheluwe P, Nissen P (2019). Structures of the heart specific SERCA2a Ca(2+)-ATPase. *The EMBO journal,* 38(5), 10.15252/embj.2018100020. Epub 2019 Feb 18.

Snipelisky D, Chaudhry SP, Stewart GC (2019). The Many Faces of Heart Failure. *Cardiac electrophysiology clinics,* 11(1), 11–20.

Sun Y, Zhou S, Guo H, Zhang J, Ma T, Zheng Y, Zhang Z, Cai L (2020). Protective effects of sulforaphane on type 2 diabetes-induced cardiomyopathy via AMPK-mediated activation of lipid metabolic pathways and NRF2 function. *Metabolism: clinical and experimental,* 102, 154002.

Tacar O, Sriamornsak P, Dass C (2013). Doxorubicin: an update on anticancer molecular action, toxicity and novel drug delivery systems. *Journal of Pharmacy and Pharmacology,* 65(2), 157–170.

Tan CMJ, Green P, Tapoulal N, Lewandowski A, Leeson P, Herring N (2018). The Role of Neuropeptide Y in Cardiovascular Health and Disease. *Frontiers in physiology,* 9, 1281–1281.

Tatemoto K (1982). Neuropeptide Y: complete amino acid sequence of the brain peptide. *Proceedings of the National Academy of Sciences of the United States of America,* 79(18), 5485–5489.

Tilemann L, Ishikawa K, Weber T, Hajjar RJ (2012). Gene therapy for heart failure. *Circulation research,* 110(5), 777–793.

Tocchetti C, Carpi A, Coppola C, Quintavalle C, Rea D, Campesan M, Arcari A, Piscopo G, Cipresso C, Monti M, De Lorenzo C, Arra C, Condorelli G, Di Lisa F, Maurea N (2014). Ranolazine protects from doxorubicin-induced oxidative stress and cardiac dysfunction. *European journal of heart failure,* 16(4), 358–366.

Tong J, Ganguly PK, Singal PK (1991). Myocardial adrenergic changes at two stages of heart failure due to adriamycin treatment in rats. *American Journal of Physiology,* 260(3), H909–H916.

Tsuji T, Del Monte F, Yoshikawa Y, Abe T, Shimizu J, Nakajima Takenaka C, Taniguchi S, Hajjar R, Takaki M (2009). Rescue of Ca2+ overload-induced left ventricular dysfunction by targeted ablation of phospholamban. *AJP-Heart and Circulatory Physiology,* 296(2), H310–H317.

Turer AT, Hill JA, Elmquist JK, Scherer PE (2012). Adipose tissue biology and cardiomyopathy: translational implications. *Circulation research,* 111(12), 1565–1577.

Ullman B, Hulting J, Lundberg JM (1994). Prognostic value of plasma neuropeptide-Y in coronary care unit patients with and without acute myocardial infarction. *European heart journal,* 15(4), 454–461.

Umlauf J & Horký M (2002). Molecular biology of doxorubicin-induced cardiomyopathy. *Experimental and clinical cardiology,* 7(1), 35–39.

Vähätalo LH, Ruohonen ST, Mäkelä S, Kovalainen M, Huotari A, Mäkelä KA, Määttä JA, Miinalainen I, Gilsbach R, Hein L, Ailanen L, Mattila M, Eerola K, Röyttä M, Herzig K, Savontaus E (2015). Neuropeptide Y in the noradrenergic neurones induces obesity and inhibits sympathetic tone in mice. *Acta physiologica,* 213(4), 902–919.

Vähätalo L, Ruohonen S, Ailanen L, Savontaus E (2016). Neuropeptide Y in noradrenergic neurons induces obesity in transgenic mouse models. *Neuropeptides,* 55, 31–37.

van Acker FA, Hulshof JW, Haenen GR, Menge WM, van der Vijgh WJ, Bast A (2001). New synthetic flavonoids as potent protectors against doxorubicin-induced cardiotoxicity. *Free radical biology & medicine,* 31(1), 31–37.

Volpe M, Rubattu S, Burnett J (2014). Natriuretic peptides in cardiovascular diseases: current use and perspectives. *European heart journal,* 35(7), 419–425.

Wang JJ, Rau C, Avetisyan R, Ren S, Romay MC, Stolin G, Gong KW, Wang Y, Lusis AJ (2016). Genetic Dissection of Cardiac Remodeling in an Isoproterenol-Induced Heart Failure Mouse Model. *PLoS genetics,* 12(7), e1006038.

Wang Y, Qian Y, Fang Q, Zhong P, Li W, Wang L, Fu W, Zhang Y, Xu Z, Li X, Liang G (2017). Saturated palmitic acid induces myocardial inflammatory injuries through direct binding to TLR4 accessory protein MD2. *Nature communications,* 8, 13997.

Wenningmann N, Knapp M, Ande A, Vaidya TR, Ait-Oudhia S (2019). Insights into Doxorubicin-induced Cardiotoxicity: Molecular Mechanisms, Preventive Strategies, and Early Monitoring. *Molecular pharmacology,* 96(2), 219–232.

Willis MS, Parry TL, Brown DI, Mota RI, Huang W, Beak JY, Sola M, Zhou C, Hicks ST, Caughey MC, D'Agostino RB,Jr, Jordan J, Hundley WG, Jensen BC (2019). Doxorubicin Exposure Causes Subacute Cardiac Atrophy Dependent on the Striated Muscle-Specific Ubiquitin Ligase MuRF1. *Circulation.Heart failure,* 12(3), e005234.

Wirth T, Parker N, Ylä Herttuala S (2013). History of gene therapy. *Gene (Amsterdam),* 525(2), 162–169.

Wolfram JA & Donahue JK (2013). Gene therapy to treat cardiovascular disease. *Journal of the American Heart Association,* 2(4), e000119.

Yi M, Li H, Wu Z, Yan J, Liu Q, Ou C, Chen M (2018). A Promising Therapeutic Target for Metabolic Diseases: Neuropeptide Y Receptors in Humans. *Cellular physiology and biochemistry: international journal of experimental cellular physiology, biochemistry, and pharmacology,* 45(1), 88–107.

Yin J, Guo J, Zhang Q, Cui L, Zhang L, Zhang T, Zhao J, Li J, Middleton A, Carmichael P, Peng S (2018). Doxorubicin-induced mitophagy and mitochondrial damage is associated with dysregulation of the PINK1/parkin pathway. *Toxicology in vitro,* 51, 1–10.

Yla-Herttuala S (2017a). Bumps in the Road for Commercial Gene Therapy for Rare Diseases. *Molecular therapy: the journal of the American Society of Gene Therapy,* 25(10), 2225.

Yla-Herttuala S (2017b). The Pharmacology of Gene Therapy. *Molecular therapy: the journal of the American Society of Gene Therapy,* 25(8), 1731–1732.

Yla-Herttuala S & Baker AH (2017). Cardiovascular Gene Therapy: Past, Present, and Future. *Molecular therapy: the journal of the American Society of Gene Therapy,* 25(5), 1095–1106.

Young M, McNulty P, Taegtmeyer H (2002). Adaptation and maladaptation of the heart in diabetes: Part II: potential mechanisms. *Circulation,* 105(15), 1861–1870.

Zarjevski N, Cusin I, Vettor R, Rohner Jeanrenaud F, Jeanrenaud B (1993). Chronic intracerebroventricular neuropeptide-Y administration to normal rats mimics hormonal and metabolic changes of obesity. *Endocrinology,* 133(4), 1753–1758.

Zhai A & Haddad H (2017). The impact of obesity on heart failure. *Current opinion in cardiology,* 32(2), 196–202.

Zhang W, Deng J, Sunkara M, Morris A, Wang C, St Clair D, Vore M (2015). Loss of multidrug resistance-associated protein 1 potentiates chronic doxorubicin-induced cardiac dysfunction in mice. *The Journal of pharmacology and experimental therapeutics,* 355(2), 280–287.

Zhang J, Qiu H, Huang J, Ding S, Huang B, Wu Q, Jiang Q (2018). Establishment of a diabetic myocardial hypertrophy model in Mus musculus castaneus mouse. *International journal of experimental pathology,* 99(6), 295–303.

Zhang S, Liu X, Bawa-Khalfe T, Lu LS, Lyu YL, Liu LF, Yeh ET (2012). Identification of the molecular basis of doxorubicin-induced cardiotoxicity. *Nature medicine,* 18(11), 1639–1642.

Zhang Y, Bao M, Dai M, Wang X, He W, Tan T, Lin D, Wang W, Wen Y, Zhang R (2015). Cardiospecific CD36 suppression by lentivirus-mediated RNA interference prevents cardiac hypertrophy and systolic dysfunction in high-fat-diet induced obese mice. *Cardiovascular diabetology,* 14, 69-015-0234-z.

Zhihao L, Jingyu N, Lan L, Michael S, Rui G, Xiyun B, Xiaozhi L, Guanwei F (2019). SERCA2a: a key protein in the Ca(2+) cycle of the heart failure. *Heart failure reviews*.

Zhu J, Zhang J, Xiang D, Zhang Z, Zhang L, Wu M, Zhu S, Zhang R, Han W (2010). Recombinant human interleukin-1 receptor antagonist protects mice against acute doxorubicin-induced cardiotoxicity. *European journal of pharmacology,* 643(2–3), 247–253.

Zhu J, Zhang J, Zhang L, Du R, Xiang D, Wu M, Zhang R, Han W (2011). Interleukin-1 signaling mediates acute doxorubicin-induced cardiotoxicity. *Biomedicine & pharmacotherapy,* 65(7), 481–485.

Zhu X, Gillespie D, Jackson E (2015). NPY1-36 and PYY1-36 activate cardiac fibroblasts: an effect enhanced by genetic hypertension and inhibition of dipeptidyl peptidase 4. *AJP-Heart and Circulatory Physiology,* 309(9), H1528–H1542.

Zima AV, Bovo E, Mazurek SR, Rochira JA, Li W, Terentyev D (2014). Ca handling during excitation-contraction coupling in heart failure. *Pflugers Archiv: European journal of physiology,* 466(6), 1129–1137.

Zsebo K, Yaroshinsky A, Rudy J, Wagner K, Greenberg B, Jessup M, Hajjar R (2014). Long-term effects of AAV1/SERCA2a gene transfer in patients with severe heart failure: analysis of recurrent cardiovascular events and mortality. *Circulation research,* 114(1), 101–108.

UNIVERSITY OF TURKU

Painosalama Oy, Turku, Finland 2020

ISBN 978-951-29-8179-3 (PRINT)
ISBN 978-951-29-8180-9 (PDF)
ISSN 0355-9483 (Print)
ISSN 2343-3213 (Online)